

TALLINN UNIVERSITY OF TECHNOLOGY
DOCTORAL THESIS
62/2025

Metabolic Characterization and Composition Control of Next Generation Probiotic Consortia

ANNA KATTEL



TALLINN UNIVERSITY OF TECHNOLOGY

School of Science

Department of Chemistry and Biotechnology

This dissertation was accepted for the defence of the degree Doctor of Philosophy in Chemistry 08/07/2025.

Supervisor:

Professor Emeritus Raivo Vilu
Tallinn University of Technology
Tallinn, Estonia

Co-supervisor:

Dr. Ranno Nahku
TFTAK
Tallinn, Estonia

Opponents:

Dr. Stéphane Chaillou
Biosphera Graduate School
INRAE, Micalis Institute
Paris-Saclay University
Paris, France

Professor Jaak Truu
Faculty of Science and Technology
Institute of Molecular and Cell Biology
University of Tartu
Tartu, Estonia

Defence of the thesis: 10/09/2025, Tallinn

Declaration:

Hereby I declare that this doctoral thesis, my original investigation and achievement, submitted for the doctoral degree at Tallinn University of Technology has not been submitted for doctoral or equivalent academic degree.

Anna Kattel

signature



Copyright: Anna Kattel, 2025

ISSN 2585-6898 (publication)

ISBN 978-9916-80-358-5 (publication)

ISSN 2585-6901 (PDF)

ISBN 978-9916-80-359-2 (PDF)

DOI

TALLINNA TEHNIKAÜLIKOOL
DOKTORITÖÖ
62/2025

Uue põlvkonna probiootiliste koosluste koostise kontroll ja metaboolne iseloomustus

ANNA KATTEL



Contents

List of Publications	7
Author's Contribution to the Publications	8
Introduction	9
Abbreviations	10
1 Literature Review	11
1.1 Definition and evolution of the microbiome field.....	11
1.2 Probiotics, next-generation probiotics, and synthetic consortia	12
1.3 Advantages and challenges of microbial consortia	15
1.4 Isothermal microcalorimetry	16
1.5 Short-chain fatty acids metabolism and genome-scale metabolic models	17
1.6 Viable cell quantification methods	20
2 Aims of the Study	22
3 Materials and Methods.....	23
3.1 Strains	23
3.2 Media	23
3.3 Cultivation	24
3.4 Microscopy and image analysis.....	25
3.5 Quantification of extracellular metabolites	25
3.6 Flow cytometry	26
3.7 DNA extraction	26
3.8 PMAx treatment and spike-in control	26
3.9 Quantitative real-time PCR	26
3.10 16S rRNA NGS.....	27
3.11 Construction of metabolic networks and flux balance analysis.....	27
4 Results and Discussion	28
4.1 Creation of the model consortium.....	28
4.2 Stability and resilience of a defined human gut microbiota consortium assessed with isothermal microcalorimetry (Publication I)	29
4.3 Evaluating diversity of 25-species model consortium (Unpublished data).....	34
4.4 Analysis of metabolism in co-cultures of <i>Anaerostipes caccae</i> and <i>Bacteroides</i> spp. (Publication II)	34
4.4.1 Screening and genome annotation analysis of candidate species	34
4.4.2 Establishing and validating co-cultures based on substrate specificity	36
4.4.3 Co-culture metabolic interactions	37
4.4.4 Species ratio determination.....	39
4.4.5 Development of co-culture bioprocess.....	40
4.4.6 Altering substrate ratios and characterizing metabolic interactions with FBA.....	41
4.5 Estimation of viable cell abundance and enumeration using PMAx and spike-in control as alternatives to traditional methods (Publication III)	44
4.5.1 Estimation of viable cell abundance using PMAx-qPCR	44
4.5.2 Bacterial enumeration using spike-in and NGS.....	47
4.5.3 Combining PMAx treatment and spike-in control.....	48
5 Conclusions	50
References	51

Acknowledgements.....	63
Abstract.....	64
Lühikokkuvõte.....	66
Appendix 1	67
Appendix 2	81
Appendix 3	95
Appendix 4	109
Curriculum vitae.....	121
Elulookirjeldus.....	123

List of Publications

The list of author's publications, on the basis of which the thesis has been prepared:

- I **Kattel, A.**, Aro, V., Lahtvee, P. J., Kazantseva, J., Jõers, A., Nahku, R., & Belouah, I. (2024). Exploring the resilience and stability of a defined human gut microbiota consortium: An isothermal microcalorimetric study. *MicrobiologyOpen*, 13(4). <https://doi.org/10.1002/mbo3.1430>
- II **Kattel, A.**, Morell, I., Aro, V., Lahtvee, P. J., Vilu, R., Jõers, A., & Nahku, R. (2023). Detailed analysis of metabolism reveals growth-rate-promoting interactions between *Anaerostipes caccae* and *Bacteroides* spp. *Anaerobe*, 79. <https://doi.org/10.1016/j.anaerobe.2022.102680>
- III Kallastu, A., Malv, E., Aro, V., Meikas, A., Vendelin, M., **Kattel, A.**, Nahku, R., & Kazantseva, J. (2023). Absolute quantification of viable bacteria abundances in food by next-generation sequencing: Quantitative NGS of viable microbes. *Current Research in Food Science*, 6(December 2022), 100443. <https://doi.org/10.1016/j.crfs.2023.100443>

Author's Contribution to the Publications

Contribution to the papers in this thesis are:

- I The author participated in the study design, experimental work and in data curation. She also participated in the editing of the manuscript.
- II The author participated in the study design and performed all the in vitro experimental work. She collected, calculated and interpreted the data, and wrote the manuscript draft. She also edited the manuscript.
- III The author participated in the experimental work and editing of the manuscript.

Introduction

The human gut microbiome plays an important role in host health, influencing various processes like nutrient digestion, immune system development and resistance to pathogens. While traditional probiotics have been used for decades to support gut health, their clinical efficiency is limited to definite strains. This has led to the emergence of next-generation probiotics (NGP), consisting of commensal microbes with targeted health benefits. However, many promising NGP candidates are strict anaerobes with poorly understood metabolic requirements, presenting significant production challenges. These may include maintaining strict anaerobic conditions, achieving consistent yields, and preserving wanted species ratios.

One potential solution is the use of defined microbial consortia – multi-strain consortia cultivated in controlled conditions, where each species is chosen with a specific purpose. Unlike monocultures, synthetic consortia can benefit from enhanced metabolic capabilities and multifunctionality through complementary metabolic functions. One species might break down complex carbohydrates, producing intermediates that support the metabolic activity of another species. This division of labour allows the processing of substrates that no single species can fully utilize on its own. At the same time, compared to multiple monoculture cultivations, co-cultivation can decrease the amount of hardware and production costs.

Co-cultivation also offers advantages in terms of stability and resilience. Microbial consortia tend to be more robust under environmental fluctuations such as changes in pH, temperature, or exposure to inhibitory compounds. Consortium members can buffer stress, compensate for lost functions, or change in abundance to maintain overall performance. Synergistic interactions, such as cross-feeding of metabolites (short-chain fatty acids such as acetate, other organic acids like lactate, vitamins), can further enhance growth and production of beneficial metabolites. Importantly, cultivating consortia instead of assembling mixed monocultures can also reduce the risk of contamination by maintaining high cell densities and ecological niches that make it harder for unwanted microbes to grow. Moreover, mimicking natural microbial ecosystems promotes stable co-existence and enables more predictable functionality in applications, from biotherapeutics to industrial fermentation.

The current thesis addresses the challenge of how to cultivate stable and controllable consortia of NGP candidate species. The main purpose of this work is to develop and validate a workflow for cultivating stable, defined microbial consortia of NGP candidates. “Unique carbon source” strategy is proposed, in which each species is provided with a carbon source that is not shared by others, thereby minimizing direct competition and enabling compositional control. Consortium growth was continuously monitored with isothermal microcalorimetry to evaluate stability, growth dynamics, and resilience under serial batch conditions. This was combined with flux balance analysis using genome-scale metabolic models to explore cross-feeding interactions. To assess viability and track species ratios, we developed microscopy-based quantification and implemented PMAXx-qPCR. Additionally, the workflow for absolute quantification of viable bacteria with next-generation sequencing was developed. The findings of this thesis have been presented at scientific seminars and conferences. Based on this work, a research service has been developed at TFTAK, which has attracted interest from international clients. Collectively, these results enhance our understanding of consortia production.

Abbreviations

<i>A. caccae</i>	<i>Anaerostipes caccae</i>
ace	Acetate pathway
<i>A. muciniphila</i>	<i>Akkermansia muciniphila</i>
<i>B. thetaiotaomicron</i>	<i>Bacteroides thetaiotaomicron</i>
but	Butyrate pathway
<i>B. vulgatus</i>	<i>Bacteroides vulgatus</i>
CDI	<i>Clostridioides difficile</i> infection
CDM	Chemically defined medium
CFU	Colony-forming unit
Cq	Quantification cycle
CRC	Colorectal cancer
FBA	Flux balance analysis
FC	Flow cytometry
FMT	Faecal microbiota transfer
<i>F. prausnitzii</i>	<i>Faecalibacterium prausnitzii</i>
GEM	Genome-scale metabolic model
glyc	Glycolysis
HPLC	High-performance liquid chromatography
IMC	Isothermal microcalorimetry
ldh	Lactate dehydrogenase
NGP	Next-generation probiotics
NGS	Next-generation sequencing
OD	Optical density
PMA	Propidium monoazide
pfl	Pyruvate formate lyase
pfr	Pyruvate ferredoxin oxidoreductase
prp	Propionate pathway
pyk	Pyruvate kinase
qPCR	Quantitative real-time PCR
SCFA	Short-chain fatty acid
suc	Succinate pathway
YCFAM	Yeast extract, casitone, fatty acids, mucin
YCM	Yeast extract, casitone, mucin

1 Literature review

1.1 Definition and evolution of the microbiome field

The study of the microbiome has evolved substantially over time. Early research between the 17th and 19th centuries laid the foundations by describing microorganisms and distinguishing microbial differences between health and disease states. A significant technological milestone in the field was the development of anaerobic cultivation techniques. Methods such as the Hungate roll-tube technique, developed in the mid-20th century, along with the later use of GasPak systems and anaerobic chambers, have been necessary for isolating and studying anaerobic microorganisms. These methods, together with the use of germ-free animal models, have been essential in highlighting the critical impact of gut microbiota on host physiology. However, they also underscore the need for continued development of cultivation techniques that enable the growth and study of diverse microbial species under laboratory conditions.

As microbiome research advanced, slightly different definitions of the microbiome began to emerge across various scientific contexts. Ecologically, the microbiome is described as an “Ecological community of commensal, symbiotic and pathogenic microorganisms within a body space or other environment” (Lederberg & Mccray, 2001). From a genomic perspective, it encompasses the full genetic material – the metagenome – of all microorganisms inhabiting a niche, such as the human gut (Nature, n.d.). In this thesis, the definition proposed by Berg et al., (2020), building upon Whipps J, 1988 is adopted: the microbiome is seen as a “characteristic microbial community occupying a reasonably well-defined habitat with distinct physio-chemical properties.” This view emphasizes that the microbiome includes not just the microorganisms themselves (such as bacteria, archaea, protozoa, fungi, and algae), but also their “theatre of activity” – a complex network of metabolites (organic acids, toxins, signalling molecules), structural components (proteins, lipids, nucleic acids), mobile genetic elements, and relic DNA. This expanded view positions the microbiome as a dynamic and integrated micro-ecosystem that both shapes and is shaped by its environment over time. When integrated within eukaryotic hosts, such as humans, the microbiome plays an essential role in maintaining host health and modulating disease risk.

Alongside growing insight into its functional importance, more precise methods have corrected earlier misconceptions about the number of microbes relative to human cells. In several scientific sources, it has been stated that microbiota outnumber human cells by a ratio of 10:1 (Pluznick, 2014; Sekirov et al., 2010; Xu et al., 2022). However, this claim has been debunked, with research suggesting that the actual ratio is closer to 1:1 (Sender et al., 2016b). It is important to note that the actual ratio is not static; it varies between individuals and can fluctuate depending on factors such as body size, gender, recent antibiotic use, and bowel habits (Sender et al., 2016a). However, revising the estimated ratio of bacteria to human cells from 10:1 to a more accurate value of approximately 1:1 does not diminish the biological significance of the microbiota.

Over the last decade the research of the microbiome in the health and well-being of a body has been remarkably accelerated. Especially the gut microbiome which has been linked to organs like brain, skin, pancreas and liver (Byrd et al., 2018; Leung et al., 2016; Sharon et al., 2016; Tripathi et al., 2018). Everyone’s gut microbiome is unique, and shaped primarily by environmental factors such as diet, medication, and lifestyle, with genetics playing only a minor role (Falony et al., 2016; Rothschild et al., 2018). This individuality

means that the composition and function of the gut microbiota can vary significantly from person to person. A diverse gut microbiome is generally considered beneficial, as it can increase resilience against pathogens and support metabolic and immune functions (Lloyd-Price et al., 2016; Lozupone et al., 2012). Conversely, reduced diversity is often linked to dysbiosis and disease. Changes in microbiome diversity and low or high abundance of species have been associated with diseases such as inflammatory bowel disease, diabetes, obesity, cardiovascular disease, and cancer (Alam et al., 2020; W.-Z. Li et al., 2020; Masheghati et al., 2024; Muscogiuri et al., 2019; Novakovic et al., 2020). Gut microbiome has been even linked to neurodegenerative diseases like Parkinson's disease (Pereira et al., 2022; Tan et al., 2021).

The concept of microbiome-based therapies dates back to fourth-century China, where fecal matter from healthy individuals was used to treat conditions such as fever, poisoning, and diarrhoea (Zhang et al., 2018). In 1958, Eisemann et al. announced the successful treatment of pseudomembranous enterocolitis with a faecal enema, now referred to as faecal microbiota transfer (FMT) (Stone, 2019). FMT is a method that has been researched in numerous clinical studies and used to treat various conditions, including ulcerative, Crohn's disease, and type 2 diabetes mellitus (Costello et al., 2019; Sokol et al., 2020; Su et al., 2022). However, clear evidence of its efficacy is currently available only for recurrent *Clostridioides difficile* infection (CDI) (Baunwall et al., 2020). While FMT has been effective for treating recurrent CDI, it has its implications. Introducing undefined live bacteria carries unpredictable risks for infections and metabolic disorders, especially in immunocompromised individuals. Although FMT is highly effective and has a good short-term safety record, it faces significant standardization challenges and potential long-term risks. Adverse events related to FMT are mostly gastrointestinal symptoms like diarrhoea, abdominal discomfort, nausea but also sore throat, rash, aspiration pneumonia and even death has been documented (Marcella et al., 2021).

Additionally, the use of postbiotics have been studied. Sterile faecal filtrates – containing bacterial debris, proteins, antimicrobial compounds, metabolic products, and DNA, but not intact microorganisms – were used to treat patients with CDI (Ott et al., 2017). In all five patients, diarrhoea and other recurrent CDI symptoms resolved, and they remained symptom-free until the end of the study, which was at least six months post-intervention. Even though the exact mechanism of action was not defined it enhances the complexity of finding treatment for different gut related diseases. For therapeutic effect it might not be necessary to transfer the entire microbiome from donor to the patient. This opens the door to rationally designed microbial therapies, such as synthetic microbial consortia, that are both safer and targeted.

1.2 Probiotics, next-generation probiotics, and synthetic consortia

Term “probiotics” refers to live microorganisms which offer health benefits upon consumption in adequate amounts (Hill et al., 2014). Probiotics can be found in traditional fermented foods (like kimchi, sauerkraut) which have a long history of consumption and are generally associated with gut health. These traditional sources contain a wide array of microorganisms, though both the quantity and composition of strains can vary considerably. Over time, specific strains have been isolated, characterized, and developed into commercially available food supplements. Decades of research have resulted in the identification of strains with targeted health benefits, some of which have undergone clinical trials and demonstrated efficacy. Probiotics are

recognized for their ability to influence the gut microbiome, and in some cases, have shown clinically validated mechanisms (Michail et al., 2006). However, effectiveness of probiotics can vary significantly depending on several factors. These include the individual's health status, the condition being targeted, the number and strain of live bacteria in the product, and whether the bacteria can survive the acidic conditions of the gastrointestinal tract. This variability makes it difficult to achieve consistent therapeutic results.

However, there are novel species with potential to have more defined therapeutic effects, specific health benefits and can become more standardized biotherapeutic products, and even drugs against diseases. These microbes, which are part of the healthy gut microbiota and have therapeutic potential are generally referred to as next-generation probiotics (NGP)(T. P. Singh & Natraj, 2021). Unlike traditional probiotics, NGP candidate species belong to diverse range of genera, have no history of use and therefore require careful safety assessments and regulations. Some promising NGP candidate species are *Akkermansia muciniphila* (*A. muciniphila*), *Bacteroides thetaiotaomicron* (*B. thetaiotaomicron*), *Faecalibacterium prausnitzii* (*F. prausnitzii*), and *Christensenella minuta* (Lalowski & Zielińska, 2024; T. P. Singh & Natraj, 2021). In addition to single species, different assembled consortia are also investigated (Clark et al., 2021; Kurt et al., 2023). NGP consortia can be customized to meet individual requirements, considering the unique composition of the microbiome and the disease being treated. While the benefits and potential have been shown in many cases, there are still many challenges to tackle. Most of the NGP candidate species are obligate anaerobes, which makes their production complicated and increases cost due to our limited knowledge of their metabolic peculiarities and the challenges associated with cultivating them (Andrade et al., 2020; Ndongo et al., 2020). And, as stated, to be classified as live biotherapeutic products, or drugs, the clinical efficacy must be proven in parallel with safety studies.

NGPs have potential applications in preventing further negative outcome of therapeutic treatments and supporting the positive effects of treatments of various conditions, including CDI, inflammatory bowel disease, colorectal cancer (CRC), and metabolic disorders (Jonkers et al., 2012). For example, it was shown in mice that *A. muciniphila* colonization significantly increased the anti-cancer effect of FOLFOX which is a combination chemotherapy regimen used to treat CRC (Hou et al., 2021). Another study investigated the effects of administering *A. muciniphila* to insulin-resistant overweight or obese human volunteers, focusing on its safety, tolerability, and impact on metabolic parameters (Depommier et al., 2019). It demonstrated that both live and pasteurized *A. muciniphila* were safe and well-tolerated over three months. *A. muciniphila* notably improved insulin sensitivity, reduced insulinemia and plasma total cholesterol. In addition, body weight, fat mass, and hip circumference decreased compared to baseline. Interestingly, pasteurized *A. muciniphila* had significantly stronger effects than live *A. muciniphila*. Observing the beneficial effect on metabolism confirms results previously shown with pasteurized *A. muciniphila* on mice (Plovier et al., 2017).

There are ongoing clinical trials testing co-cultures as biotherapeutic products for safety and efficacy. Phase I-II clinical trials have been completed to evaluate the safety and tolerability of a live biotherapeutic product comprising 11 commensal bacterial strains in combination with nivolumab for the treatment of different types of advanced or metastatic cancer including CRC (NCT04208958). Currently there are two FDA-approved microbiota-based therapeutics on the market. One of them is SER-109, which is an oral live biotherapeutic product derived from faecal microbiota, mainly consisting of purified

Firmicutes spores, which helps to prevent the recurrence of CDI (Blair, 2024). Another one is RBX2660, a live faecal microbiota suspension for rectal use, also meant for preventing recurrence of CDI (Blair, 2023). Both of them are manufactured from donated human faecal matter and the detailed mechanisms by which they are effective are unknown. No synthetically produced consortia have gained the approval of FDA.

In addition to their therapeutic potential as next-generation probiotics, defined microbial consortia also play important roles in diverse fields such as bioprocessing, fermentation, and environmental science (Chen et al., 2014; Shin et al., 2010; Wang et al., 2016). Synthetic microbial consortia are typically developed using a closed-loop design-build-test-learn cycle. Their construction commonly follows two main strategies: the bottom-up approach, which assembles consortia from individually characterized strains, and the top-down approach, which simplifies complex natural communities (Lawson et al., 2019). In practice, many designs also employ hybrid strategies that combine elements of both methods.

Synthetic microbial consortia can also be constructed based on different design principles, such as cross-feeding and trait-based selection (Liang et al., 2022). Cross-feeding is a common microbial interaction where one species produces metabolites that others consume. This strategy promotes diversity, stability, and functional specialization through metabolic division of labour. Cross-feeding can occur in unidirectional, bidirectional, or multidirectional forms and usually involves metabolites but can also involve extracellular enzymes. Various mathematical models such as generalized Lotka–Volterra equations and flux balance analysis can help predict and optimize these interactions. An example of cross-feeding-based design is the study by Ziesack et al., (2019), in which a synthetic consortium of four gut-associated bacteria was engineered for obligate amino acid cross-feeding. Each species overproduced one amino acid while depending on the others for three, resulting in increased population evenness and reduced antagonism.

However, constructing stable consortia based on cross-feeding presents several challenges. Despite their cooperative nature, these systems are vulnerable to negative effects of competition, evolutionary instability, and the emergence of strains that exploit shared resources without contributing themselves. For instance, marine bacteria *Prochlorococcus* and SAR11 exhibit a commensal cross-feeding interaction (lactate and acetate provided by *Prochlorococcus*), but their possible competition for limited sulphur compounds could destabilize the co-culture (Becker et al., 2019).

Trait-based construction of synthetic microbial consortia involves selecting species based on defined physiological or ecological characteristics, such as substrate preferences, environmental tolerances, or metabolic functions. In trait-based microbial consortia, each species is chosen to perform a specific, non-overlapping function – such as breaking down a certain substrate or producing a needed compound. This complementary role distribution reduces overlap in resource use, which minimizes direct competition among members. In contrast to cross-feeding-based consortia, which behaviour depends on metabolic exchanges between species, trait-based approaches rely on the independent functional capabilities of each member. Krieger et al., (2021) demonstrate how temperature ranges of different species can be used to adjust their abundance in a consortium. They applied temperature cycles to a consortium of *Escherichia coli* and *Pseudomonas putida* to exploit their different growth patterns at various temperatures. This approach integrates a trait-based perspective (bottom-up design) with environmental

control, which is a characteristic of a top-down approach. In another example, Clark et al., (2021) used a model-guided approach to construct synthetic human gut microbiome optimized for butyrate production. By selecting species based on traits related to growth dynamics and butyrate production, and accounting for environmental factors like pH and hydrogen sulphide levels, they successfully assembled consortia with enhanced metabolic function.

However, the effectiveness of trait-based approach depends on how reliably traits are expressed in co-culture. Microbial traits observed in monoculture may not behave similarly in complex consortia due to factors like regulatory shifts, microbial interactions, or stress responses (Lawson et al., 2019; Widder et al., 2016).

Defined microbial consortia are designed through theoretical strategies and validated with experimental models. One example of this is a study in which bottom-up design was used to select nine strains for a consortium that mimics the carbohydrate fermentation processes of a healthy human gut (Kurt et al., 2023). These bacteria were cultured together, and they formed a stable and reproducible consortium. At the same time, if grown individually, none of the strains showed increased growth but rather poor or equal growth compared to consortium growth. While it is an example of a bottom-up approach it also highlights the importance and benefits of co-cultivation and the need for novel cultivation techniques. Moreover, it was shown that consortium growth and metabolic activity differed from a mix of the same strain's monocultures. Co-cultivated consortium was found to be as effective as FMT for treating acute colitis induced by dextran sodium sulphate in mice, but the equivalent mix of individually cultured strains did not achieve the same effectiveness.

1.3 Advantages and challenges of microbial consortia

While the design of microbial consortia can be complex, they offer several advantages. Microbial consortia tend to be more resilient and resistant to stress than monocultures. Overlapping metabolic functions and having redundancy mean if one species is under stress, others can compensate for preserving functionality (Embree et al., 2015). For example, gut microbiota can withstand disturbances like antibiotics better than a single strain, because surviving members can fill the functional roles of those who were lost. Additionally, species abundances within a consortium can shift dynamically in response to environmental changes, allowing the community to maintain a stable overall function through complex feedback interactions, such as cross-feeding and substrate competition (McCarty & Ledesma-Amaro, 2019). Monocultures, lacking such internal redundancy, are more vulnerable – if the single strain fails under stress, the function is lost.

Consortia also benefit from division of labour among different microbes, enabling degradation or synthesis of compounds that no single strain could accomplish alone (Z. Li et al., 2019). In bioremediation, mixed microbial communities can break down complex pollutants (like petroleum) via sequential and cooperative metabolism, achieving degradation where monocultures cannot (Zanaroli et al., 2010). Similarly, in industrial biotechnology, co-cultures allow compartmentalization of metabolic pathways across strains, reducing the burden on any one cell and improving overall efficiency (McCarty & Ledesma-Amaro, 2019). This wide range of cooperative benefits is seen in soil consortia and plant root microbiomes. Combinations of bacteria and fungi provide enhanced nutrient cycling and stress tolerance for plants, surpassing the capabilities of single inoculants (Santoyo et al., 2021). In short, a consortium's functional

diversity allows for niche saturation, where available ecological niches and resources are fully exploited.

Furthermore, a well-established microbial consortium can protect itself against invading pathogens through competitive exclusion and production of inhibitory compounds. Diverse consortia occupy a wide array of niches and consume available nutrients, leaving little opportunity for pathogens to establish themselves. In the gut, the existing microbiome can affect whether incoming species successfully establish themselves, primarily through competitive exclusion, when both incoming and resident species rely on the same niche and resources, coexistence becomes unlikely (Le Roy et al., 2019; Maldonado-Gómez et al., 2016; Martínez et al., 2018).

These advantages can offer notable economic and operational benefits as well. Use of cheap, complex feedstocks that is possible due to division of labour. As well the overall enhanced productivity and efficiency (Roell et al., 2019). In addition, the hardware requirements for cultivating consortia in a single bioreactor are considerably lower than those needed to grow each monoculture separately, which can reduce equipment costs and save time in operational workflows.

Despite the strengths, microbial consortia can be harder to control and reliably reproduce. Complex interactions and dynamic shifts in species composition may lead to variability in performance. In industrial or clinical applications, monocultures often provide more reproducibility – a single well-characterized strain tends to behave predictably under set conditions, whereas consortia might exhibit a drift in composition and ensuring the same ratio of species can be challenging. Similarly, in cultivation processes, co-cultures require careful tuning of growth conditions, and an imbalance can lead to one species overgrowing and diminishing the consortium's intended function. Monocultures, with no inter-species competition, are simpler to optimize.

From a practical standpoint, monocultures are still essential in applications requiring precise, high-yield production of a target compound. Engineered monocultures avoid the uncertainty of interactions between species, though they sacrifice the resilience and multifunctionality of consortia. Microbial consortia offer strength in numbers – greater stress resistance, metabolic diversity, and ecological stability – while monocultures offer simplicity and predictability. Finding the right balance between these trade-offs is important, as the benefits of cooperative microbial consortia must be weighed against the need for precise control and consistent performance.

1.4 Isothermal microcalorimetry

Isothermal microcalorimetry (IMC) is a unique method that has been used for shelf-life studies, on-line monitoring of growth and metabolism of microorganisms including biofilm formation and fermentation in milk (Kabanova et al., 2009; Kütt et al., 2023; Morozova et al., 2020; Stulova et al., 2015; Sultan et al., 2022).

IMC is an extremely sensitive technique for monitoring the heat generation by metabolically active microorganisms within hermetically sealed ampoules maintained at a constant temperature. The rate of heat generation directly correlates with the rate of biomass production, and the shape of the heat production curve reflects the metabolic activities of the microorganisms (Forrest W.W. & Walker D.J., 1963).

IMC has several advantages in microbiology compared to other methods. Firstly, the sensitivity; heat generated by even a small number of microorganisms can be detected by IMC. Detectable cell concentration is starting from 2.5×10^4 and 1.0×10^5 CFU per mL which is significantly lower than detection level of spectrophotometer that measures

turbidity (10^7 – 10^8 CFU mL⁻¹)(Braissant et al., 2010). An additional advantage of IMC is its suitability for cultivation in anaerobic conditions, making it particularly useful for studying human gut microbiome species. Furthermore, heat production is unaffected by the growth medium opacity. Mucin is one of the medium ingredients that is mostly insoluble in water, but a necessary substrate for some NGP candidate species. Mucin-containing media are not transparent but biochemical reactions in them could be readily investigated using IMC.

Besides high sensitivity, IMC allows to measure heat flows changes with high accuracy – approximately 1%. This is due to instruments ability to maintain the temperature of the ampoule's within ± 0.1 °C, and measure heat flow across a large range, while having only small baseline drift, typically by only 0.2 μ W over 24 hours. In addition to this, IMC provides continuous on-line measurements which allows to observe experiments in real time. Also, the heat measurements are non-invasive, as it occurs externally without altering the samples inside the ampoules. This allows the samples to be used for additional analyses afterwards, such as quantifying organic acids, amino acids, and carbohydrates (Kattel et al., 2023, 2024).

Each method has its limitations; for IMC, samples must reach the set temperature before measurements can begin. Typical equilibration period is approximately one hour during which no data can be acquired. Secondly, only batch processes can be studied in the IMC. In the batch process, the cell concentration as well as substrate and product concentrations are changing. In serial batch format, microorganisms are inoculated into the medium and grown until stationary phase. Fraction of the grown culture is then transferred into fresh medium. This process is repeated and helps to mimic industrial production processes where several seed batches are needed to be produced as inocula for higher volume cultivations.

1.5 Short-chain fatty acids metabolism and genome-scale metabolic models

Short-chain fatty acids (SCFA) are key microbial metabolites with significant physiological roles in the human gut. Understanding how these compounds are produced, utilized, and cross-fed among microbial species requires both experimental and computational tools. Methods like IMC describe phenotypic traits but genome-scale metabolic models (GEMs) can be used to simulate metabolic behaviour and to predict interactions under various conditions.

To effectively model microbial interactions using GEMs, it is necessary to understand the diversity and metabolic roles of SCFA-producing bacteria. Metabolism of human gut microbiota species is diverse while they convert indigestible substrates into SCFA. Based on the substrate preferences or metabolism end products gut microbiota species can be categorized into several subgroups: asaccharolytic bacteria, mucin degraders, butyrate producers, lactic acid producers, succinate and propionate producers, acetate and ethanol producers. Figure 1 provides a schematic overview of the key anaerobic metabolic pathways and enzymes involved in SCFA production by different gut microbiota subgroups. SCFA play a role in modulating interactions between the host and microbiota, influencing inflammatory processes and our health overall. Among the SCFAs, acetate is the most prevalent but has received less research attention compared to propionate and butyrate, which are often regarded as more functional (Münste & Hartmann, 2025).

Butyrate is an important SCFA that serves not only as a fermentation product but also as an energy source for colonocytes through β -oxidation and the Krebs cycle (Donohoe et al., 2011). In the gut, butyrate has anti-inflammatory and immunoregulatory effects (Chang et al., 2014; Recharla et al., 2023; N. Singh et al., 2014). It also accelerates the assembly of tight junctions, which are necessary for the barrier function formation and maintenance (Peng et al., 2009).

While butyrate is an energy source for colonocytes, other SCFAs like acetate and propionate, which are not metabolized, travel to the liver with the portal vein. Once absorbed, propionate is rapidly metabolized by hepatocytes, while acetate can either be utilized in the liver or enter peripheral circulation for use by other tissues (den Besten et al., 2013). At the same time, there is SCFA and other organic acid cross-feeding in the intestine between different species. The main acetate producers can be found among several phyla like Bacteroidetes, Firmicutes, Actinobacteria, and Verrucomicrobia (Hosmer et al., 2024; Mukherjee et al., 2020). This acetate can be consumed by other Firmicutes like *Anaerostipes caccae* who utilize the acetyl-CoA pathway and convert it together with lactate into butyrate (Duncan et al., 2004; Schwartz et al., 2002). Also, succinate that is produced by Bacteroidetes can be converted into propionate by succinate-utilizers like *Phascolarctobacterium faecium* via succinate pathway (Ikeyama et al., 2020). As cross-feeding interactions can be used to design stable microbial consortia, it is important to understand the metabolism of species and characterize inter-species metabolic interactions in detail.

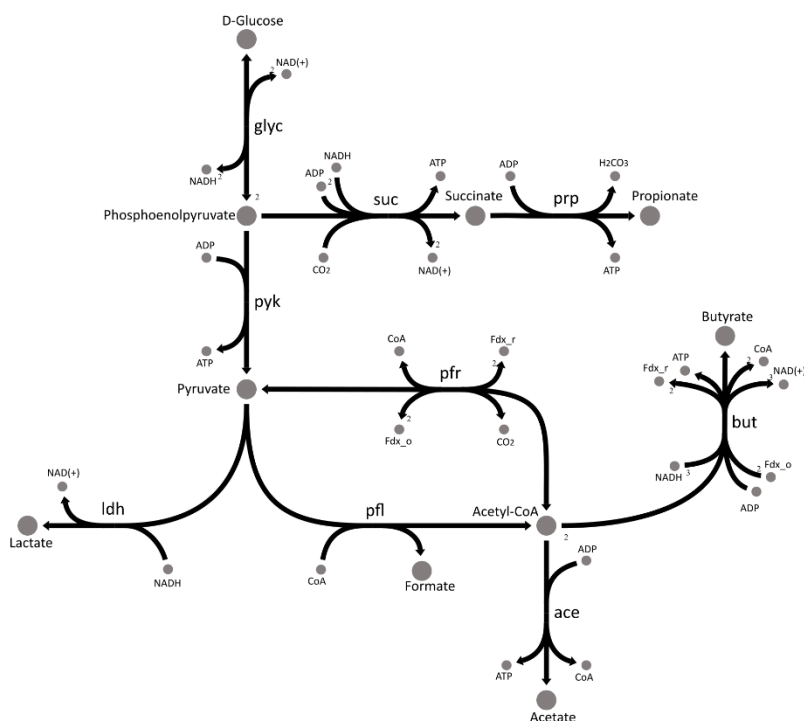


Figure 1. Anaerobic central carbon metabolism and short-chain fatty acid production. The map illustrates the flow of metabolites from glucose through glycolysis (glyc), which in this scheme includes eight enzymes: glucose-6-phosphate isomerase, 6-phosphofructokinase, fructose-bisphosphate aldolase, triose-phosphate isomerase, glyceraldehyde-3-phosphate dehydrogenase, phosphoglycerate kinase, phosphoglycerate mutase, and enolase. The final glycolytic step, conversion of phosphoenolpyruvate to pyruvate, is catalyzed by pyruvate kinase (pyk). Pyruvate is further metabolized via multiple branch points including lactate dehydrogenase (ldh), pyruvate formate lyase (pfl), and pyruvate ferredoxin oxidoreductase (pfr). Conversion of acetyl-CoA to acetate occurs via acetate kinase and phosphate acetyltransferase (ace). The butyrate production pathway (but) includes six enzymatic steps, catalyzed by acetyl-CoA C-acetyltransferase, 3-hydroxybutyryl-CoA dehydrogenase, 3-hydroxybutyryl-CoA dehydratase, butyryl-CoA dehydrogenase, butyryl-CoA phosphate butyryltransferase, and butyrate kinase. The succinate pathway (suc) includes phosphoenolpyruvate carboxykinase, malate dehydrogenase, fumarate hydratase, and fumarate reductase. The propionate pathway (prp) is a sum of reactions catalyzed by succinate-CoA ligase, methylmalonyl-CoA mutase, (S)-methylmalonyl-CoA decarboxylase, propionyl-CoA phosphate propionyltransferase, and propionate kinase. Stoichiometric coefficients are shown to indicate the number of molecules involved in each reaction step.

GEMs map out gene-protein-reaction associations for an organism's metabolic genes and use a stoichiometric matrix to predict metabolic fluxes, enabling analysis of metabolism at the whole-cell level (Thiele & Palsson, 2010). One of the advantages is that GEMs provide a detailed understanding of an organism's metabolic network, which can be used to predict metabolic fluxes and identify key metabolic pathways. GEMs serve as a platform for generating hypotheses about metabolic functions and interactions, which can then be tested experimentally. However, data quality plays an important role in the accuracy of these models. The completeness of GEMs is limited by the availability of high-quality genomic data. Both the data quality and the number of degrees of

freedom i.e. complexity of metabolism in the metabolic model significantly impacts the accuracy of the computational procedures. The outcome of calculations is also strongly affected by both the availability and reliability of genomic and protein annotation data for respective microbial species. Incomplete or poorly annotated genomes can lead to gaps in the metabolic network, reducing the model's accuracy. Outside model organisms, many reactions included in GEMs are predicted based on genomic data and have not been experimentally validated.

1.6 Viable cell quantification methods

Accurate and reliable quantification of viable microbes is essential for informed decision-making and quality control in the production of NGP and other applications. To date, plating remains the most widely accepted method for this purpose. CFU counts are specific, detection requires cells to be alive and able to reproduce, providing a definitive measure of viable organisms. Most probable number dilution assays provide a comparable alternative for viability quantification in liquid media, but they also rely on the growth of culturable organisms and use statistical calculations rather than direct cell counts (Oblinger & Koburger, 1975). While both methods are affordable and technically straightforward, they share significant limitations, especially when applied to complex microbial communities. Samples containing diverse species, such as those with NGP candidates, may require different culture media or growth conditions, making universal cultivation difficult. Furthermore, some bacteria are unculturable under standard laboratory conditions, cultivation does not provide taxonomic information, and obtaining results can take several days (Stewart, 2012).

Use of fluorescent stains that distinguish live and dead cells based on membrane integrity do not require cultivation. Dyes such as SYTO9 (penetrates all cells) and propidium iodide (penetrates only cells with compromised membranes) are used together to label intact and membrane-damaged cells (Baena-Ruano et al., 2006). Live cells fluoresce green while dead cells fluoresce red, enabling direct counts via flow cytometry (FC). FC allows thousands of individual cells to be analysed per second and is a high-throughput tool for viability assessment across fields ranging from water disinfection to food and industrial bioprocessing (Bunthof et al., 2001; Grey & Steck, 2001; Hoefel et al., 2003). However, not all dead cells immediately lose membrane integrity, so dyes can misclassify some dead cells as viable, potentially overestimating live counts (Truchado et al., 2020). Conversely, injured cells with leaky membranes might be counted as dead even if they could recover.

RNA-based methods, such as transcriptomics, offer an alternative approach for identifying only viable cells. Since RNA is an unstable molecule that is rapidly degraded after cell death, its presence indicates metabolically active live bacteria. This allows the sequencing workflow to begin directly from RNA isolation. But due to RNA's short lifespan and associated technical challenges, this method is not widely adopted. Although RNASeq offers high resolution, sensitivity, and suitability for low-biomass samples, it remains expensive and time-consuming, making it impractical for routine use.

Other modern molecular methods, including next-generation sequencing (NGS), PCR, and immunoassays, offer detailed information on the abundance of specific bacterial species (Cao et al., 2017). However, they also have certain limitations. PCR and immunoassays are designed to detect selected target microorganisms, offering rapid and quantitative results. Yet, their sensitivity often depends on prior culturing to increase the number of cells, and they are limited to detecting only those bacteria that have been

specifically predefined in the analysis. The primary advantage of NGS over these methods is its ability to uncover previously unknown microorganisms. Unlike targeted techniques, NGS does not require prior knowledge of the sample's microbial composition. 16S rRNA gene (16S) amplicon NGS offers a comprehensive profile of bacterial consortia by providing the relative abundance of all detected taxa (Adamberg, Raba, et al., 2020; Ji & Nielsen, 2015). However, obtaining absolute abundance data remains challenging due to significant variation in 16S rRNA gene copy numbers among taxa, PCR amplification biases introduced during library preparation, and complexities in data analysis like setting appropriate thresholds.

One solution is to use quantitative microbiome profiling where FC is used to normalize 16S sequencing data by estimating total bacterial load (Vandeputte et al., 2017). Alternatively, spike-in controls added during DNA extraction help account for DNA loss and improve quantification. Introducing spike-in controls at the DNA extraction stage helps to monitor the entire sequencing workflow and minimize biases. Two main types of spike-in controls have been developed: synthetic DNA molecules and whole cells (Piwosz et al., 2018; Smets et al., 2016; Tkacz et al., 2018; Zemb et al., 2020). Synthetic DNA is highly precise and flexible but does not account for biases introduced during cell lysis or DNA extraction. In contrast, spike-in cells typically comprising a mix of Gram-positive and Gram-negative bacteria better reflect processing steps but may not match the specific characteristics of the native microbial community. By combining the known quantity of spike-in material with the relative abundance data from sequencing, absolute microbial counts can be obtained.

An affordable and technically simple option for converting relative data to absolute is quantitative real-time PCR (qPCR). Standard qPCR yields absolute or relative abundance of target gene copies, but it does not differentiate live and dead cells, DNA from dead cells can persist in samples and be amplified. To address this, viability PCR techniques have been developed using photoreactive dyes like ethidium monoazide, propidium monoazide (PMA), and PMAxx (advanced version of PMA). PMAxx-qPCR involves treating a sample with PMAxx before DNA extraction. PMA penetrates cells with compromised membranes and covalently binds their DNA upon light activation, thereby inhibiting the amplification of DNA from dead bacteria. It has been successfully applied in a wide range of contexts, including probiotics research, food safety testing, and the analysis of environmental water and soil microbiomes (Alonso et al., 2014; Ditommaso et al., 2015; Scariot et al., 2018). Limitations of this method are similar to those observed with fluorescent dyes and FC, if some dead cells have intact membranes, dye might fail to enter and their DNA will be mistakenly counted as viable, leading to overestimation (Nocker et al., 2017). On the other hand, high PMA concentrations or cell membrane differences can sometimes exclude DNA from slightly damaged but recoverable cells. Given the complexity of distinguishing viable from non-viable microbes, no single method is universally sufficient for all applications. A combined, sample-dependent approach balancing accuracy and feasibility is important for reliable microbial viability assessment across research and industry settings.

2 Aims of the Study

The aim of this thesis is to develop and validate scalable workflows for the cultivation, characterization, and compositional control of defined microbial consortia, with a focus on NGP candidates. The specific aims were as follows:

- Evaluating consortium stability and resilience using isothermal calorimetry.
- Exploring metabolic interactions and cross-feeding mechanisms through co-culture experiments.
- Establishing a substrate-based strategy to control species abundance in co-cultures.
- Establishing robust viability assessment and enumeration methods.

3 Materials and Methods

Below is a summary of the methods used in this study. More details for every method are provided in Publications I–III.

3.1 Strains

The following bacterial strains were used across the three publications and in the thesis: *Akkermansia muciniphila* (DSM 22959), *Alistipes shahii* (DSM 19121), *Anaerostipes caccae* (DSM 14662), *Anaerotruncus colihominis* (DSM 17241), *Bacteroides thetaiotaomicron* (DSM 2079), *Bacteroides caccae* (DSM 19024), *Bacteroides ovatus* (DSM 1896), *Bacteroides uniformis* (DSM 6597), *Bacteroides vulgatus* (DSM 3289), *Bifidobacterium adolescentis* (DSM 20087), *Bifidobacterium longum* subsp. *infantis* (DSM 20088), *Blautia faecis* (DSM 27629), *Blautia hydrogenotrophica* (DSM 10507), *Butyricimonas faecihominis* (DSM 105721), *Christensenella minuta* (DSM 22607), *Catenibacterium mitsuokai* (DSM 15897), *Collinsella aerofaciens* (DSM 13712), *Dorea formicigenerans* (DSM 3992), *Dorea longicatena* (DSM 13814), *Eisenbergiella tayi* (DSM 26961), *Eubacterium rectale* (DSM 17629), *Faecalibacterium prausnitzii* (DSM 17677), *Odoribacter splanchnicus* (DSM 20712), *Prevotella copri* (DSM 18205), and *Roseburia faecis* (DSM 16840). All strains were obtained from the German Collection of Microorganisms and Cell Cultures (DSMZ).

Several species included in this thesis have undergone reclassification based on genomic evidence. Specifically, *Faecalibacterium prausnitzii* has been reclassified; the strain used in this thesis corresponds to *Faecalibacterium duncaniae* (Sakamoto et al., 2022). Similarly, *Eubacterium rectale* has been reclassified as *Agathobacter rectalis*, *Prevotella copri* as *Segatella copri*, and *Bacteroides vulgatus* as *Phocaeicola vulgatus* (Hahnke et al., 2016; Hitch et al., 2022; Rosero et al., 2016). For consistency with existing literature and publications this thesis is based on, historical species names have been retained in results and plots. However, the updated taxonomic names are used in the phylogenetic tree (Figure 3), which is based on the current NCBI taxonomy as retrieved using the taxize R package.

The lyophilized strains were revived in suitable media tailored for each organism (see Publication II for the medium composition). After cultivation, bacterial stocks were washed with Dulbecco's phosphate-buffered saline supplemented with 1% L-Cysteine hydrochloride. Long-term storage was carried out at -80°C in Dulbecco's phosphate-buffered saline containing 20% glycerol and 1% L-Cysteine hydrochloride.

To prepare the multi-strain stock (20 strains), the number of cells in each strain stock culture was estimated by measuring optical density at 600 nm (OD600), assuming that an OD600 of 1 corresponds approximately to 10^9 CFU per mL. From each stock, 5×10^8 cells were taken and combined into the mixture, resulting in a final OD600 of 0.98 for the mixed culture. To prepare the multi-strain stock (25 strains), from each stock, 2×10^8 cells were taken and combined into the mixture.

3.2 Media

Different types of complex and defined media were used in this thesis to describe co-culture growth. Complex yeast extract, casitone, fatty acids, mucin (YCFAM) medium was used in Publication I (composition and preparation details provided there). In Publication II, several versions of chemically defined media (CDM) were tested,

the details of which are provided in the supplementary data of that publication. For evaluating diversity of 25-species model consortium we used yeast extract, casitone, mucin (YCM) medium. YCM medium consisted of (per litre): 2.5 g casitone (Tryptone Plus, Sigma-Aldrich), 2.5 g yeast extract (NuCel 545, Bio Springer), 1 g L-cysteine HCl (Alfa Aesar), 1 mg resazurin sodium salt (Acros Organics), 2.93 g K₂HPO₄ (Sigma-Aldrich), 4.65 g KH₂PO₄ (Sigma-Aldrich), 0.9 g (NH₄)₂SO₄ (Alfa Aesar), 0.9 g NaCl (Acros Organics), 0.28 g KOH (Fluka), 1 g NaHCO₃ (Sigma-Aldrich), 10 mg hemin (Sigma-Aldrich), 10 µg biotin (Merck), 10 µg cobalamin (Fisher Bioreagents), 30 µg para-aminobenzoic acid (Sigma-Aldrich), 150 µg pyridoxamine (Carbosynth), 50 µg folate (Alfa Aesar), 0.09 g MgSO₄·7H₂O (Alfa Aesar), 0.09 g CaCl₂·H₂O (ApliChem). Mucin from porcine stomach type III (Sigma-Aldrich) was used as a substrate at concentration of 1 g L⁻¹. Sterilization was performed using the same procedure as described for the YCFAM medium (Publication I).

In all cases, media was kept overnight in an anaerobic chamber (COY box, Coy Laboratory Products Inc., Grass Lake, MI, USA) with an atmosphere of 2.5 ± 0.5% H₂, 10% CO₂, and balanced N₂.

3.3 Cultivation

Different systems were used for anaerobic cultivation throughout the thesis. Culture preparations were always done in an anaerobic chamber. Most experiments were conducted using isothermal microcalorimetry (IMC)—TAM III and TAM IV-48 (TA Instruments, New Castle, DE, USA). These included the stability and resilience study of the three-species consortium in Publication I, as well as the small-scale co-culture production and substrate validation experiments in Publication II. Except for the substrate validation and acetate/lactate supplementation study (see Table 2, Table S3, Table S4), all IMC experiments followed a serial batch design: each batch lasted 23–24 h, and 20 µL (1% v/v) of the culture was transferred into 1.98 mL of fresh medium at the start of each new batch (Figure 2). The cultivation period ranged from three to seven consecutive batches.

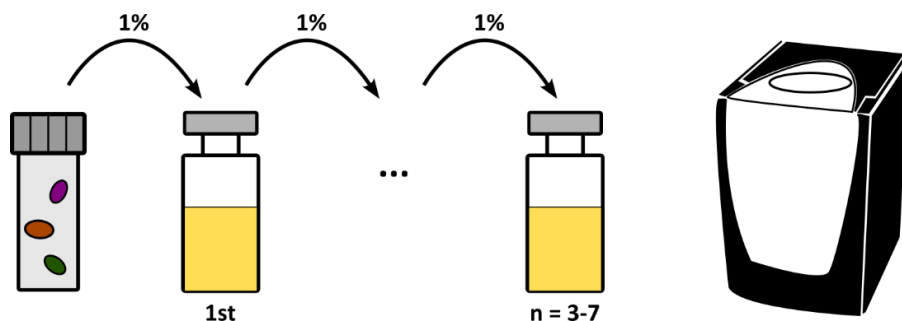


Figure 2. This figure presents the workflow scheme for serial batch cultivations using IMC, conducted with both mono- and co-cultures. Bacteria or bacterial mixtures were inoculated into glass ampoules, which were then hermetically sealed and placed into the IMC. After 23–24 hours of incubation, 1% of the culture volume was transferred into fresh medium. Depending on the experimental setup, three to seven consecutive batch cultivations were carried out.

Strain screening in chemically defined media containing glucose was performed using a BioTek Synergy H1 Multi-Mode Reader (Agilent Technologies Inc., Santa Clara, CA, USA), as described in Publication II. Upscaling from IMC conditions was carried out using 1.25 L Biobundle bioreactors (Applikon, Delft, Netherlands), with further details provided in Publication II.

3.4 Microscopy and image analysis

In Publication II we developed a microscopy image-based method to estimate the species ratios in the co-cultures. Bacterial cultures (*A. caccae*, *B. thetaiotaomicron*, *B. vulgatus*) were adjusted to an OD of 1 and vortexed to disperse the cells. Gram staining was performed using the Biogram 4 Kit (Biognost Ltd., Croatia), and samples were examined with a Nikon Eclipse E200-LED microscope (Japan) using a 100× oil immersion lens. Brightfield images were captured with a Nikon D5200 camera and analyzed in Fiji software. Cells were segmented via color thresholding to determine cell area. *B. thetaiotaomicron* and *B. vulgatus* were defined as cells under 0.85 mm², while *A. caccae* ranged from 0.85–2 mm². For clusters of *A. caccae* exceeding 2 mm², the area was divided by 1.6 mm² (average area of *A. caccae*) to estimate cell count. Each sample included 1200–8900 measured cells. Results are based on triplicate measurements and standard error was calculated accordingly.

In Publication III, a similar procedure was used to study the morphology of selected strains. The same staining protocol and microscope configuration were applied, and brightfield images were captured using the Nikon D5200 camera. No image analysis was performed in Fiji; only the images were collected.

3.5 Quantification of extracellular metabolites

For metabolite analysis (Publication I and II), fermentation samples were centrifuged at 14000 g for 5 minutes at 4 °C and the supernatant was filtered using 0.2 µm syringe filters (Millipore Millex-LG filters 13 mm Millex PTFE 0.2 µm non-sterile SLLGH13NK; Millipore Corp.). Medium samples were filtered directly without centrifugation.

Metabolite concentrations were measured using high-performance liquid chromatography (Waters 2695 HPLC system; Waters Corporation, Milford, MA, USA). The system was equipped with an HPX-87H column (Bio-Rad Laboratories, Richmond, CA, USA) and used isocratic elution with 0.005 M H₂SO₄ at a flow rate of 0.6 mL min⁻¹. The column temperature was maintained at 35 °C. Detection was performed with both refractive index (RI) and ultraviolet (UV) detectors, and quantification was based on external standard curves. The following metabolites were quantified: acetate, butyrate, citrate, ethanol, formate, isobutyrate, isovalerate, lactate, malate, propionate, succinate, valerate, D-galacturonic acid, D-sorbitol, and D-xylose.

Free amino acids were quantified from the same supernatant using a Waters UPLC-PDA system (Waters Corporation, Milford, MA, USA). Samples were derivatized with 6-aminoquinolyl-N-hydroxysuccinimidyl carbamate using the AccQ-Tag Ultra Derivatization Kit (Waters Corporation), and separated on an AccQ-Tag Ultra column using a gradient of eluents A and B. Amino acids were detected by photodiode array and analysed with Empower 3 software (Waters Corporation).

3.6 Flow cytometry

A50-Micro Flow Cytometer (Apogee Flow Systems, UK) was used to assess the viability of 20 individual strains as well as the mixed 20-strain consortia glycerol stock. Membrane integrity was assessed using a dual-staining approach. SYTO24 (SYTO™ 24 Green Fluorescent Nucleic Acid Stain, 5 mM solution in dimethyl sulfoxide; Invitrogen, USA) was used to label all bacterial cells, while propidium iodide (1.0 mg/mL solution in water; Invitrogen, USA) stained only those with compromised membranes. The sample preparation and instrument setup are described in more detail in Publication III.

3.7 DNA extraction

Genomic DNA extraction was performed using two different kits depending on the publication. In Publications I and II, DNA was extracted using the GenElute Bacterial Genomic DNA Kit (Merck, Germany), and the resulting DNA was diluted to a concentration of approximately 10 ng/μL to fit the requirements of the downstream analysis. For Publication III, genomic DNA from the 20-strain consortia samples was isolated using the ZymoBIOMICS™ DNA Miniprep Kit (Zymo Research, Irvine, CA, USA), following the manufacturer's protocol. DNA concentrations were measured using a Qubit™ 4 Fluorometer (Thermo Fisher Scientific, Waltham, MA, USA) in combination with the Qubit dsDNA BR Assay Kit (Thermo Fisher Scientific).

3.8 PMAxx treatment and spike-in control

To evaluate cell viability of twenty bacterial species as well as the 20-strain consortia, propidium monoazide (PMAxx) treatment was used prior to qPCR. Cell suspensions were mixed with PMAxx™ solution in water (Biotium, Fremont, CA, USA) to achieve a final concentration of 25 μM. The mixtures were incubated in the dark on a shaker for 10 minutes. Following incubation, the samples were exposed to blue light using the PMA-Lite™ LED Photolysis device (Biotium) for 20 minutes, with intermittent inversion to ensure even exposure. After light treatment, the samples were centrifuged at 5000 × g for 15 minutes at 4 °C. The resulting pellets were resuspended in phosphate-buffered saline. A defined number of ZymoBIOMICS™ Spike-in Control I (High Microbial Load, Zymo Research, Irvine, CA, USA) was added to the samples if relevant.

3.9 Quantitative real-time PCR

In Publication II, the relative abundances of *A. caccae*, *B. thetaiotaomicron*, and *B. vulgatus* were measured using quantitative real-time PCR (qPCR). Specific primers targeting the Peptidase S41 family gene of *B. thetaiotaomicron*, the sorbitol operon transcription regulator gene of *A. caccae*, and the 16S rRNA gene of *B. vulgatus* were used. Standard curves were constructed from genomic DNA of each species using five concentrations ranging from 0.002 to 36 ng mL⁻¹. PCR reactions were run in triplicate in a final volume of 20 μL using 5× HOT FirePol EvaGreen qPCR Mix Plus (Solis BioDyne, Estonia) and primers at 10 μM. Reactions were set up in white 96-well plates (BIOplastics, Netherlands) sealed with Opti-seal™ Optical Disposable Adhesive. Amplification was carried out with qTOWER³ (Analytik Jena GmbH, Germany) using the following thermal profile: initial denaturation at 95 °C for 15 minutes; 40 cycles of 95 °C for 15 seconds, 60 °C for 20 seconds, 72 °C for 20 seconds, one cycle of 95 °C for 5 seconds, 60 °C for 1 minute, and a melting curve from 60 °C to 97 °C.

While qPCR was also used in Publication III, additional steps were included to assess viability of 20 individual and mixed 20-strain consortium stocks. There were slight differences in the thermal protocol (see Publication III). Viability was determined using strain-specific primers and calculated from the ΔCq (based on the quantification cycle (Cq)) between PMAxx-treated and untreated samples. Viable cell percentages were calculated using the following equation:

$$\% \text{ viable} = \frac{100}{2^{\Delta Cq}}$$

3.10 16S rRNA NGS

In Publication I and III, relative abundances of the three-species consortium were determined using 16S rRNA sequencing. For 16S rRNA gene sequencing, the V4 region was amplified using primers F515 and R806, and libraries were prepared using a standard protocol. Sequencing was performed using the Illumina iSeq 100. Read identification and quantification were performed using BION-META software. In Publication I the relative abundances were normalized based on known 16S rRNA gene copy numbers (3 for *A. muciniphila*, 5 for *B. thetaiotaomicron*, and 6 for *F. prausnitzii*; (Stoddard et al., 2015)).

3.11 Construction of metabolic networks and flux balance analysis

In Publication I genome-scale metabolic networks for *A. muciniphila*, *B. thetaiotaomicron*, and *F. prausnitzii* were obtained from public database (Machado et al., 2018) and the curated with MEMOTE (Lieven et al., 2020). Intracellular flux patterns were analysed using flux balance analysis (FBA) and flux variability analysis (FVA), with biomass production (growth rate) set as the objective function.

In Publication II, metabolic networks were built for *A. caccae* and *B. thetaiotaomicron*, consisting of 371 metabolites and 490 reactions for *A. caccae*, and 447 metabolites and 584 reactions for *B. thetaiotaomicron*. These individual models were merged into a consortium-level metabolic network by introducing a shared extracellular metabolite pool and eliminating duplicate exchange reactions. The resulting consortium network included a total of 760 metabolites and 1025 reactions.

FBA model was created in Wolfram Mathematica format using in-house software developed in MATLAB (Orth et al., 2010). All calculations were carried out using Wolfram Mathematica version 8.01. The model was constrained using input flux data, and ATP production was set as the objective function. To find a feasible solution, the input flux error margin was increased stepwise by $\pm 1\%$. To evaluate how well the measured metabolite data reflected the organisms' known metabolism, a carbon mass balance analysis was also conducted. Additionally, flux variability analysis was applied to selected exchange fluxes to explore potential cross-feeding interactions between *A. caccae* and *B. thetaiotaomicron* in co-culture conditions (Mahadevan & Schilling, 2003).

4 Results and Discussion

4.1 Creation of the model consortium

Model consortium was created of 25 human gut microbiome species, many of them are also NGP candidates (Figure 3). The selection was done based on existing literature to ensure both diversity and similarity to the typical Estonian gut microbiome (Adamberg, Jaagura, et al., 2020). Additionally, the availability of the strains' genomes and their safety levels were taken into account. The model consortium includes various bacteria with distinct metabolic roles. Several species – such as *Faecalibacterium prausnitzii* (now *F. duncaniae*), *Agathobacter rectalis*, *Roseburia faecis*, *A. caccae*, *Blautia* spp., and *Butyricimonas faecihominis* – are known producers of butyrate and/or acetate, SCFAs associated with anti-inflammatory effects. *A. muciniphila* is specialized in degrading mucin, while *Bacteroides* species efficiently break down a wide range of dietary polysaccharides. Bile salt hydrolase genes, which contribute to bile acid metabolism, have been identified in genera such as *Bacteroides*, *Bifidobacterium*, *Collinsella*, and *Blautia* (Song et al., 2019). This thesis investigates the metabolic traits of selected consortium members in more detail than others, with particular attention to their roles in cross-feeding and consortium stability.

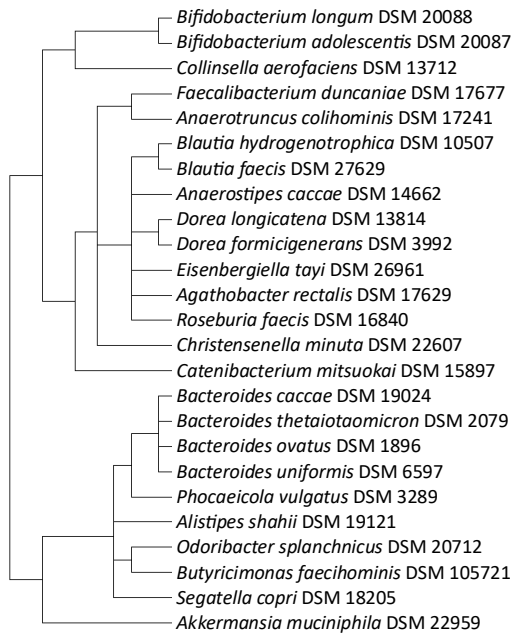


Figure 3. Phylogenetic tree of 25 human gut microbiome species constructed using NCBI taxonomy data. The tree was generated using the R package taxize (version 0.10.0) in RStudio (version 2025.05.0), based on NCBI Taxonomy IDs and visualized using R plotting functions. Tree structure reflects taxonomic relationships as defined by NCBI and is not inferred from sequence data. Four species included in this thesis have undergone taxonomic reclassification: *Faecalibacterium prausnitzii* to *Faecalibacterium duncaniae*, *Eubacterium rectale* to *Agathobacter rectalis*, *Prevotella copri* to *Segatella copri*, and *Bacteroides vulgatus* to *Phocaeicola vulgatus* (Hahnke et al., 2016; Hitch et al., 2022; Rosero et al., 2016; Sakamoto et al., 2022). The phylogenetic tree reflects the updated taxonomy, but the original names are retained throughout the thesis for consistency with publications this thesis is based on.

4.2 Stability and resilience of a defined human gut microbiota consortium assessed with isothermal microcalorimetry (Publication I)

Stability and resilience are important characteristics of consortia as they ensure consistent metabolic activity and species ratio which are essential for achieving desired biotechnological outcomes. Additionally, resilience helps in managing environmental fluctuations, providing a foundation for experimental and industrial applications. To investigate these characteristics, we employed a calorimetric approach, chosen for its wide range of advantages, and implemented serial batch cultivation. This way we can simulate conditions in production processes where multiple seed batches are required to produce inocula for larger volumes. Our consortium of choice consisted of human gut microbiota species, but these methods could be applied to other consortia as well. To simplify the 25 species model consortium and gain deeper insight into interspecies interactions, we chose three species with different metabolic types for the study: *A. muciniphila*, *B. thetaiotaomicron*, and *F. prausnitzii*. These species were characterized in both monoculture and consortium settings.

Using an isothermal microcalorimeter, we determined that the consortium's stability was achieved when the heat flow curves became reproducible over the course of seven passages. A passage was defined by the transfer of 1% (v/v) of the preceding bacterial culture into fresh YCFAM medium, plus the fermentation time (approximately 24h). Principal component analysis based on the collected heat flow data showed that the consortium and individual strains required a different number of passages to reach stability (Figure 4). *A. muciniphila* monoculture needed four passages, while *B. thetaiotaomicron* and *F. prausnitzii* monocultures needed only two passages. The consortium was stable after three passages. Stability was also confirmed by 16S rRNA sequencing, which confirmed the presence of all three species in the consortium. At the end of the seventh passage, *B. thetaiotaomicron*, *A. muciniphila*, and *F. prausnitzii* ratios were 54 ± 1 %, 31 ± 1 %, and 15 ± 0 %, respectively ($n = 3$) (Figure 5B).

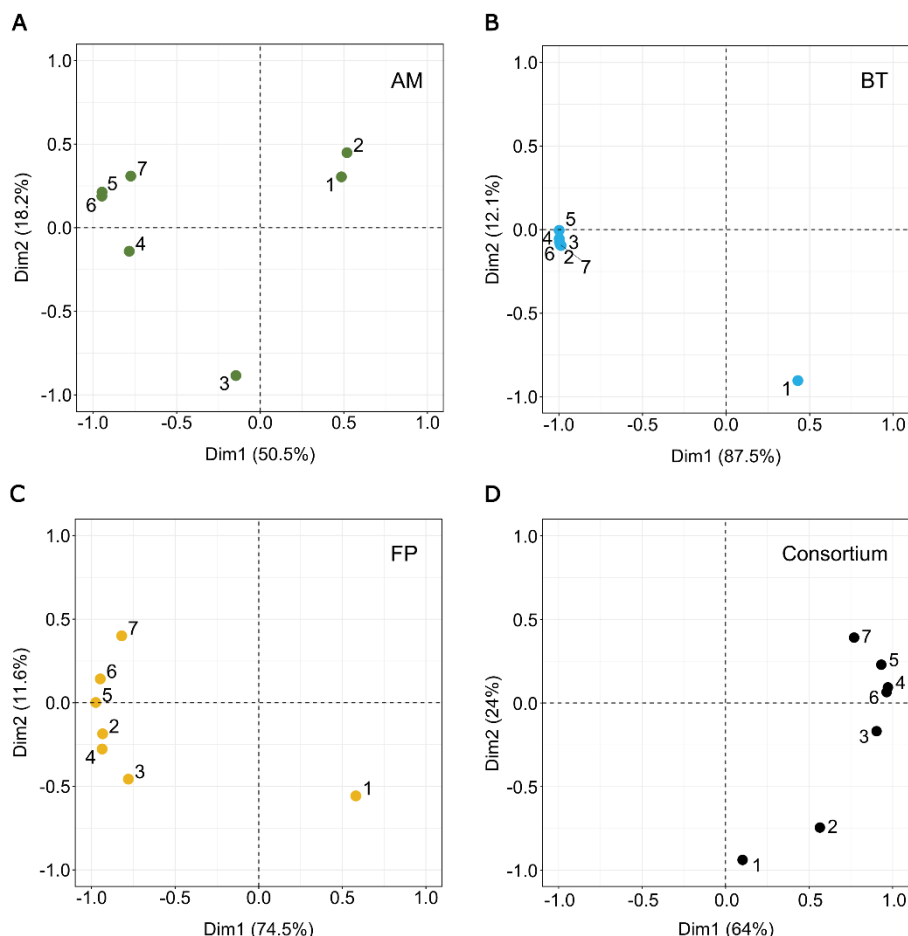


Figure 4. Stability was reached at different passage numbers for the consortium and individual strains. Principal component analysis was performed on heat flow data obtained with isothermal microcalorimetry (IMC) across seven consecutive passages (1 through 7, $n = 3$). Panels a–d represent the following: A. *muciniphila* (green), B. *thetaiotaomicron* (blue), F. *prausnitzii* (yellow), and the consortium (black). Reproduced from: Kattel et al., (2024), *MicrobiologyOpen*, Wiley. Licensed under CC BY 4.0.

To further characterize the strains and their possible influence on each other, their growth rates were determined in monoculture and in the consortium. Hourly samples were taken to determine the relative abundance of each strain in the consortium using 16S rRNA sequencing. The total heat generated by the consortium was used, along with these abundances, to reconstruct the growth curves of each individual strain (Figure 5C). In case of monocultures heat data from the fifth, sixth and seventh passage were used. *A. muciniphila* specific growth rate in the monoculture was $0.57 \pm 0.02 \text{ h}^{-1}$ (Figure S1A,B), which is similar to its growth rate in consortium 0.62 h^{-1} (Figure 5C). Multiple phases were observed in the heat flow curves of *B. thetaiotaomicron* and *F. prausnitzii* monocultures (Figure S1A, C, D). The depletion of the most preferred substrate(s) likely triggered metabolic switches, which in turn slowed the growth rate during each new phase. Both strains had fast first initial growth phases, specific growth rates in

monocultures were $0.88 \pm 0.06 \text{ h}^{-1}$ and $1.00 \pm 0.08 \text{ h}^{-1}$ for *B. thetaiotaomicron* and *F. prausnitzii* respectively. Then entered a slower second ($0.20 \pm 0.01 \text{ h}^{-1}$ and $0.21 \pm 0.01 \text{ h}^{-1}$, respectively) and third phase ($0.07 \pm 0.002 \text{ h}^{-1}$ and $0.09 \pm 0.004 \text{ h}^{-1}$, respectively). The growth rates calculated from the reconstructed growth curves closely match those observed in monocultures (Figure 5C).

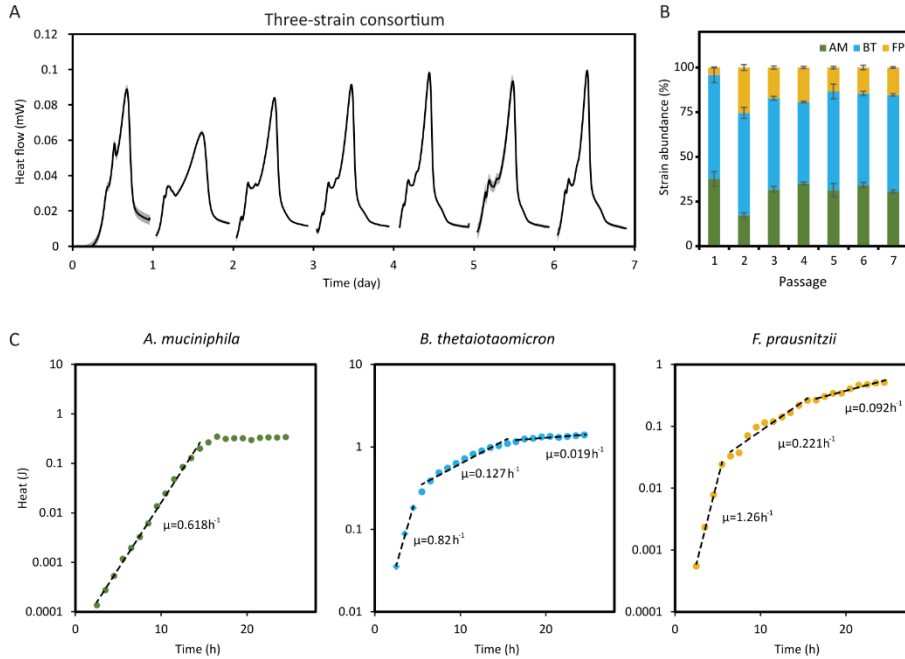


Figure 5. Stability of the consortium composition throughout serial passages. (a) Growth of the consortium was assessed in YCFAM medium across seven consecutive passages using IMC. For each passage, average heat flow and its standard deviation ($n = 3$) are illustrated by full lines and ribbon, respectively. (b) The relative abundance of each strain within the consortium was analyzed at the end of each passage via 16S rRNA gene sequencing. *A. muciniphila*, *B. thetaiotaomicron*, and *F. prausnitzii* are indicated by green, blue, and yellow bars, respectively. (c) Individual growth rates (h^{-1}) were calculated based on the total heat (J) produced by the consortium and the relative abundance of each strain within the consortium. Reproduced from: Kattel et al., (2024), *MicrobiologyOpen*, Wiley. Licensed under CC BY 4.0.

Community's ability to recover from different types of disturbances by growth, physiological, or genetic adaptation is defined as resilience (Allison & Martiny, 2008). The stability of the community can be affected by pH, medium composition, and species initial abundance over serial passages (Goldford et al., 2018; Niehaus et al., 2019). We challenged the stability of the consortium and assessed its resilience by altering the initial species abundances. Three combinations were tested, each with the concentration of one species reduced 100-fold compared to the other two species in the inoculum. At the end of all passages, species ratio was quantified using 16S rRNA sequencing. If the composition of the consortia and growth kinetics were to match the reference consortium (equal inoculation rate, Figure 5), the disturbance would be considered overcome. If this were not achieved, the consortium would not be resilient.

Firstly, the growth kinetics were assessed. Two consortia, where *A. muciniphila* and *B. thetaiotaomicron* were inoculated at a lower concentration respectively, had notably different growth kinetics than the reference consortium (Figure 6A). The consortium with a low *A. muciniphila* inoculation rate overcame the disturbance after four passages. In the case of consortia with low *B. thetaiotaomicron* and *F. prausnitzii*, two passages were sufficient to recover from the disturbance. Consistent with the heat flow data, 16S rRNA sequencing also confirmed that all three consortia were able to overcome the disturbances and return to stable composition by the end of the fifth passage (Figure 6B). The obtained consortia compositions after each passage are presented in Table S1. This indicates that there is no strong competition for growth-dependent substrate(s), and species are not heavily dependent on each other, although cross-feeding possibilities exist.

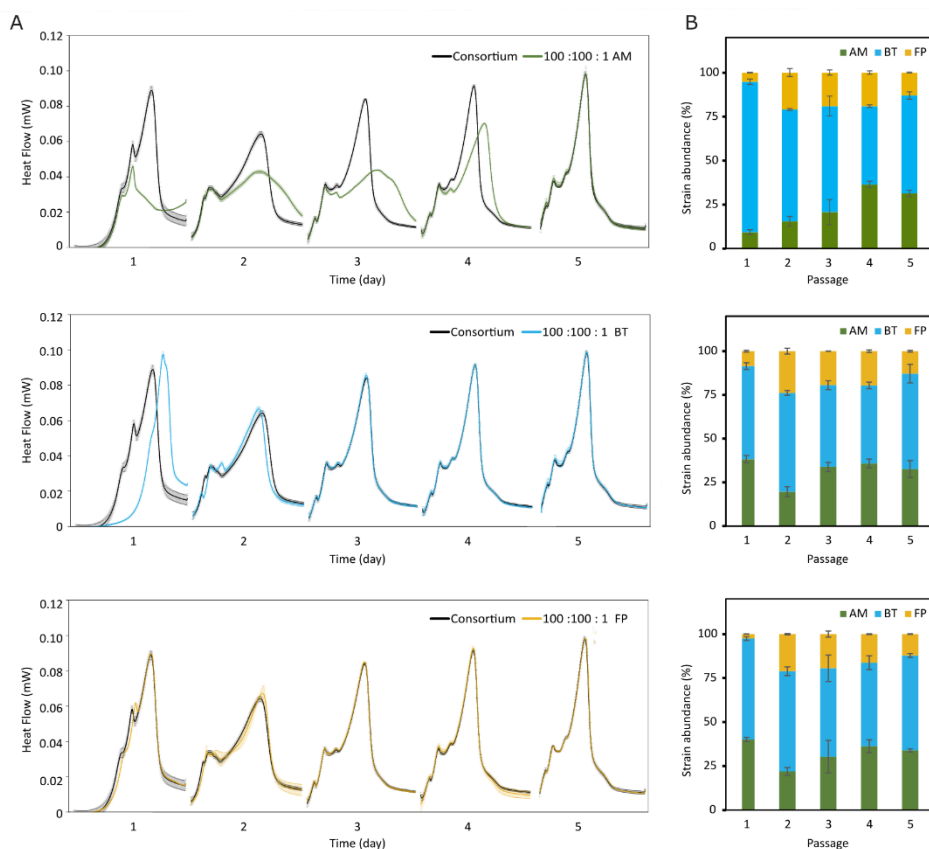


Figure 6. Resilience of the consortium. (a) To assess the resilience of the consortium, three experimental setups were designed where either *A. muciniphila* (AM), *B. thetaiotaomicron* (BT), or *F. prausnitzii* (FP) was initially inoculated at a 100-fold lower concentration than the other two strains (from top to bottom, respectively). Average heat flow and its standard deviation ($n = 3$) are shown as solid line and ribbon respectively. Resilience was considered achieved once the heat flow profile matched that of the original consortium (Figure 5). (b) The relative abundance of *A. muciniphila* (green), *B. thetaiotaomicron* (blue), and *F. prausnitzii* (yellow) was determined with 16S rRNA gene sequencing at the end of each passage ($n = 3$). Reproduced from: Kattel et al., (2024), *MicrobiologyOpen*, Wiley. Licensed under CC BY 4.0.

To further investigate the interactions in the consortium, we looked into the main metabolites (Figure 7). SCFA were quantified at the end of the fifth, sixth, and seventh passages in the consortium (equal inoculation rate) as well as the monoculture samples. Results from the three monoculture samples were summarized to allow for a better comparison with the consortium. The consortium had a significantly higher concentration of acetate, butyrate, and succinate compared to the sum of monocultures. Propionate concentration was significantly lower in the consortium than in the sum of monocultures. These results indicate that species are not completely independent of one another. As butyrate is only produced by *F. prausnitzii*, the higher concentration indicates beneficial cross-feeding with acetate producers. Despite the presence of acetate consumption, its concentration remains higher in the consortium compared to the sum of monocultures, likely due to overall increased production, suggesting complex metabolic interplay.

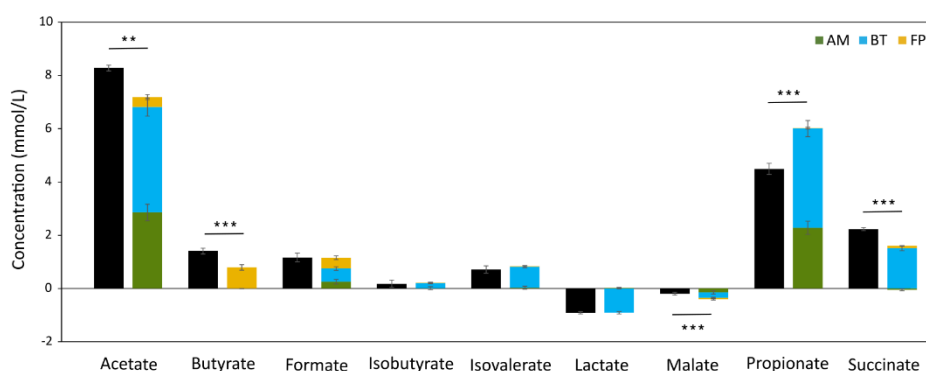


Figure 7. Production of external metabolites in monocultures and the consortium. Concentrations of organic acids (mmol/L) were measured following the fifth, sixth, and seventh passages. Green, blue, and yellow bars indicate the monocultures of *A. muciniphila* (AM), *B. thetaiotaomicron* (BT), and *F. prausnitzii* (FP), respectively, while black bars depict the consortium. To represent the expected outcome without interspecies interactions, metabolite concentrations from individual strains were stacked up. Statistical significance between consortium and the mathematical sum of monocultures was calculated with a Student's t-test (* $p < 0.05$, ** $p < 0.01$, *** $p < 0.001$). Reproduced from: Kattel et al., (2024), *MicrobiologyOpen*, Wiley. Licensed under CC BY 4.0.

Flux balance analysis (FBA) was also performed using the available data; however, many of the predictions were not confirmed by in vitro data, especially the quantification of amino acids. While FBA provides valuable hypotheses, it is limited by data quality and model-specific constraints such as steady-state growth and objective functions. In our case, the use of a complex undefined medium and the inability to quantify carbon source consumption further constrained the accuracy of FBA predictions. Our results indicate that further refinement, particularly the use of chemically defined media and dynamic sampling, will be essential to align predictions with empirical data. Nonetheless, we concluded that each strain likely had a different growth-limiting substrate, supporting the idea that each species in the consortia is limited by a different primary growth substrate.

4.3 Evaluating diversity of 25-species model consortium (Unpublished data)

As our three-species consortium was stable, we proceeded to test a more diverse model consortium. We cultivated 25 species in complex YCM medium over three passages, again using an isothermal microcalorimeter. All species except *Prevotella copri* were present after day 3, and the Shannon diversity index was 2.26. The Shannon diversity index, often referred to as the Shannon-Wiener index, quantifies community diversity by incorporating both the number of species and relative abundance of those species (Shannon, 1948). It should be noted that 16S rRNA gene sequencing could not differentiate between *Bifidobacterium adolescentis* and *Bifidobacterium longum*, as well as *Roseburia faecis* and *Eubacterium rectale*, so these species were grouped together in the analysis.

Odoribacter splanchnicus had the highest relative abundance (30.4%), while *Bacteroides* spp. accounted for a combined 44.8%. Butyrate producers, excluding *Odoribacter splanchnicus*, made up 5.4% of the consortium. Considering that the consortium consisted of strict anaerobes and often difficult-to-cultivate species, the observed diversity was relatively high, with 14 species exceeding 1% abundance.

At this stage, we lacked effective tools to selectively increase or decrease the abundance of individual species and thereby modulate overall consortium diversity. One potential strategy was to supplement the medium with additional substrates. However, without a clear understanding of how these changes would impact consortium dynamics, such modifications could lead to unpredictable and undesirable outcomes. This challenge motivated the development of a unique substrate-based approach for consortia production.

4.4 Analysis of metabolism in co-cultures of *Anaerostipes caccae* and *Bacteroides* spp. (Publication II)

Many NGP candidate species are cultivated in rich complex media due to limited knowledge of their metabolism. To enable detailed metabolic studies, we switched from complex rich media to a chemically defined medium (CDM). This approach allows precise quantification of substrates and yields more accurate data for FBA. Although we anticipated that some species might not be culturable in CDM, the resulting loss in diversity was acceptable, as the aim was not to replicate gut complexity but to develop a controlled production workflow.

4.4.1 Screening and genome annotation analysis of candidate species

We assessed the growth of 25 species in CDM, where glucose was the primary carbon source, using a microtiter plate reader. Out of the 25 species, growth was observed for 12 species (Table 1). Species with extremely slow growth rates, long lag-phases, or no detectable growth were excluded from subsequent experiments. Following the initial screening, eight species were selected for further analysis: *Anaerostipes caccae* (*A. caccae*), *Bifidobacterium longum*, *Bifidobacterium adolescentis*, *B. thetaiotaomicron*, *B. vulgatus*, *Bacteroides ovatus*, *Bacteroides caccae*, and *Bacteroides uniformis*.

Table 1. Overview of the average measured and calculated growth parameters in a glucose-containing defined medium. The following species did not exhibit measurable growth and were therefore excluded from the table: *Christensenella minuta*, *Alistipes shahii*, *Anaerotruncus colihominis*, *Blautia faecis*, *Blautia hydrogenotrophica*, *Butyrivimonas faecihominis*, *Prevotella copri*, *Eubacterium rectale*, *Akkermansia muciniphila*, *Faecalibacterium prausnitzii*, *Roseburia faecis*, *Eisenbergiella tayi*, and *Odoribacter splanchnicus*. Reported errors represent the standard error of four biological replicates. * – Growth parameters for *Catenibacterium mitsuokai* are unavailable due to cell clumping during cultivation, which resulted in unreliable OD measurements. Adapted from: Kattel et al., (2023), *Anaerobe*, Elsevier. Used under author rights.

Organism	Maximum OD at 600 nm	Lag phase, h	Specific growth rate, h ⁻¹
<i>Anaerostipes caccae</i>	0.59 ± 0.03	10.4 ± 0.1	0.59 ± 0.01
<i>Bacteroides vulgatus</i>	0.61 ± 0.01	3.6 ± 0.3	0.27 ± 0.01
<i>Bacteroides caccae</i>	0.82 ± 0.00	2.0 ± 0.1	0.37 ± 0.01
<i>Bacteroides ovatus</i>	0.66 ± 0.01	2.6 ± 0.2	0.34 ± 0.01
<i>Bacteroides thetaiotaomicron</i>	0.70 ± 0.00	2.9 ± 0.1	0.45 ± 0.00
<i>Bacteroides uniformis</i>	0.71 ± 0.01	2.4 ± 0.1	0.34 ± 0.01
<i>Bifidobacterium longum</i> subsp. <i>infantis</i>	0.35 ± 0.01	6.3 ± 0.1	0.31 ± 0.01
<i>Bifidobacterium adolescentis</i>	0.41 ± 0.01	5.3 ± 0.0	0.24 ± 0.01
<i>Collinsella aerofaciens</i>	0.32 ± 0.02	5.7 ± 0.2	0.09 ± 0.00
<i>Dorea formicigenerans</i>	0.11 ± 0.00	21.2 ± 0.6	0.05 ± 0.00
<i>Dorea longicatena</i>	1.40 ± 0.08	15.7 ± 0.5	0.39 ± 0.02
<i>Catenibacterium mitsuokai</i>		NA*	

Next, we looked into the metabolic pathways to determine the substrate utilization capabilities of these species (Table S2), focusing on monosaccharides and their derivatives such as sugar alcohols and acids. These substrates were selected due to the availability of reliable analytical methods for their quantification, which is crucial for high-quality metabolic modelling and assessing cross-feeding interactions.

The pathway analysis revealed that *Bifidobacterium longum* and *Bifidobacterium adolescentis* lacked unique degradation pathways that were not also present in *A. caccae* and the *Bacteroides* species. Therefore, *Bifidobacteria* were excluded from further experiments. In summary, among the remaining six species, pathway analysis revealed 13 different degradation pathways across 12 selected carbohydrates. Glucose was replaced with these substrates (at equimolar concentrations) in CDM, and growth profiles were recorded (Table 2). Due to the limited number of unique substrates identified among the six species, we were restricted to conducting pairwise co-culture experiments. Substrate was considered to be unique if it was exclusively consumed by single species in the co-culture.

Table 2. Validation of in silico metabolic predictions. Shown are the average growth rates (μ , h^{-1}) for six different species grown on selected substrates. Growth rates were calculated based on heat production data, with standard errors calculated from two biological replicates. AC – *A. caccae*, BC – *B. caccae*, BO – *B. ovatus*, BT – *B. thetaiotaomicron*, BU – *B. uniformis*, BV – *B. vulgatus*, ND – growth not detected. Adapted from: Kattel et al., (2023), *Anaerobe*, Elsevier. Used under author rights.

Substrate	AC	BC	BO	BT	BU	BV
D-Fructose	0.35 \pm 0.01	0.51 \pm 0.03	0.33 \pm 0.06	0.48 \pm 0.03	0.55 \pm 0.08	0.57 \pm 0.01
D-Galactose	0.50 \pm 0.00	0.56 \pm 0.02	0.43 \pm 0.05	0.66 \pm 0.00	0.55 \pm 0.00	0.32 \pm 0.01
D-Xylose	ND	0.61 \pm 0.00	0.44 \pm 0.02	0.56 \pm 0.05	0.54 \pm 0.01	0.42 \pm 0.01
L-Arabinose	ND	0.53 \pm 0.00	0.50 \pm 0.00	0.58 \pm 0.01	0.51 \pm 0.02	0.56 \pm 0.02
D-Galacturonic acid	ND	0.31 \pm 0.02	0.19 \pm 0.02	0.27 \pm 0.01	0.22 \pm 0.02	0.21 \pm 0.02
L-Rhamnose	ND	0.14 \pm 0.00	0.15 \pm 0.00	0.15 \pm 0.01	ND	0.30 \pm 0.01
L-Fucose	ND	0.29 \pm 0.01	0.12 \pm 0.00	0.22 \pm 0.01	ND	ND
D-Mannitol	0.08 \pm 0.00	ND	0.34 \pm 0.01	ND	ND	ND
D-Sorbitol	0.17 \pm 0.00	ND	ND	ND	ND	ND
Dulcitol	0.05 \pm 0.00	ND	ND	ND	ND	ND
Xylitol	ND	ND	ND	ND	ND	ND
D-Lyxose	ND	ND	ND	ND	ND	ND

4.4.2 Establishing and validating co-cultures based on substrate specificity

Based on the growth data (Table 2) we identified multiple unique substrate-based co-culture pairs and tested *A. caccae* (D-sorbitol; specific growth rate 0.17 h^{-1}) with *B. thetaiotaomicron* (D-xylose; 0.56 h^{-1}) and *B. vulgatus* (D-galacturonic acid; 0.21 h^{-1}). These combinations allowed us to pair the butyrate-producer *A. caccae* with succinate/propionate producers – *B. thetaiotaomicron* and *B. vulgatus*. Firstly, we needed to confirm that in multi-substrate conditions, species selectively utilized their designated unique carbon source and that there would be no consumption of the other one.

Growth medium containing a unique carbon source along with a non-utilizable carbon source for each species was prepared and used in a serial batch format. Growth kinetics of monocultures remained consistent across three consecutive batches. In D-xylose + D-sorbitol medium, total heat production by *B. thetaiotaomicron* was 0.68 \pm 0.02 J mL $^{-1}$ (day 3)(Figure 8A), and in D-galacturonic acid + D-sorbitol medium, *B. vulgatus* produced 0.44 \pm 0.04 J mL $^{-1}$ of heat on day 3 (Figure 8B). The heat produced by *A. caccae* remained unchanged whether D-sorbitol medium was supplemented with D-xylose (0.35 \pm 0.02 J mL $^{-1}$) or D-galacturonic acid (0.33 \pm 0.02 J mL $^{-1}$). No significant difference was observed ($p = 0.48$). Quantification of the sugars at the end of the experiments confirmed the depletion of the main carbon sources: D-sorbitol by *A. caccae*, D-xylose by *B. thetaiotaomicron*, and D-galacturonic acid by *B. vulgatus*.

We then studied co-cultures of *A. caccae* with *B. thetaiotaomicron* or *B. vulgatus* in the same dual-substrate media. Our hypothesis was that, in the absence of interactions, total heat production would equal or be similar to the sum of monocultures. However, measured heat was 1.1 to 1.5 times higher in both co-cultures across all three batches (Figure 8), suggesting positive metabolic interactions.

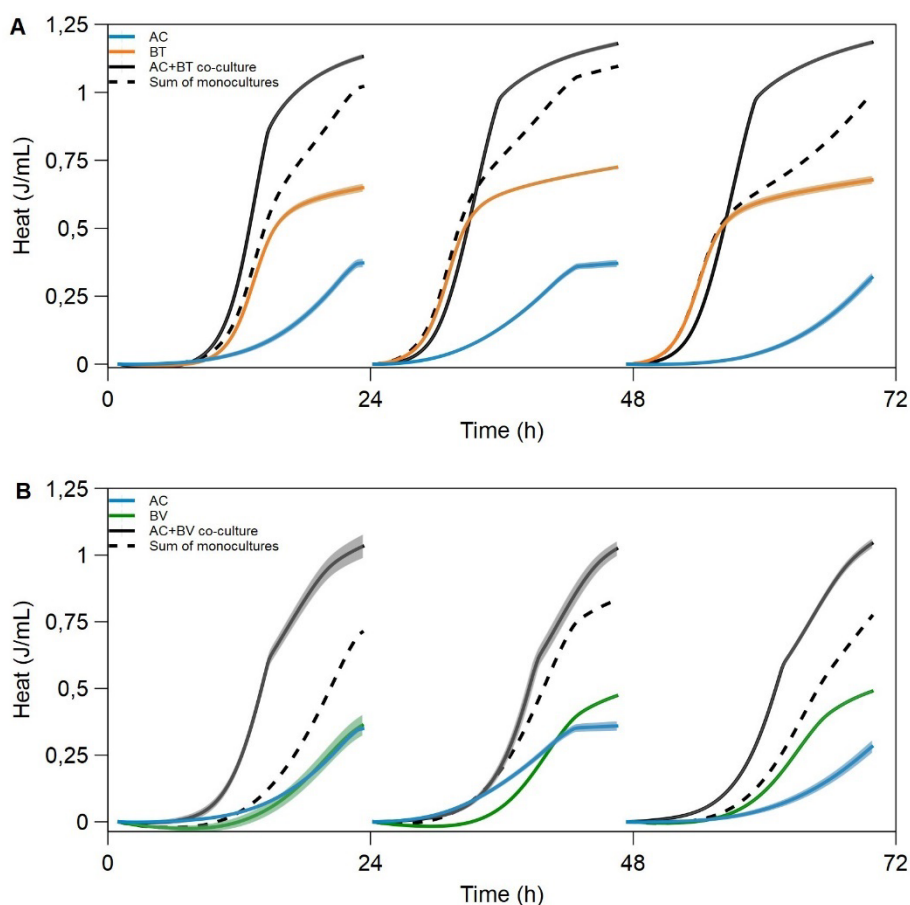


Figure 8. Monitoring of monoculture and co-culture growth kinetics using IMC. (A) Heat flow profiles for *A. caccae* (AC), *B. thetaiotaomicron* (BT), and their co-culture (AC + BT) cultivated in D-sorbitol and D-xylose medium. (B) Heat flow for AC, *B. vulgatus* (BV), and their co-culture (AC + BV) cultivated in D-sorbitol and D-galacturonic acid medium. Full line and ribbon represent the average and standard deviation of the heat, respectively ($n=3$), for each batch. The dashed line indicates the mathematical sum of the two monoculture heat profiles. Reproduced from: Kattel et al., (2023), *Anaerobe*, Elsevier. Used under author rights.

4.4.3 Co-culture metabolic interactions

Figure 8 illustrates that co-cultures generated consistently throughout three batches more heat than the sum of individual monocultures, indicating metabolic interactions. We compared final organic acid concentrations in co-cultures to the sum of monocultures (Table 3, Table 4). Significant differences were observed for acetate, butyrate, and lactate.

In the *A. caccae* + *B. thetaiotaomicron* co-culture on day 3, acetate levels were 2-fold lower and lactate 50-fold lower when compared to the sum of monoculture results (Table 3). In the co-culture, butyrate and propionate concentrations were 3.1-fold and 1.3-fold higher, respectively. Acetate and propionate were produced exclusively by *B. thetaiotaomicron*, whereas lactate and butyrate were produced solely by *A. caccae*.

Therefore, these results indicate mutual metabolic benefits likely via cross-feeding of acetate for butyrate synthesis (Chia et al., 2018; Duncan et al., 2004; Falony et al., 2006).

A. caccae + *B. vulgatus* co-culture had similar changes regarding the metabolite concentrations (Table 4). When comparing the day 3 results, acetate and lactate levels in the co-culture were 1.4-fold and 6-fold lower, respectively, than the combined values from the *A. caccae* and *B. vulgatus* monocultures. In contrast, concentrations of butyrate and propionate were higher 2.9-fold and 2-fold, respectively in the co-culture.

To assess the potential growth-promoting effects of acetate on *A. caccae* and lactate on *B. thetaiotaomicron*, supplementation experiments were conducted in the IMC. A range of acetate and lactate concentrations (0 to 20 mM) was tested. When grown on D-sorbitol without acetate, *A. caccae* exhibited a specific growth rate of $0.24 \pm 0.00 \text{ h}^{-1}$. The addition of 2 mM acetate significantly increased specific growth rate up to $0.74 \pm 0.00 \text{ h}^{-1}$ ($p < 0.001$). Increasing acetate concentrations further (4 to 20 mM) produced an additional though smaller effect, with maximal specific growth rates ranging from 0.85 to 1.05 h^{-1} ($p < 0.001$).

Regardless of the acetate concentration, all D-sorbitol ($5.5 \pm 0.1 \text{ mM}$) was consumed by *A. caccae* (Table S3). When 6 mM of acetate or more was in the medium, approximately $4.2 \pm 0.2 \text{ mM}$ of acetate was taken up. At lower acetate concentrations (2 mM and 4 mM), acetate was depleted. This corresponds to a molar consumption ratio of acetate to D-sorbitol of roughly 0.8:1. The conversion of acetate to butyrate requires one NADH molecule per reaction via a non-bifurcative pathway (KEGG, Kanehisa & Goto, 2000), whereas converting D-sorbitol to butyrate yields one NADH per molecule of D-sorbitol. Theoretically, the expected molar ratio of acetate to D-sorbitol should be 1:1. The observed deviation from this ratio likely comes from the consumption of free amino acids and the potential utilization of bifurcative butyrate synthesis pathways, both of which reduce intracellular NADH levels (F. Li et al., 2008). Additionally, as the acetate concentration in the medium was increased, lactate production decreased (Table S3). When added acetate concentrations were 6 mM or higher, steep decrease in lactate production was observed, implying that limited NADH availability may limit acetate uptake.

The effect of lactate supplementation on the growth of *B. thetaiotaomicron* was evaluated across a same range of concentrations: 2 mM, 4 mM, 6 mM, 8 mM, 10 mM, and 20 mM. Despite varying lactate levels, the effect on specific growth rate remained relatively consistent. Without lactate, *B. thetaiotaomicron* exhibited a specific growth rate of $0.38 \pm 0.00 \text{ h}^{-1}$, which increased to 0.53 – 0.56 h^{-1} upon lactate addition ($p < 0.01$). The maximum observed lactate consumption was $3.2 \pm 0.0 \text{ mM}$, while $4.7 \pm 0.0 \text{ mM}$ of D-xylose was metabolized, resulting in a lactate to D-xylose molar consumption ratio of 0.7:1 (Table S4). Under anaerobic conditions, converting lactate to pyruvate is not energetically favourable and requires a bifurcative pathway involving reduced ferredoxin with a low redox potential as a co-substrate (Weghoff et al., 2015). This conversion yields two NADH molecules. Given that pyruvate ferredoxin oxidoreductase is the primary source of reduced ferredoxin in succino- and propionigenic bacteria, lactate consumption is likely constrained by the availability of reduced ferredoxin (Blaschkowski et al., 1982). The NADH generated from concentration dependent lactate uptake is subsequently channeled into the production of succinate and propionate. As lactate concentrations in the medium increase, the molar ratio of these acids to consumed D-xylose also rises from 0.4:1 to 0.7:1. These findings strongly suggest that the extent of cross-feeding between the species is limited by intracellular availability of NADH and/or reduced ferredoxin.

Table 3. Production of major metabolites on day 3 in the co-culture (*A. caccae* + *B. thetaiotaomicron*) and in the respective monocultures (*A. caccae*, *B. thetaiotaomicron*). Average values (mM) \pm standard errors (n = 3) are presented. Statistical significance between the co-culture and the combined monocultures was determined using Student's t-test (*p < 0.05, **p < 0.01, *p < 0.001). ND – not detected. Adapted from: Kattel et al., (2023), Anaerobe, Elsevier. Used under author rights.**

	acetate	butyrate	formate	lactate	propionate	succinate
<i>A. caccae</i>	ND	1.32 \pm 0.02	0.73 \pm 0.03	4.68 \pm 0.06	ND	ND
<i>B. thetaiotaomicron</i>	2.53 \pm 0.01	ND	0.60 \pm 0.01	ND	1.53 \pm 0.01	1.95 \pm 0.01
<i>A. caccae</i> + <i>B. thetaiotaomicron</i> co-culture	1.38 \pm 0.01***	4.49 \pm 0.01***	0.41 \pm 0.00***	0.10 \pm 0.00***	2.00 \pm 0.01***	1.73 \pm 0.00***
Sum of <i>A. caccae</i> and <i>B. thetaiotaomicron</i>	2.53 \pm 0.01	1.32 \pm 0.02	1.33 \pm 0.04	4.68 \pm 0.06	1.53 \pm 0.01	1.95 \pm 0.01

Table 4. Production of major metabolites on day 3 in the co-culture (*A. caccae* + *B. vulgatus*) and in the respective monocultures (*A. caccae*, *B. vulgatus*). Average values (mM) \pm standard errors (n = 3) are presented. Statistical significance between the co-culture and the combined monocultures was determined using Student's t-test (*p < 0.05, **p < 0.01, *p < 0.001). ND – not detected. Adapted from: Kattel et al., (2023), Anaerobe, Elsevier. Used under author rights.**

	acetate	butyrate	formate	lactate	propionate	succinate
<i>A. caccae</i>	ND	1.19 \pm 0.01	0.7 \pm 0.03	4.28 \pm 0.15	ND	ND
<i>B. vulgatus</i>	4.29 \pm 0.01	ND	0.24 \pm 0.00	ND	0.57 \pm 0.00	0.99 \pm 0.00
<i>A. caccae</i> + <i>B. vulgatus</i> co-culture	3.12 \pm 0.02***	3.73 \pm 0.03***	0.61 \pm 0.01**	1.03 \pm 0.06***	1.04 \pm 0.01***	1.11 \pm 0.01**
Sum of <i>A. caccae</i> and <i>B. vulgatus</i>	4.29 \pm 0.01	1.19 \pm 0.01	0.94 \pm 0.03	4.28 \pm 0.15	0.57 \pm 0.00	0.99 \pm 0.00

4.4.4 Species ratio determination

Accurately determining species ratios is critical for understanding co-culture dynamics, as the ratio of the species can determine the overall functionality of the co-culture. While 16S sequencing and qPCR are commonly used in research, extracting DNA from different species presents challenges, and it is important to evaluate and optimize protocols specifically for the species of interest (Clark et al., 2021; Oba et al., 2020). We tested DNA extraction and qPCR protocol using artificial mixes of *A. caccae*, *B. thetaiotaomicron*, and *B. vulgatus*. In an equal mix (ratio based on OD measurements), *B. thetaiotaomicron* and *B. vulgatus* were overestimated (47% \pm 2% and 41% \pm 1%), and *A. caccae* was underestimated (12% \pm 1%)(Table S5). A second test mix, where the expected OD-based ratio was 80% *A. caccae*, 10% *B. thetaiotaomicron*, and 10% *B. vulgatus*, yielded 52% *A. caccae*, 27% *B. thetaiotaomicron*, and 21% *B. vulgatus*. In these test experiments, we used the GenElute™ Bacterial Genomic DNA Kit (Merck, Germany) for DNA extraction. We also evaluated an alternative kit, the ZymoBIOMICS™ DNA Miniprep Kit, (Zymo Research, Irvine, CA, USA); however, this did not improve the extraction yield for *A. caccae* (data not shown). Alternative primers were also designed for all three strains; however, consistent with previous results, *A. caccae* was still underestimated (data not shown).

A potential reason for this bias is the difference in cell wall structures: *A. caccae* is gram-variable, while the *Bacteroides* spp. are gram-negative (Schwiertz et al., 2002; Weiss & Rettger, 1937). These differences likely affect DNA extraction efficiency. Therefore, DNA-based methods may not reliably quantify species ratios but can be used to determine stability in co-cultivation experiments.

The qPCR analysis confirmed that the strain ratios remained consistent throughout the serial batch experiment (Table S6). However, we needed a method that could measure the species ratio as the goal was to also change the ratio later and only using metabolome data would not have been sufficient. To determine cell ratios more accurately, we developed a microscopy-based image analysis method leveraging the distinct morphologies of *A. caccae* and *Bacteroides* spp. At the end of the serial batch experiment (day 3), microscopy image analysis showed average species ratios of 49:51 ($\pm 3\%$) for *A. caccae*:*B. thetaiotaomicron* and 37:63 ($\pm 1\%$) for *A. caccae*:*B. vulgatus*, indicating that both species were present in approximately equal cell concentrations in both co-cultures.

4.4.5 Development of co-culture bioprocess

IMC is a good method for screening experiments but for more technical control and additional analysis we developed high density processes in Applikon bioreactors. Now we had an opportunity to perform through growth gas analysis and elevate both carbon source and amino acid concentrations three to five times for higher biomass densities. Final OD values for monocultures were consistent: 2.3 ± 0.0 for *A. caccae*, 2.1 ± 0.1 for *B. thetaiotaomicron*, and 1.6 ± 0.1 for *B. vulgatus*. Co-cultures showed nearly doubled biomass: 4.1 ± 0.2 for *A. caccae* + *B. thetaiotaomicron* and 3.5 ± 0.1 for *A. caccae* + *B. vulgatus*.

The *A. caccae* + *B. vulgatus* co-culture had a similar specific growth rate ($0.52 \pm 0.02 \text{ h}^{-1}$) with *A. caccae* + *B. thetaiotaomicron* co-culture ($0.48 \pm 0.05 \text{ h}^{-1}$). As in IMC experiments, co-cultures showed higher butyrate and propionate levels, and lower acetate and lactate levels, than monocultures (Table 5). Since qPCR could not be used to determine the species ratio, microscopy images were taken from samples at the end of fermentation. Based on cell size, *Bacteroides* spp. and *A. caccae* were differentiated. Microscopy confirmed species ratios: 43:57 (*A. caccae*:*B. thetaiotaomicron*) and 49:51 (*A. caccae*:*B. vulgatus*), demonstrating maintained control upon scale-up.

Table 5. Production of major metabolites was determined in monocultures of *A. caccae*, *B. thetaiotaomicron*, and *B. vulgatus*, as well as in their respective two-species co-cultures in bioreactor experiments. Average concentrations (mM) \pm standard errors ($n \geq 2$) are shown. A Student's *t*-test was used to assess statistical significance between co-culture values and the sum of monoculture values (* $p < 0.05$, ** $p < 0.01$, * $p < 0.001$). ND – not detected. Adapted from: Kattel et al., (2023), *Anaerobe*, Elsevier. Used under author rights.**

	acetate	butyrate	formate	lactate	propionate	succinate
<i>A. caccae</i>	ND	4.31 \pm 0.03	0.45 \pm 0.01	13.40 \pm 0.29	ND	ND
<i>B. thetaiotaomicron</i>	9.24 \pm 0.10	ND	3.71 \pm 0.15	0.35 \pm 0.18	1.22 \pm 0.05	6.96 \pm 0.04
<i>B. vulgatus</i>	16.68 \pm 0.68	ND	2.74 \pm 0.04	0.05 \pm 0.05	0.62 \pm 0.01	2.78 \pm 0.22
<i>A. caccae</i> + <i>B. thetaiotaomicron</i> co-culture	3.11 \pm 0.34**	9.51 \pm 0.51**	2.52 \pm 0.11**	8.58 \pm 0.69**	1.85 \pm 0.21	5.48 \pm 0.62
<i>A. caccae</i> + <i>B. vulgatus</i> co-culture	6.11 \pm 1.02***	14.06 \pm 0.50***	4.82 \pm 1.17	3.80 \pm 0.59***	1.10 \pm 0.09***	2.03 \pm 0.23
Sum of <i>A. caccae</i> and <i>B. thetaiotaomicron</i>	9.24 \pm 0.10	4.31 \pm 0.03	4.17 \pm 0.15	13.76 \pm 0.34	1.22 \pm 0.05	6.96 \pm 0.04
Sum of <i>A. caccae</i> and <i>B. vulgatus</i>	16.68 \pm 0.68	4.31 \pm 0.03	3.20 \pm 0.04	13.45 \pm 0.30	0.62 \pm 0.01	2.78 \pm 0.22

4.4.6 Altering substrate ratios and characterizing metabolic interactions with FBA

One key aspect of the workflow was the ability to control species ratios. This is essential when product efficacy depends on specific ratio. Initially, we used a 50:50 (percentage wise) substrate ratio (D-sorbitol:D-xylose), expecting corresponding species ratios. To demonstrate substrate-based control, we altered the ratio to 80:20 and 20:80 while keeping the ratio in the inoculum same as before: 50:50 (*A. caccae*:*B. thetaiotaomicron*).

For the 80:20 substrate ratio we increased the target concentration of D-sorbitol (*A. caccae* substrate) to 66.8 mM and maintained the target concentration of D-xylose (substrate for *B. thetaiotaomicron*) at 16.7 mM. These concentrations were based on values set during experimental design and the actual concentrations measured by HPLC showed some deviation, as expected. Under these conditions, we observed a longer lag phase, likely due to insufficient acetate production by *B. thetaiotaomicron*. Acetate remained undetectable until 12.4 h and previously observed high growth rate was not reached. We monitored hydrogen production throughout the growth as an indicator of *A. caccae*'s metabolic activity. Microscopy at the end showed an 82:18 ratio (*A. caccae*:*B. thetaiotaomicron*).

Subsequently, we reversed the substrate concentrations, increasing the target concentration of D-xylose (substrate for *B. thetaiotaomicron*) to 66.8 mM while maintaining the D-sorbitol (substrate for *A. caccae*) target concentration at 16.7 mM. This also resulted in a significantly longer lag-phase compared to the 50:50 substrate ratio. Hydrogen production ceased at 17.8 h, indicating the depletion of D-sorbitol and the onset of the asaccharolytic phase for *A. caccae*. At the end of fermentation, based on microscopy images, the cell ratio was 29:71 (*A. caccae*:*B. thetaiotaomicron*).

For metabolic modelling, the organisms' growth was separated into two main phases: saccharolytic and asaccharolytic. Model calculations indicated that the computationally

estimated metabolomes differed from experimental observations by 2–5%, leading to a surplus in carbon balance ranging from 1–4%. Flux variability analysis showed obligatory cross-feeding under several experimental scenarios (Figure 9). Based on exometabolome data, acetate was conclusively cross-fed by *A. caccae* in the saccharolytic phase of the 80:20 (D-sorbitol:D-xylose) setup, while *B. thetaiotaomicron* exhibited lactate cross-feeding during the asaccharolytic phase. Additionally, in the 20:80 (D-sorbitol:D-xylose) setup, *A. caccae* also displayed lactate cross-feeding in the asaccharolytic phase, therefore confirming metabolic interactions between the two species in the co-culture.

One of the earlier studies also looked into interactions between *A. caccae* and *B. thetaiotaomicron*, reporting metabolite changes such as lactate depletion and reductions in acetate and malate levels in co-cultures compared to monocultures (Chia et al., 2020). In agreement with these observations, we detected declines in short-chain fatty acids, specifically acetate and lactate, both substrates utilized by *A. caccae* (Duncan et al., 2004; Schwieritz et al., 2002). Although acetate utilization by *B. thetaiotaomicron* has been documented, lactate metabolism had not previously been demonstrated. Conversely, study with a different *B. thetaiotaomicron* strain (LMG 11262) indicated an inability to metabolize lactate (Falony et al., 2009). Additionally, we measured a significant increase in butyrate and propionate concentrations in our cultivation experiments, indicating mutual benefits from co-cultivation, with butyrate produced only by *A. caccae* and propionate only by *B. thetaiotaomicron*.

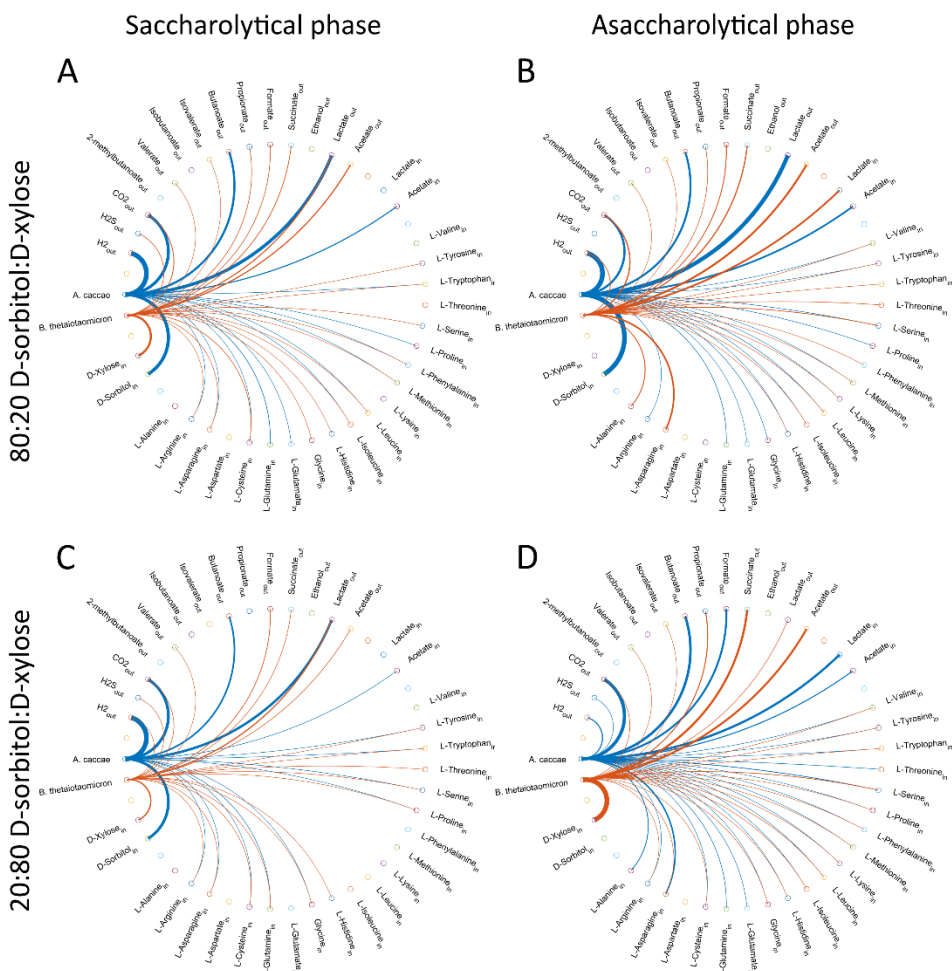


Figure 9. Metabolic cross-feeding between *A. caccae* and *B. thetaiotaomicron* in co-culture. After depletion of the primary carbon sources, both species continued growth, therefore growth was divided into saccharolytic and asaccharolytic phases. Varying the initial carbon source concentrations resulted in different metabolic scenarios. Metabolic flux distributions are shown for the 80:20 (D-sorbitol:D-xylose) setup, where both species are saccharolytic (A), and where BT transitions to the asaccharolytic phase (B). In this phase, BT consumes lactate produced by AC, while AC predominantly utilizes D-sorbitol and acetate. In the 20:80 (D-sorbitol:D-xylose) setup, panel C illustrates a scenario where both species remain in saccharolytic phase, while panel D depicts a condition in which AC is in asaccharolytic phase. In the asaccharolytic phase, AC consumes lactate and acetate, while BT mainly utilizes D-xylose. Orange and blue lines represent metabolic fluxes from AC and BT, respectively, with line thickness correlating with the corresponding flux value. Compounds labelled as “in” are consumed, and those labelled as “out” are produced. Adapted from: Kattel et al., (2023), Anaerobe, Elsevier. Used under author rights.

4.5 Estimation of viable cell abundance and enumeration using PMAXx and spike-in control as alternatives to traditional methods (Publication III)

4.5.1 Estimation of viable cell abundance using PMAXx-qPCR

Accurate viability assessment is critical for evaluating the biological functionality of microbial products. Specifically, their ability to perform intended metabolic roles and for ensuring the quality and consistency of synthetic microbial consortia. Traditional plating methods, while commonly used, are limited by their low throughput, labour intensiveness, and lack of species-level taxonomic information without further downstream analysis such as MALDI-TOF or PCR. Additionally, not all bacteria are culturable or grow on very specific medium. These limitations are especially pronounced in complex consortia where precise species-level viability data are crucial.

To address these challenges, we implemented a combination of propidium monoazide (PMAXx) and qPCR for viability assessment (Emerson et al., 2017; Navarro et al., 2020). PMAXx is a photo-reactive dye that selectively penetrates dead cells with compromised membranes and binds covalently to DNA upon exposure to light, thereby inhibiting its amplification in subsequent PCR reactions. By comparing the qPCR amplification of PMAXx-treated samples to untreated controls, we could estimate the proportion of viable cells within the sample. Strain specific primers were used to carry out the qPCR.

Flow cytometry (FC) was used to benchmark the PMAXx-qPCR results. Using SYTO24 and propidium iodide staining, we assessed the viability of each of the 20 individual strains as well as the viability of the mixed 20-strain consortia glycerol stock. The viability values obtained from FC varied significantly among individual strains, with viability ranging from 4% (*Bacteroides caccae*) to 96% (*Butyricimonas faecihominis*) (Table 6). The viability of the mixed 20-strain consortium was 68%. Importantly, PMAXx-qPCR results showed strong correlation with FC data (Figure 10) ($R^2 = 0.884$ when outliers were excluded), validating the accuracy of the method.

Table 6. The viability of 20 bacterial strains was evaluated using both FC and qPCR. *- Universal primers targeting the 16S rRNA gene V4 region were used instead of specific ones. Adapted from: Kallastu et al., (2023), *Current Research in Food Science, Elsevier*. Licensed under CC BY 4.0.

Species (acronym)	Gram stain	Viability by FC, %	Viability by qPCR, %
<i>Akkermansia muciniphila</i> (AM)	negative	66.11 ± 0.03	81.22 ± 13.47
<i>Alistipes shahii</i> (AS)	negative	62.40 ± 7.63	78.51 ± 12.18
<i>Anaerostipes caccae</i> (AC)	variable	60.69 ± 9.86	90.01 ± 5.02
<i>Anaerotruncus colihominis</i> (ACo)	positive	23.35 ± 0.90	40.15 ± 13.87
<i>Bacteroides caccae</i> (BC)	negative	3.76 ± 2.16	9.28 ± 0.26
<i>Bacteroides thetaiotaomicron</i> (BT)	negative	63.88 ± 8.26	56.87 ± 2.51
<i>Bacteroides uniformis</i> (BU)	negative	88.59 ± 1.82	100.00 ± 8.84
<i>Bifidobacterium adolescentis</i> (BA)	positive	83.72 ± 1.55	90.26 ± 7.07
<i>Blautia hydrogenotrophica</i> (BH)	positive	35.06 ± 14.86	24.63 ± 1.62
<i>Butyrivibrio faecihominis</i> (BF)	negative	95.88 ± 0.85	92.47 ± 27.24
<i>Catenibacterium mitsuokai</i> (CM)	positive	6.14 ± 1.86	0.46 ± 0.01
<i>Christensenella minuta</i> (ChM)	negative	40.40 ± 0.46	34.66 ± 7.18
<i>Collinsella aerofaciens</i> (CA)	positive	4.31 ± 0.13	11.25 ± 1.51
<i>Dorea formicigenerans</i> (DF)	positive	81.80 ± 1.19	90.18 ± 8.42
<i>Dorea longicatena</i> (DL)	positive	14.91 ± 1.49	22.70 ± 0.89
<i>Eisenbergiella tayi</i> (ET)	positive but Gram-stain negative	8.95 ± 1.57	43.96 ± 2.16
<i>Faecalibacterium prausnitzii</i> (FP)	positive	72.23 ± 5.40	74.70 ± 14.27
<i>Odoribacter splanchnicus</i> (OS)	negative	87.06 ± 0.54	93.38 ± 4.83
<i>Prevotella copri</i> (PC)	negative	32.88 ± 4.00	73.56 ± 21.67
<i>Roseburia faecis</i> (RF)	negative or variable	67.84 ± 4.32	87.07 ± 2.16
Mix of 20 strains		68.41 ± 0.18	60.92 ± 3.98*

However, some discrepancies between the two approaches were observed. For example, in the case of *Catenibacterium mitsuokai*, FC showed several-fold higher viability than qPCR, whereas in the case of *Eisenbergiella tayi*, the opposite was observed. Both FC and PMAxx-qPCR have distinct advantages and limitations. FC allows rapid detection of membrane integrity using fluorescent dyes, although its throughput is limited by sample preparation and instrument settings. It struggles with species exhibiting atypical morphologies, forming long chains or aggregates (like *Dorea longicatena*), which complicate gating strategies and can lead to underestimation or misclassification. Additionally, FC cannot provide taxonomic resolution unless paired with fluorescent in situ hybridization or other markers.

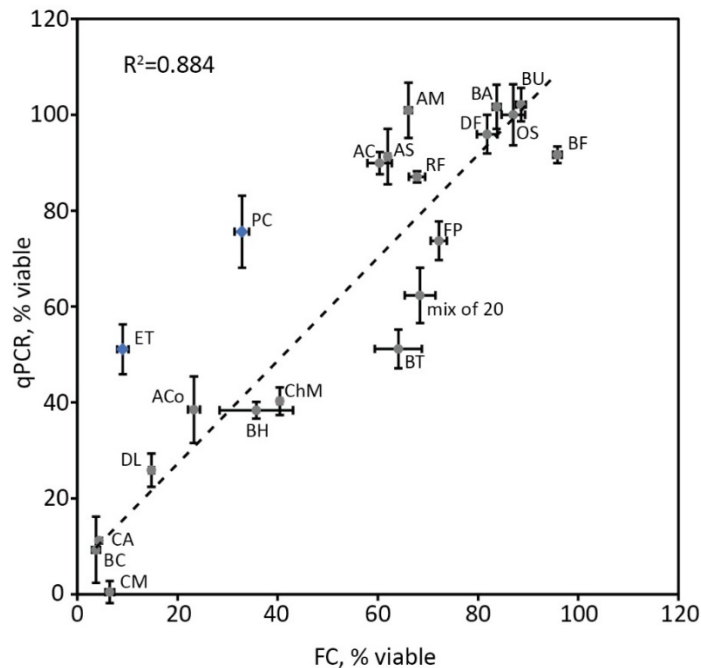


Figure 10. Scatterplot showing cell viability results obtained by FC and qPCR using strain-specific primers. The dotted line shows the regression trendline, with R^2 representing correlation strength. Grey circles are included in the regression analysis; blue squares are outliers. Acronyms for bacterial strains are provided in the Table 6. Reproduced from: Kallastu et al., (2023), *Current Research in Food Science*, Elsevier. Licensed under CC BY 4.0.

PMAxx-qPCR, in contrast, offers high taxonomic specificity by using strain-specific primers, making it suitable for studying complex microbial consortia. PMAxx-qPCR is compatible with plate-based and automated workflows, enhancing scalability in both research and industrial contexts. Nonetheless, PMAxx-qPCR is not without limitations. Its accuracy depends heavily on consistent and efficient DNA extraction, which may vary significantly between strains due to differences in cell wall structure. Gram-positive and Gram-variable species, such as *A. cacciae*, may yield lower DNA quantities, leading to an underestimation of viability. Also, the primer specificity and PCR efficiency play an important role in getting accurate results. The effectiveness of PMAxx also relies on light exposure and the optical clarity of the suspension. In coloured or turbid matrices, the efficiency of dye-DNA crosslinking may decrease, potentially allowing dead cell DNA to be amplified. Furthermore, both FC and PMAxx-qPCR rely on the differential permeability of fluorescent dyes, introducing a potential bias if dye uptake is inconsistent between species.

Overall, qPCR in combination with PMAxx showed higher levels of viable cells than FC. To further understand the discrepancies between two methods, microscopy analysis was done selectively to visually confirm species morphology and cellular arrangement. Based on FC and PMAxx-qPCR results, we selected representative species to investigate whether structural characteristics such as clumping could explain the differences in viability estimates. Some selected species showed agreement between both methods and others had clear discrepancies. Figure 11B shows that species with discrepancies between FC and qPCR data tend to form clusters and fiber-like structures. These formations can impact

cloud formation and complicate the analysis of FC data. In conclusion, PMAxx dye offers a reliable approach for distinguishing viable from dead microbial cells when used in combination with qPCR. This combination provides species-level resolution and improved accuracy in viability assessments, particularly in complex microbial communities.

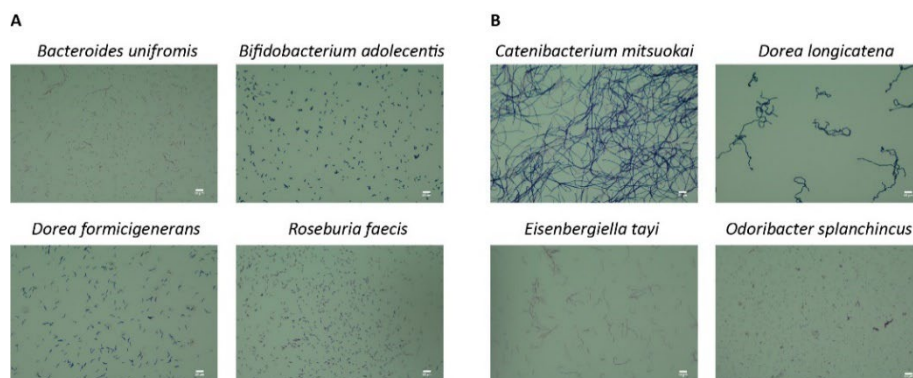


Figure 11. Microscopy images of bacterial strains: (A) examples where FC and qPCR data were similar, and (B) examples where FC and qPCR data differed. The white scale bar in the bottom right corner indicates 10 μm . Reproduced from: Kallastu et al., (2023), *Current Research in Food Science*, Elsevier. Licensed under CC BY 4.0.

4.5.2 Bacterial enumeration using spike-in and NGS

In some cases, the composition of microbial consortia is unknown. In such situations, NGS is a suitable alternative to PCR as it provides taxonomic information on all the species present in the sample. When combined with PMAxx, it can also distinguish between viable and non-viable cells. Additionally, incorporating a spike-in control allows for quantification of the total bacterial load not only relative abundance of bacteria.

To estimate the number of bacteria in our mixed 20-strain consortium stock, a spike-in control was incorporated prior to DNA extraction. We picked out the commercially available High-load Spike-in control (ZymoResearch) which contains a known quantity of two rarely occurring bacterial strains: *Allobacillus halotolerans* and *Imtechella halotolerans*. These strains underwent the entire NGS workflow alongside the sample and knowing the precise quantity of the spike-in strains allowed us to estimate the number of all bacteria in each sample. It is important to add the spike-in cells before the DNA extraction, so that they undergo the same experimental workflow as the target cells, ensuring methodological consistency.

To confirm that the number of added spike-in cells correlates with their NGS read counts linearly, we added them at different concentrations. As expected, varying the spike-in concentration resulted in a linear correlation with the total bacterial count (Pearson correlation coefficient, $r = 0.9981$). Therefore, for reliable estimation of microbial cell numbers, it is not required to add spike-in at an exact amount.

Based on OD600 measurement, our 20-strain mix sample taken for analysis had approximately 1.50×10^9 cells. Spike-in control reads, and species reads were used to estimate the total cell count of the mix sample using NGS. With the exact spike-in cell numbers known, we calculated the number of total cells in our sample (Table 7). Across different spike-in concentrations (0.5, 1.0, and 2.5%), the average calculated number of total cells was $1.55 \pm 0.18 \times 10^9$ which is similar to the theoretical value based on OD600 measurement (1.50×10^9 cells).

Table 7. Using spike-in for absolute quantification of total cells in 20 strain mix sample. NA – not available. Adapted from: Kallastu et al., (2023), *Current Research in Food Science*, Elsevier. Licensed under CC BY 4.0.

		20 st mix	20 st mix 0.5%	20 st mix 1%	20 st mix 2.5%
Number of added spike-in cells		0.00	7.50×10^6	1.50×10^7	3.75×10^7
Calculated abundance of added spike-in, %	<i>Allobacillus halotolerans</i>	0.00	0.25	0.72	1.13
	<i>Imtechella halotolerans</i>	0.00	0.18	0.35	1.28
SUM of spike-in, %		0.00	0.43	1.07	2.42
Calculated abundance of 20 strains, %		100	99.57	98.93	97.58
Calculated number of total cells in 20 strain mix sample		NA	1.74×10^9	1.39×10^9	1.51×10^9

As mentioned before, spike-in control should be added before DNA extraction. However, this is not always feasible or the quantitative information about bacterial load is needed retrospectively. In such cases, the only option is by measuring microbial gDNA concentration. Real-time quantitative PCR is a widely accepted method for obtaining quantitative DNA data, as the concentration of microbial gDNA is directly proportional to the number of bacterial cells. We decided to test it by performing qPCR with degenerate primers targeting the conserved 16S V4 region. Using a calibration curve, the microbial gDNA concentration was converted into an estimated total bacterial cell count of $1.16 \pm 0.12 \times 10^9$ cells. When compared to the theoretical value, the total cell count estimated with the qPCR was of the same order of magnitude but slightly lower.

According to our findings, the application of a spike-in control resulted in highly accurate enumeration of microbes, yielding results comparable to those obtained with FC, while qPCR-based estimation was slightly lower. Similar observations were made by Zemb et al., (2020), who reported that qPCR underestimated bacterial counts by approximately 1.9-fold compared to values obtained using an artificial internal spike-in standard.

4.5.3 Combining PMAxx treatment and spike-in control

Next, we combined PMAxx treatment with a spike-in control to assess both total and viable bacterial populations. Cells were either left untreated or treated with PMAxx, followed by the addition of the spike-in control. The complete 16S amplicon sequencing workflow was then performed. To quantify viable bacteria, three parallel analyses were conducted (20St 0.5PMA, 20St 1PMA, 20St 2.5PMA), each differing in the concentration of spike-in control added. Sequencing results confirmed the presence of all 20 bacterial species (Figure 12). The taxonomic profiles of viable bacteria across the three replicates were consistent with one another but differed from the total bacteria profile. For example, *Catenibacterium mitsuokai* and *Collinsella aerofaciens* were found in total consortia, but not among viable cells, aligning well with results from FC and qPCR (Figure 12, Table 6). Overall, the viability determined by NGS showed strong agreement with FC and qPCR data.

To express the results in absolute cell numbers, the data was normalized using either spike-in or qPCR quantification (Figure 12B). The total number of bacteria detected via spike-in control was $1.55 \pm 0.18 \times 10^9$, closely matching the FC result of $1.56 \pm 0.17 \times 10^9$ and aligning with the theoretical estimate (Table 8). In terms of viable cells, spike-in

quantification yielded $1.05 \pm 0.12 \times 10^9$ cells per sample, while qPCR yielded a lower count of $7.03 \pm 0.25 \times 10^8$ cells. FC viability results were consistent with the spike-in data, reporting $1.06 \pm 0.17 \times 10^9$ viable cells in the sample. Across all methods, calculated viability ranged between 61% and 68% (Table 8).

Table 8. Total and viable cell counts obtained with different methods. Mean values (cells) \pm standard deviations ($n = 3$) are presented. Adapted from: Kallastu et al., (2023), *Current Research in Food Science, Elsevier*. Licensed under CC BY 4.0.

Sample	Cell number	Viability, %
20 st mix theoretical	1.50×10^9	
20 st mix FC	$1.56 \pm 0.17 \times 10^9$	68.41 ± 0.18
20 st mix FC alive	$1.06 \pm 0.17 \times 10^9$	
20 st spike-in	$1.55 \pm 0.18 \times 10^9$	67.79 ± 8.19
20 st spike-in alive	$1.05 \pm 0.12 \times 10^9$	
20 st mix qPCR	$1.16 \pm 0.12 \times 10^9$	60.92 ± 3.98
20 st mix qPCR alive	$7.03 \pm 0.25 \times 10^8$	

In summary, cell number estimates for both total and viable cells were closely aligned between the FC and spike-in control combined with NGS, whereas qPCR consistently yielded lower counts. This integrated approach, combining a viability reagent with either spike-in control and NGS analysis or qPCR, proved effective for characterizing microbial consortia. Although applied here to a bacterial mixture with a known composition, the method is versatile and can be extended to a range of microbial samples, including those derived from food, environmental, or clinical sources.

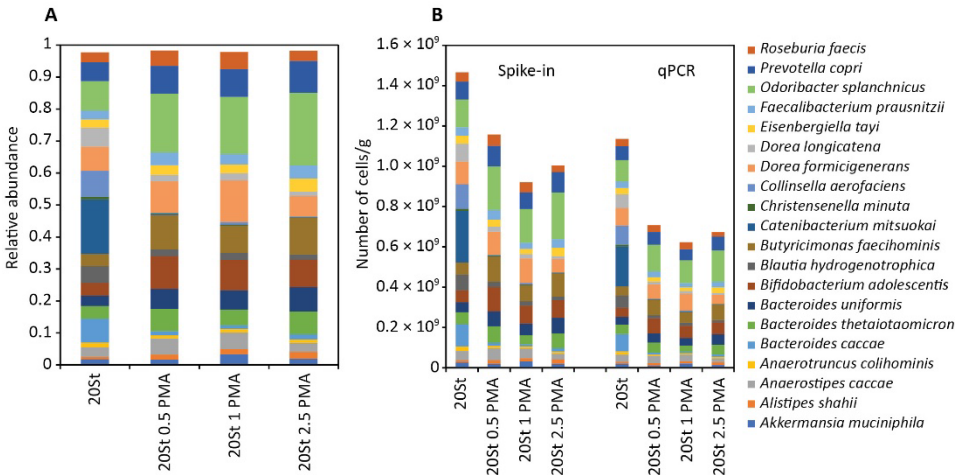


Figure 12. Identification of bacterial composition in total (20St) and viable (20St 0.5PMA, 20St 1PMA, 20St 2.5PMA) consortia samples using 16S V4 amplicon NGS. (A) Distribution of bacterial relative abundance. (B) Normalized NGS data using either spike-in control or qPCR-based quantification. Reproduced from: Kallastu et al., (2023), *Current Research in Food Science, Elsevier*. Licensed under CC BY 4.0.

5 Conclusions

This thesis set out to develop and validate scalable methodologies for cultivating, characterizing, and controlling defined microbial consortia composed of next-generation probiotic candidates. While traditional probiotic applications have focused on single-strain cultures, the complexity of gut microbiota and the emerging role of strict anaerobes in health and disease necessitate co-culture approaches. This work provides insights into designing robust consortia by combining trait-based design principles, isothermal calorimetry, and genome-scale metabolic modelling. The main conclusions that can be drawn from this work are:

- A three-species model consortium (*A. muciniphila*, *B. thetaiotaomicron*, *F. prausnitzii*) maintained stable composition across serial passages and showed resilience when initial species ratios were notably altered. The consortium recovered its original composition, demonstrating robustness and compositional stability during serial batch cultivation.
- Metabolic interactions, such as cross-feeding, were observed through changes in SCFA profiles and confirmed that co-cultivation can enhance metabolite production compared to monocultures. Notably, butyrate concentrations were significantly higher in consortia, suggesting beneficial interactions.
- Genome-scale metabolic models and flux balance analysis were used to support experimental findings. In Publication I, model accuracy was limited by data quality due to complex media. However, in Publication II, defined media and metabolite measurements enabled more accurate metabolic modelling, confirming single substrate utilization and confirming cross-feeding interactions.
- An approach based on unique carbon sources was implemented to control species abundance in co-culture. Each species was provided with a carbon source not shared by others, reducing competition and allowing stable co-cultivation. This compositional control strategy was validated using isothermal microcalorimetry, bioreactors, flux balance analysis, and microscopy-based species ratio analysis.
- Viability quantification method PMAxx-qPCR was adapted for strict anaerobes, enabling accurate assessment of species viability in mixed cultures. In addition, the workflow for absolute quantification of viable bacteria with next-generation sequencing was developed by adding PMAxx reagent and spike-in control. This method can be used for defined microbial consortia as well as for unknown samples.

In summary, this thesis outlines a workflow for the cultivation and control of defined microbial consortia composed of strict anaerobes. While the developed methodologies offer a step forward in the field of synthetic gut microbiota, further work is needed to improve scale-up strategies, and functionality validation under relevant conditions.

References

- Adamberg, K., Jaagura, M., Aaspõllu, A., Nurk, E., & Adamberg, S. (2020). The composition of faecal microbiota is related to the amount and variety of dietary fibres. *International Journal of Food Sciences and Nutrition*, 71(7), 845–855. <https://doi.org/10.1080/09637486.2020.1727864>
- Adamberg, K., Raba, G., & Adamberg, S. (2020). Use of Changestat for Growth Rate Studies of Gut Microbiota. *Frontiers in Bioengineering and Biotechnology*, 8. <https://doi.org/10.3389/fbioe.2020.00024>
- Alam, M. T., Amos, G. C. A., Murphy, A. R. J., Murch, S., Wellington, E. M. H., & Arasaradnam, R. P. (2020). Microbial imbalance in inflammatory bowel disease patients at different taxonomic levels. *Gut Pathogens*, 12(1). <https://doi.org/10.1186/s13099-019-0341-6>
- Allison, S. D., & Martiny, J. B. H. (2008). *Resistance, resilience, and redundancy in microbial communities*. www.pnas.org/cgi/content/full/
- Alonso, J. L., Amorós, I., & Guy, R. A. (2014). Quantification of viable *Giardia* cysts and *Cryptosporidium* oocysts in wastewater using propidium monoazide quantitative real-time PCR. *Parasitology Research*, 113(7), 2671–2678. <https://doi.org/10.1007/s00436-014-3922-9>
- Andrade, J. C., Almeida, D., Domingos, M., Seabra, C. L., Machado, D., Freitas, A. C., & Gomes, A. M. (2020). Commensal obligate anaerobic bacteria and health: Production, storage, and delivery strategies. In *Frontiers in Bioengineering and Biotechnology* (Vol. 8, pp. 1–23). Frontiers Media S.A. <https://doi.org/10.3389/fbioe.2020.00550>
- Baena-Ruano, S., Jiménez-Ot, C., Santos-Dueñas, I. M., Cantero-Moreno, D., Barja, F., & García-García, I. (2006). Rapid method for total, viable and non-viable acetic acid bacteria determination during acetification process. *Process Biochemistry*, 41(5), 1160–1164. <https://doi.org/10.1016/j.procbio.2005.12.016>
- Baunwall, S. M. D., Lee, M. M., Eriksen, M. K., Mullish, B. H., Marchesi, J. R., Dahlerup, J. F., & Hvas, C. L. (2020). Faecal microbiota transplantation for recurrent *Clostridioides difficile* infection: An updated systematic review and meta-analysis. *EClinicalMedicine*, 29–30. <https://doi.org/10.1016/j.eclinm.2020.100642>
- Becker, J. W., Hogle, S. L., Rosendo, K., & Chisholm, S. W. (2019). Co-culture and biogeography of *Prochlorococcus* and SAR11. *ISME Journal*, 13(6), 1506–1519. <https://doi.org/10.1038/s41396-019-0365-4>
- Berg, G., Rybakova, D., Fischer, D., Cernava, T., Vergès, M. C. C., Charles, T., Chen, X., Cocolin, L., Eversole, K., Corral, G. H., Kazou, M., Kinkel, L., Lange, L., Lima, N., Loy, A., Macklin, J. A., Maguin, E., Mauchline, T., McClure, R., ... Schlöter, M. (2020). Microbiome definition re-visited: old concepts and new challenges. In *Microbiome* (Vol. 8, Issue 1). BioMed Central Ltd. <https://doi.org/10.1186/s40168-020-00875-0>
- Blair, H. A. (2023). RBX2660 (REBYOTA®) in preventing recurrence of *Clostridioides difficile* infection: a profile of its use in the USA. *Drugs and Therapy Perspectives*, 39(10), 331–338. <https://doi.org/10.1007/s40267-023-01023-y>
- Blair, H. A. (2024). SER-109 (VOWST™): A Review in the Prevention of Recurrent *Clostridioides difficile* Infection. *Drugs*. <https://doi.org/10.1007/s40265-024-02006-7>

- Blaschkowski, H. P., Neuer, G., Ludwig-Festl, M., & Knappe, J. (1982). Routes of Flavodoxin and Ferredoxin Reduction in *Escherichia coli* CoA-Acylating Pyruvate: Flavodoxin and NADPH: Flavodoxin Oxidoreductases Participating in the Activation of Pyruvate Formate-Lyase. *European Journal of Biochemistry*, 123(3), 563–569. <https://doi.org/10.1111/j.1432-1033.1982.tb06569.x>
- Braissant, O., Wirz, D., Göpfert, B., & Daniels, A. U. (2010). Use of isothermal microcalorimetry to monitor microbial activities. In *FEMS Microbiology Letters* (Vol. 303, Issue 1, pp. 1–8). Blackwell Publishing Ltd. <https://doi.org/10.1111/j.1574-6968.2009.01819.x>
- Bunthof, C. J., Van Schalkwijk, S., Meijer, W., Abee, T., & Hugenholtz, J. (2001). Fluorescent Method for Monitoring Cheese Starter Permeabilization and Lysis. *Applied and Environmental Microbiology*, 67(9), 4264–4271. <https://doi.org/10.1128/AEM.67.9.4264-4271.2001>
- Byrd, A. L., Belkaid, Y., & Segre, J. A. (2018). The human skin microbiome. In *Nature Reviews Microbiology* (Vol. 16, Issue 3, pp. 143–155). Nature Publishing Group. <https://doi.org/10.1038/nrmicro.2017.157>
- Cao, Y., Fanning, S., Proos, S., Jordan, K., & Srikumar, S. (2017). A review on the applications of next generation sequencing technologies as applied to food-related microbiome studies. In *Frontiers in Microbiology* (Vol. 8, Issue SEP). Frontiers Media S.A. <https://doi.org/10.3389/fmicb.2017.01829>
- Chang, P. V., Hao, L., Offermanns, S., & Medzhitov, R. (2014). The microbial metabolite butyrate regulates intestinal macrophage function via histone deacetylase inhibition. *Proceedings of the National Academy of Sciences of the United States of America*, 111(6), 2247–2252. <https://doi.org/10.1073/pnas.1322269111>
- Chen, Y., Li, C., Zhou, Z., Wen, J., You, X., Mao, Y., Lu, C., Huo, G., & Jia, X. (2014). Enhanced biodegradation of alkane hydrocarbons and crude oil by mixed strains and bacterial community analysis. *Applied Biochemistry and Biotechnology*, 172(7), 3433–3447. <https://doi.org/10.1007/s12010-014-0777-6>
- Chia, L. W., Hornung, B. V. H., Aalvink, S., Schaap, P. J., de Vos, W. M., Knol, J., & Belzer, C. (2018). Deciphering the trophic interaction between *Akkermansia muciniphila* and the butyrogenic gut commensal *Anaerostipes caccae* using a metatranscriptomic approach. *Antonie van Leeuwenhoek, International Journal of General and Molecular Microbiology*, 111(6), 859–873. <https://doi.org/10.1007/s10482-018-1040-x>
- Chia, L. W., Mank, M., Blijenberg, B., Aalvink, S., Bongers, R. S., Stahl, B., Knol, J., & Belzer, C. (2020). *Bacteroides thetaiotaomicron* fosters the growth of butyrate-producing *anaerostipes caccae* in the presence of lactose and total human milk carbohydrates. *Microorganisms*, 8(10), 1–13. <https://doi.org/10.3390/microorganisms8101513>
- Clark, R. L., Connors, B. M., Stevenson, D. M., Hromada, S. E., Hamilton, J. J., Amador-Noguez, D., & Venturelli, O. S. (2021). Design of synthetic human gut microbiome assembly and butyrate production. *Nature Communications*, 12(1), 1–16. <https://doi.org/10.1038/s41467-021-22938-y>

- Costello, S. P., Hughes, P. A., Waters, O., Bryant, R. V., Vincent, A. D., Blatchford, P., Katsikeros, R., Makanyanga, J., Campaniello, M. A., Mavrangelos, C., Rosewarne, C. P., Bickley, C., Peters, C., Schoeman, M. N., Conlon, M. A., Roberts-Thomson, I. C., & Andrews, J. M. (2019). Effect of Fecal Microbiota Transplantation on 8-Week Remission in Patients with Ulcerative Colitis: A Randomized Clinical Trial. *JAMA - Journal of the American Medical Association*, 321(2), 156–164. <https://doi.org/10.1001/jama.2018.20046>
- den Besten, G., van Eunen, K., Groen, A. K., Venema, K., Reijngoud, D. J., & Bakker, B. M. (2013). The role of short-chain fatty acids in the interplay between diet, gut microbiota, and host energy metabolism. In *Journal of Lipid Research* (Vol. 54, Issue 9, pp. 2325–2340). <https://doi.org/10.1194/jlr.R036012>
- Depommier, C., Everard, A., Druart, C., Plovier, H., Van Hul, M., Vieira-Silva, S., Falony, G., Raes, J., Maiter, D., Delzenne, N. M., de Barse, M., Loumaye, A., Hermans, M. P., Thissen, J. P., de Vos, W. M., & Cani, P. D. (2019). Supplementation with *Akkermansia muciniphila* in overweight and obese human volunteers: a proof-of-concept exploratory study. *Nature Medicine*, 25(7), 1096–1103. <https://doi.org/10.1038/s41591-019-0495-2>
- Ditommaso, S., Ricciardi, E., Giacomuzzi, M., Arauco Rivera, S. R., & Zotti, C. M. (2015). Legionella in water samples: How can you interpret the results obtained by quantitative PCR? *Molecular and Cellular Probes*, 29(1), 7–12. <https://doi.org/10.1016/j.mcp.2014.09.002>
- Donohoe, D. R., Garge, N., Zhang, X., Sun, W., O'Connell, T. M., Bunger, M. K., & Bultman, S. J. (2011). The microbiome and butyrate regulate energy metabolism and autophagy in the mammalian colon. *Cell Metabolism*, 13(5), 517–526. <https://doi.org/10.1016/j.cmet.2011.02.018>
- Duncan, S. H., Louis, P., & Flint, H. J. (2004). Lactate-utilizing bacteria, isolated from human feces, that produce butyrate as a major fermentation product. *Applied and Environmental Microbiology*, 70(10), 5810–5817. <https://doi.org/10.1128/AEM.70.10.5810-5817.2004>
- Embree, M., Liu, J. K., Al-Bassam, M. M., & Zengler, K. (2015). Networks of energetic and metabolic interactions define dynamics in microbial communities. *Proceedings of the National Academy of Sciences of the United States of America*, 112(50), 15450–15455. <https://doi.org/10.1073/pnas.1506034112>
- Emerson, J. B., Adams, R. I., Román, C. M. B., Brooks, B., Coil, D. A., Dahlhausen, K., Ganz, H. H., Hartmann, E. M., Hsu, T., Justice, N. B., Paulino-Lima, I. G., Luongo, J. C., Lymperopoulou, D. S., Gomez-Silvan, C., Rothschild-Mancinelli, B., Balk, M., Huttenhower, C., Nocker, A., Vaishampayan, P., & Rothschild, L. J. (2017). Schrödinger's microbes: Tools for distinguishing the living from the dead in microbial ecosystems. In *Microbiome* (Vol. 5, Issue 1, p. 86). <https://doi.org/10.1186/s40168-017-0285-3>
- Falony, G., Calmeyer, T., Leroy, F., & De Vuyst, L. (2009). Coculture fermentations of bifidobacterium species and bacteroides thetaiotaomicron reveal a mechanistic insight into the prebiotic effect of inulin-type fructans. *Applied and Environmental Microbiology*, 75(8), 2312–2319. <https://doi.org/10.1128/AEM.02649-08>

- Falony, G., Joossens, M., Vieira-Silva, S., Wang, J., Darzi, Y., Faust, K., Kurilshikov, A., Bonder, M. J., Valles-Colomer, M., Vandeputte, D., Tito, R. Y., Chaffron, S., Rymenans, L., Verspecht, C., De Sutter, L., Lima-Mendez, G., D'hoë, K., Jonckheere, K., Homola, D., ... Raes, J. (2016). Population-level analysis of gut microbiome variation. *American Association for the Advancement of Science*, 352(6285), 560–564. <https://doi.org/10.1126/science.aad3503>
- Falony, G., Vlachou, A., Verbrugghe, K., & De Vuyst, L. (2006). Cross-feeding between *Bifidobacterium longum* BB536 and acetate-converting, butyrate-producing colon bacteria during growth on oligofructose. *Applied and Environmental Microbiology*, 72(12), 7835–7841. <https://doi.org/10.1128/AEM.01296-06>
- Forrest W.W., & Walker D.J. (1963). Calorimetric measurements of energy of maintenance of *Streptococcus faecalis*. *Biochemical and Biophysical Research Communications*, 13(3), 217–222.
- Goldford, J. E., Lu, N., Bajić, D., Estrela, S., Tikhonov, M., Sanchez-Gorostiaga, A., Segrè, D., Mehta, P., & Sanchez, A. (2018). *Emergent simplicity in microbial community assembly*. <https://doi.org/10.1126/science.aat1168>
- Grey, B., & Steck, T. R. (2001). Concentrations of Copper Thought to Be Toxic to *Escherichia coli* Can Induce the Viable but Nonculturable Condition. *Applied and Environmental Microbiology*, 67(3–12), 5325–5327. <https://doi.org/10.1128/aem.67.11.5325-5327.2001>
- Hahnke, R. L., Meier-Kolthoff, J. P., García-López, M., Mukherjee, S., Huntemann, M., Ivanova, N. N., Woyke, T., Kyrpides, N. C., Klenk, H. P., & Göker, M. (2016). Genome-based taxonomic classification of Bacteroidetes. *Frontiers in Microbiology*, 7(DEC). <https://doi.org/10.3389/fmicb.2016.02003>
- Hill, C., Guarner, F., Reid, G., Gibson, G. R., Merenstein, D. J., Pot, B., Morelli, L., Canani, R. B., Flint, H. J., Salminen, S., Calder, P. C., & Sanders, M. E. (2014). The international scientific association for probiotics and prebiotics consensus statement on the scope and appropriate use of the term probiotic. *Nature Reviews Gastroenterology and Hepatology*, 11(8), 506–514. <https://doi.org/10.1038/nrgastro.2014.66>
- Hitch, T. C. A., Bisdorf, K., Afrizal, A., Riedel, T., Overmann, J., Strowig, T., & Clavel, T. (2022). A taxonomic note on the genus *Prevotella*: Description of four novel genera and emended description of the genera *Hallella* and *Xylanibacter*. *Systematic and Applied Microbiology*, 45(6). <https://doi.org/10.1016/j.syapm.2022.126354>
- Hoefel, D., Grooby, W. L., Monis, P. T., Andrews, S., & Saint, C. P. (2003). Enumeration of water-borne bacteria using viability assays and flow cytometry: A comparison to culture-based techniques. *Journal of Microbiological Methods*, 55(3), 585–597. [https://doi.org/10.1016/S0167-7012\(03\)00201-X](https://doi.org/10.1016/S0167-7012(03)00201-X)
- Hosmer, J., McEwan, A. G., & Kappler, U. (2024). Bacterial acetate metabolism and its influence on human epithelia. In *Emerging Topics in Life Sciences* (Vol. 8, Issue 1, pp. 1–13). Portland Press Ltd. <https://doi.org/10.1042/ETLS20220092>
- Hou, X., Zhang, P., Du, H., Chu, W., Sun, R., Qin, S., Tian, Y., Zhang, Z., & Xu, F. (2021). *Akkermansia muciniphila* Potentiates the Antitumor Efficacy of FOLFOX in Colon Cancer. *Frontiers in Pharmacology*, 12. <https://doi.org/10.3389/fphar.2021.725583>

- Ikeyama, N., Murakami, T., Toyoda, A., Mori, H., Iino, T., Ohkuma, M., & Sakamoto, M. (2020). Microbial interaction between the succinate-utilizing bacterium *Phascolarctobacterium faecium* and the gut commensal *Bacteroides thetaiotaomicron*. *MicrobiologyOpen*, 9(10). <https://doi.org/10.1002/mbo3.1111>
- Ji, B., & Nielsen, J. (2015). From next-generation sequencing to systematic modeling of the gut microbiome. In *Frontiers in Genetics* (Vol. 6, Issue JUN). Frontiers Media S.A. <https://doi.org/10.3389/fgene.2015.00219>
- Jonkers, D., Penders, J., Masclee, A., & Pierik, M. (2012). Probiotics in the management of inflammatory bowel disease: A systematic review of intervention studies in adult patients. *Drugs*, 72(6), 803–823. <https://doi.org/10.2165/11632710-000000000-00000>
- Kabanova, N., Kazarjan, A., Stulova, I., & Vilu, R. (2009). Microcalorimetric study of growth of *Lactococcus lactis* IL1403 at different glucose concentrations in broth. *Thermochimica Acta*, 496(1–2), 87–92. <https://doi.org/10.1016/j.tca.2009.07.003>
- Kallastu, A., Malv, E., Aro, V., Meikas, A., Vendelin, M., Kattel, A., Nahku, R., & Kazantseva, J. (2023). Absolute quantification of viable bacteria abundances in food by next-generation sequencing: Quantitative NGS of viable microbes. *Current Research in Food Science*, 6(December 2022), 100443. <https://doi.org/10.1016/j.crfs.2023.100443>
- Kanehisa, M., & Goto, S. (2000). KEGG: Kyoto Encyclopedia of Genes and Genomes. *Nucleic Acids Research*, 28(1), 27–30. <https://doi.org/10.3892/ol.2020.11439>
- Kattel, A., Aro, V., Lahtvee, P. J., Kazantseva, J., Jöers, A., Nahku, R., & Belouah, I. (2024). Exploring the resilience and stability of a defined human gut microbiota consortium: An isothermal microcalorimetric study. *MicrobiologyOpen*, 13(4). <https://doi.org/10.1002/mbo3.1430>
- Kattel, A., Morell, I., Aro, V., Lahtvee, P. J., Vilu, R., Jöers, A., & Nahku, R. (2023). Detailed analysis of metabolism reveals growth-rate-promoting interactions between *Anaerostipes caccae* and *Bacteroides* spp. *Anaerobe*, 79. <https://doi.org/10.1016/j.anaerobe.2022.102680>
- Krieger, A. G., Zhang, J., & Lin, X. N. (2021). Temperature regulation as a tool to program synthetic microbial community composition. *Biotechnology and Bioengineering*, 118(3), 1381–1392. <https://doi.org/10.1002/bit.27662>
- Kurt, F., Leventhal, G. E., Spalinger, M. R., Anthamatten, L., Rogalla von Bieberstein, P., Menzi, C., Reichlin, M., Meola, M., Rosenthal, F., Rogler, G., Lacroix, C., & de Wouters, T. (2023). Co-cultivation is a powerful approach to produce a robust functionally designed synthetic consortium as a live biotherapeutic product (LBP). *Gut Microbes*, 15(1). <https://doi.org/10.1080/19490976.2023.2177486>
- Kütt, M. L., Orgusaar, K., Stulova, I., Priidik, R., Pismennõi, D., Vaikma, H., Kallastu, A., Zhogoleva, A., Morell, I., & Kriščiunaite, T. (2023). Starter culture growth dynamics and sensory properties of fermented oat drink. *Heliyon*, 9(5). <https://doi.org/10.1016/j.heliyon.2023.e15627>
- Lalowski, P., & Zielińska, D. (2024). The Most Promising Next-Generation Probiotic Candidates—Impact on Human Health and Potential Application in Food Technology. *Fermentation*, 10(9), 444. <https://doi.org/10.3390/fermentation10090444>

- Lawson, C. E., Harcombe, W. R., Hatzenpichler, R., Lindemann, S. R., Löffler, F. E., O'Malley, M. A., García Martín, H., Pfleger, B. F., Raskin, L., Venturelli, O. S., Weissbrodt, D. G., Noguera, D. R., & McMahon, K. D. (2019). Common principles and best practices for engineering microbiomes. In *Nature Reviews Microbiology* (Vol. 17, Issue 12, pp. 725–741). Nature Publishing Group. <https://doi.org/10.1038/s41579-019-0255-9>
- Le Roy, T., Debédat, J., Marquet, F., Da-Cunha, C., Ichou, F., Guerre-Millo, M., Kapel, N., Aron-Wisniewsky, J., & Clément, K. (2019). Comparative evaluation of microbiota engraftment following fecal microbiota transfer in mice models: Age, kinetic and microbial status matter. *Frontiers in Microbiology*, 10(JAN). <https://doi.org/10.3389/fmicb.2018.03289>
- Lederberg, J., & McCray, A. T. (2001). 'Ome Sweet 'Omics-A Genealogical Treasury of Words. *The Scientist*, 15(8), 8–8. www.ics.com
- Leung, C., Rivera, L., Furness, J. B., & Angus, P. W. (2016). The role of the gut microbiota in NAFLD. In *Nature Reviews Gastroenterology and Hepatology* (Vol. 13, Issue 7, pp. 412–425). Nature Publishing Group. <https://doi.org/10.1038/nrgastro.2016.85>
- Li, F., Hinderberger, J., Seedorf, H., Zhang, J., Buckel, W., & Thauer, R. K. (2008). Coupled ferredoxin and crotonyl coenzyme A (CoA) reduction with NADH catalyzed by the butyryl-CoA dehydrogenase/Etf complex from *Clostridium kluyveri*. *Journal of Bacteriology*, 190(3), 843–850. <https://doi.org/10.1128/JB.01417-07>
- Li, W.-Z., Stirling, K., Yang, J.-J., & Zhang, L. (2020). Gut microbiota and diabetes: From correlation to causality and mechanism. *World Journal of Diabetes*, 11(7), 293–308. <https://doi.org/10.4239/wjd.v11.i7.293>
- Li, Z., Wang, X., & Zhang, H. (2019). Balancing the non-linear rosmarinic acid biosynthetic pathway by modular co-culture engineering. *Metabolic Engineering*, 54, 1–11. <https://doi.org/10.1016/j.ymben.2019.03.002>
- Liang, Y., Ma, A., & Zhuang, G. (2022). Construction of Environmental Synthetic Microbial Consortia: Based on Engineering and Ecological Principles. In *Frontiers in Microbiology* (Vol. 13). Frontiers Media S.A. <https://doi.org/10.3389/fmicb.2022.829717>
- Lieven, C., Beber, M. E., Olivier, B. G., Bergmann, F. T., Ataman, M., Babaei, P., Bartell, J. A., Blank, L. M., Chauhan, S., Correia, K., Diener, C., Dramp, A., Ebert, B. E., Edirisinghe, J. N., Faria, P., Feist, A. M., Fengos, G., T Fleming, R. M., Garcamp, B., ... Zhang, C. (2020). MEMOTE for standardized genome-scale metabolic model testing. *Nature Biotechnology*, 38, 272–276. <https://doi.org/10.5281/zenodo.2636858>
- Lloyd-Price, J., Abu-Ali, G., & Huttenhower, C. (2016). The healthy human microbiome. In *Genome Medicine* (Vol. 8, Issue 1). BioMed Central Ltd. <https://doi.org/10.1186/s13073-016-0307-y>
- Lozupone, C. A., Stombaugh, J. I., Gordon, J. I., Jansson, J. K., & Knight, R. (2012). Diversity, stability and resilience of the human gut microbiota. In *Nature* (Vol. 489, Issue 7415, pp. 220–230). <https://doi.org/10.1038/nature11550>
- Machado, D., Andrejev, S., Tramontano, M., & Patil, K. R. (2018). Fast automated reconstruction of genome-scale metabolic models for microbial species and communities. *Nucleic Acids Research*, 46(15), 7542–7553. <https://doi.org/10.1093/nar/gky537>

- Mahadevan, R., & Schilling, C. H. (2003). The effects of alternate optimal solutions in constraint-based genome-scale metabolic models. *Metabolic Engineering*, 5(4), 264–276. <https://doi.org/10.1016/j.ymben.2003.09.002>
- Maldonado-Gómez, M. X., Martínez, I., Bottacini, F., O’Callaghan, A., Ventura, M., van Sinderen, D., Hillmann, B., Vangay, P., Knights, D., Hutkins, R. W., & Walter, J. (2016). Stable Engraftment of *Bifidobacterium longum* AH1206 in the Human Gut Depends on Individualized Features of the Resident Microbiome. *Cell Host and Microbe*, 20(4), 515–526. <https://doi.org/10.1016/j.chom.2016.09.001>
- Marcella, C., Cui, B., Kelly, C. R., Ianiro, G., Cammarota, G., & Zhang, F. (2021). Systematic review: the global incidence of faecal microbiota transplantation-related adverse events from 2000 to 2020. In *Alimentary Pharmacology and Therapeutics* (Vol. 53, Issue 1, pp. 33–42). Blackwell Publishing Ltd. <https://doi.org/10.1111/apt.16148>
- Martinez, I., Maldonado-Gomez, M. X., Gomes-Neto, J. C., Kittana, H., Ding, H., Schmaltz, R., Joglekar, P., Cardona, R. J., Marsteller, N. L., Kembel, S. W., Benson, A. K., Peterson, D. A., Ramer-Tait, A. E., & Walter, J. (2018). Experimental evaluation of the importance of colonization history in early-life gut microbiota assembly. *Elife*. <https://doi.org/10.7554/eLife.36521.001>
- Masheghati, F., Asgharzadeh, M. R., Jafari, A., Masoudi, N., & Maleki-Kakelar, H. (2024). The role of gut microbiota and probiotics in preventing, treating, and boosting the immune system in colorectal cancer. In *Life Sciences* (Vol. 344). Elsevier Inc. <https://doi.org/10.1016/j.lfs.2024.122529>
- McCarty, N. S., & Ledesma-Amaro, R. (2019). Synthetic Biology Tools to Engineer Microbial Communities for Biotechnology. In *Trends in Biotechnology* (Vol. 37, Issue 2, pp. 181–197). Elsevier Ltd. <https://doi.org/10.1016/j.tibtech.2018.11.002>
- Michail, S., Sylvester, F., Fuchs, G., & Issenman, R. (2006). Clinical efficacy of probiotics: Review of the evidence with focus on children. In *Journal of Pediatric Gastroenterology and Nutrition* (Vol. 43, Issue 4, pp. 550–557). <https://doi.org/10.1097/01.mpg.0000239990.35517.bf>
- Morozova, K., Bulbarello, A., Schaefer, C., Funda, E., Porta, F., & Scampicchio, M. (2020). Novel isothermal calorimetry approach to monitor micronutrients stability in powder forms. *LWT*, 117. <https://doi.org/10.1016/j.lwt.2019.108594>
- Mukherjee, A., Lordan, C., Ross, R. P., & Cotter, P. D. (2020). Gut microbes from the phylogenetically diverse genus *Eubacterium* and their various contributions to gut health. In *Gut Microbes* (Vol. 12, Issue 1). Taylor and Francis Inc. <https://doi.org/10.1080/19490976.2020.1802866>
- Münste, E., & Hartmann, P. (2025). The Role of Short-Chain Fatty Acids in Metabolic Dysfunction-Associated Steatotic Liver Disease and Other Metabolic Diseases. In *Biomolecules* (Vol. 15, Issue 4). Multidisciplinary Digital Publishing Institute (MDPI). <https://doi.org/10.3390/biom15040469>
- Muscogiuri, G., Cantone, E., Cassarano, S., Tuccinardi, D., Barrea, L., Savastano, S., & Colao, A. (2019). Gut microbiota: a new path to treat obesity. *International Journal of Obesity Supplements*, 9(1), 10–19. <https://doi.org/10.1038/s41367-019-0011-7>
- Nature. (n.d.). *Microbiome*. Retrieved December 12, 2024, from URL: <https://www.nature.com/subjects/microbiome>
- Navarro, Y., Torija, M. J., Mas, A., & Beltran, G. (2020). Viability-PCR allows monitoring yeast population dynamics in mixed fermentations including viable but non-culturable yeasts. *Foods*, 9(10). <https://doi.org/10.3390/foods9101373>

- Ndongo, S., Khelaifia, S., Lagier, J. C., & Raoult, D. (2020). From anaerobes to aerointolerant prokaryotes. In *Human Microbiome Journal* (Vol. 15). Elsevier Ltd. <https://doi.org/10.1016/j.humic.2019.100068>
- Niehaus, L., Boland, I., Liu, M., Chen, K., Fu, D., Henckel, C., Chaung, K., Miranda, S. E., Dyckman, S., Crum, M., Dedrick, S., Shou, W., & Momeni, B. (2019). Microbial coexistence through chemical-mediated interactions. *Nature Communications*, 10(1). <https://doi.org/10.1038/s41467-019-10062-x>
- Nocker, A., Cheswick, R., Dutheil de la Rochere, P. M., Denis, M., Léziart, T., & Jarvis, P. (2017). When are bacteria dead? A step towards interpreting flow cytometry profiles after chlorine disinfection and membrane integrity staining. *Environmental Technology (United Kingdom)*, 38(7), 891–900. <https://doi.org/10.1080/09593330.2016.1262463>
- Novakovic, M., Rout, A., Kingsley, T., Kirchoff, R., Singh, A., Verma, V., Kant, R., & Chaudhary, R. (2020). Role of gut microbiota in cardiovascular diseases. In *World Journal of Cardiology* (Vol. 12, Issue 4, pp. 110–122). Baishideng Publishing Group Co. <https://doi.org/10.4330/wjc.v12.i4.110>
- Oba, S., Sunagawa, T., Tanihiro, R., Awashima, K., Sugiyama, H., Odani, T., Nakamura, Y., Kondo, A., Sasaki, D., & Sasaki, K. (2020). Prebiotic effects of yeast mannan, which selectively promotes *Bacteroides thetaiotaomicron* and *Bacteroides ovatus* in a human colonic microbiota model. *Scientific Reports*, 10(1), 1–11. <https://doi.org/10.1038/s41598-020-74379-0>
- Oblinger, J. L., & Koburger, J. A. (1975). Understanding and Teaching the Most Probable Number Technique. *Journal of Food Protection*, 38(9), 540–545.
- Orth, J. D., Thiele, I., & Palsson, B. O. (2010). What is flux balance analysis? In *Nature Biotechnology* (Vol. 28, Issue 3, pp. 245–248). <https://doi.org/10.1038/nbt.1614>
- Ott, S. J., Waetzig, G. H., Rehman, A., Moltzau-Anderson, J., Bharti, R., Grasis, J. A., Cassidy, L., Tholey, A., Fickenscher, H., Seegert, D., Rosenstiel, P., & Schreiber, S. (2017). Efficacy of Sterile Fecal Filtrate Transfer for Treating Patients With *Clostridium difficile* Infection. *Gastroenterology*, 152(4), 799–811.e7. <https://doi.org/10.1053/j.gastro.2016.11.010>
- Peng, L., Li, Z. R., Green, R. S., Holzman, I. R., & Lin, J. (2009). Butyrate enhances the intestinal barrier by facilitating tight junction assembly via activation of AMP-activated protein kinase in Caco-2 cell monolayers. *Journal of Nutrition*, 139(9), 1619–1625. <https://doi.org/10.3945/jn.109.104638>
- Pereira, P. A. B., Trivedi, D. K., Silverman, J., Duru, I. C., Paulin, L., Auvinen, P., & Scheperjans, F. (2022). Multiomics implicate gut microbiota in altered lipid and energy metabolism in Parkinson's disease. *Npj Parkinson's Disease*, 8(1). <https://doi.org/10.1038/s41531-022-00300-3>
- Piwoz, K., Shabarova, T., Tomasch, J., Šimek, K., Kopejtká, K., Kahl, S., Pieper, D. H., & Koblížek, M. (2018). Determining lineage-specific bacterial growth curves with a novel approach based on amplicon reads normalization using internal standard (ARNIS). *ISME Journal*, 12(11), 2640–2654. <https://doi.org/10.1038/s41396-018-0213-y>
- Plovier, H., Everard, A., Druart, C., Depommier, C., Van Hul, M., Geurts, L., Chilloux, J., Ottman, N., Duparc, T., Lichtenstein, L., Myridakis, A., Delzenne, N. M., Klievink, J., Bhattacharjee, A., Van Der Ark, K. C. H., Aalvink, S., Martinez, L. O., Dumas, M. E., Maiter, D., ... Cani, P. D. (2017). A purified membrane protein from *Akkermansia muciniphila* or the pasteurized bacterium improves metabolism in obese and diabetic mice. *Nature Medicine*, 23(1), 107–113. <https://doi.org/10.1038/nm.4236>

- Pluznick, J. L. (2014). Gut microbes and host physiology: What happens when you host billions of guests? In *Frontiers in Endocrinology* (Vol. 5, Issue JUN). Frontiers Research Foundation. <https://doi.org/10.3389/fendo.2014.00091>
- Recharla, N., Geesala, R., & Shi, X. Z. (2023). Gut Microbial Metabolite Butyrate and Its Therapeutic Role in Inflammatory Bowel Disease: A Literature Review. In *Nutrients* (Vol. 15, Issue 10). Multidisciplinary Digital Publishing Institute (MDPI). <https://doi.org/10.3390/nu15102275>
- Roell, G. W., Zha, J., Carr, R. R., Koffas, M. A., Fong, S. S., & Tang, Y. J. (2019). Engineering microbial consortia by division of labor. In *Microbial Cell Factories* (Vol. 18, Issue 1). BioMed Central Ltd. <https://doi.org/10.1186/s12934-019-1083-3>
- Rosero, J. A., Killer, J., Sechovcová, H., Mrázek, J., Benada, O., Fliegerová, K., Havlík, J., & Kopečný, J. (2016). Reclassification of *Eubacterium rectale* (Hauduroy et al. 1937) prévot 1938 in a new genus *agathobacter* gen. nov. as *Agathobacter rectalis* comb. nov., and description of *Agathobacter ruminis* sp. nov., isolated from the rumen contents of sheep and cows. *International Journal of Systematic and Evolutionary Microbiology*, 66(2), 768–773. <https://doi.org/10.1099/ijsem.0.000788>
- Rothschild, D., Weissbrod, O., Barkan, E., Kurilshikov, A., Korem, T., Zeevi, D., Costea, P. I., Godneva, A., Kalka, I. N., Bar, N., Shilo, S., Lador, D., Vila, A. V., Zmora, N., Pevsner-Fischer, M., Israeli, D., Kosower, N., Malka, G., Wolf, B. C., ... Segal, E. (2018). Environment dominates over host genetics in shaping human gut microbiota. *Nature*, 555(7695), 210–215. <https://doi.org/10.1038/nature25973>
- Sakamoto, M., Sakurai, N., Tanno, H., Iino, T., Ohkuma, M., & Endo, A. (2022). Genome-based, phenotypic and chemotaxonomic classification of *Faecalibacterium* strains: proposal of three novel species *Faecalibacterium duncaniae* sp. nov., *Faecalibacterium hattorii* sp. nov. and *Faecalibacterium gallinarum* sp. nov. *International Journal of Systematic and Evolutionary Microbiology*, 72(4). <https://doi.org/10.1099/ijsem.0.005379>
- Santoyo, G., Guzmán-Guzmán, P., Parra-Cota, F. I., de los Santos-Villalobos, S., Orozco-Mosqueda, M. D. C., & Glick, B. R. (2021). Plant growth stimulation by microbial consortia. In *Agronomy* (Vol. 11, Issue 2). MDPI AG. <https://doi.org/10.3390/agronomy11020219>
- Scariot, M. C., Venturelli, G. L., Prudêncio, E. S., & Arisi, A. C. M. (2018). Quantification of *Lactobacillus paracasei* viable cells in probiotic yoghurt by propidium monoazide combined with quantitative PCR. *International Journal of Food Microbiology*, 264, 1–7. <https://doi.org/10.1016/j.ijfoodmicro.2017.10.021>
- Schwartz, A., Hold, G. L., Duncan, S. H., Gruhl, B., Collins, M. D., Lawson, P. A., Flint, H. J., & Blaut, M. (2002). *Anaerostipes caccae* gen. nov., sp. nov., a new saccharolytic, acetate-utilising, butyrate-producing bacterium from human faeces. *Systematic and Applied Microbiology*, 25(1), 46–51. <https://doi.org/10.1078/0723-2020-00096>
- Sekirov, I., Russell, S. L., Caetano, L., Antunes, M., & Finlay, B. B. (2010). *Gut Microbiota in Health and Disease*. <https://doi.org/10.1152/physrev.00045.2009>.-Gut
- Sender, R., Fuchs, S., & Milo, R. (2016a). Are We Really Vastly Outnumbered? Revisiting the Ratio of Bacterial to Host Cells in Humans. *Cell*, 164(3), 337–340. <https://doi.org/10.1016/j.cell.2016.01.013>
- Sender, R., Fuchs, S., & Milo, R. (2016b). Revised Estimates for the Number of Human and Bacteria Cells in the Body. *PLoS Biology*, 14(8), 1–14. <https://doi.org/10.1371/journal.pbio.1002533>

- Shannon, C. E. (1948). A Mathematical Theory of Communication. *The Bell System Technical Journal*, 27(3), 379–423.
- Sharon, G., Sampson, T. R., Geschwind, D. H., & Mazmanian, S. K. (2016). The Central Nervous System and the Gut Microbiome. In *Cell* (Vol. 167, Issue 4, pp. 915–932). Cell Press. <https://doi.org/10.1016/j.cell.2016.10.027>
- Shin, H. D., McClendon, S., Vo, T., & Chen, R. R. (2010). Escherichia coli binary culture engineered for direct fermentation of hemicellulose to a biofuel. *Applied and Environmental Microbiology*, 76(24), 8150–8159. <https://doi.org/10.1128/AEM.00908-10>
- Singh, N., Gurav, A., Sivaprakasam, S., Brady, E., Padia, R., Shi, H., Thangaraju, M., Prasad, P. D., Manicassamy, S., Munn, D. H., Lee, J. R., Offermanns, S., & Ganapathy, V. (2014). Activation of Gpr109a, receptor for niacin and the commensal metabolite butyrate, suppresses colonic inflammation and carcinogenesis. *Immunity*, 40(1), 128–139. <https://doi.org/10.1016/j.immuni.2013.12.007>
- Singh, T. P., & Natraj, B. H. (2021). Next-generation probiotics: a promising approach towards designing personalized medicine. In *Critical Reviews in Microbiology* (Vol. 47, Issue 4, pp. 479–498). Taylor and Francis Ltd. <https://doi.org/10.1080/1040841X.2021.1902940>
- Smets, W., Leff, J. W., Bradford, M. A., McCulley, R. L., Lebeer, S., & Fierer, N. (2016). A method for simultaneous measurement of soil bacterial abundances and community composition via 16S rRNA gene sequencing. *Soil Biology and Biochemistry*, 96, 145–151. <https://doi.org/10.1016/j.soilbio.2016.02.003>
- Sokol, H., Landman, C., Seksik, P., Berard, L., Montil, M., Nion-Larmurier, I., Bourrier, A., Le Gall, G., Lalande, V., De Rougemont, A., Kirchgessner, J., Dagueneil, A., Cachanado, M., Rousseau, A., Drouet, É., Rosenzweig, M., Hagege, H., Dray, X., Klatzman, D., ... Simon, T. (2020). Fecal microbiota transplantation to maintain remission in Crohn's disease: A pilot randomized controlled study. *Microbiome*, 8(1), 1–14. <https://doi.org/10.1186/s40168-020-0792-5>
- Song, Z., Cai, Y., Lao, X., Wang, X., Lin, X., Cui, Y., Kalavagunta, P. K., Liao, J., Jin, L., Shang, J., & Li, J. (2019). Taxonomic profiling and populational patterns of bacterial bile salt hydrolase (BSH) genes based on worldwide human gut microbiome. *Microbiome*, 7(1). <https://doi.org/10.1186/s40168-019-0628-3>
- Stewart, E. J. (2012). Growing unculturable bacteria. In *Journal of Bacteriology* (Vol. 194, Issue 16, pp. 4151–4160). <https://doi.org/10.1128/JB.00345-12>
- Stoddard, S. F., Smith, B. J., Hein, R., Roller, B. R. K., & Schmidt, T. M. (2015). rrnDB: Improved tools for interpreting rRNA gene abundance in bacteria and archaea and a new foundation for future development. *Nucleic Acids Research*, 43(D1), D593–D598. <https://doi.org/10.1093/nar/gku1201>
- Stone, L. (2019). Faecal microbiota transplantation for Clostridioides difficile infection. *Nature Milestones*.
- Stulova, I., Kabanova, N., Kriščiunaite, T., Adamberg, K., Laht, T. M., & Vilu, R. (2015). Microcalorimetric study of the growth of Streptococcus thermophilus in renneted milk. *Frontiers in Microbiology*, 6(FEB). <https://doi.org/10.3389/fmicb.2015.00079>
- Su, L., Hong, Z., Zhou, T., Jian, Y., Xu, M., Zhang, X., Zhu, X., & Wang, J. (2022). Health improvements of type 2 diabetic patients through diet and diet plus fecal microbiota transplantation. *Scientific Reports*, 12(1), 1–12. <https://doi.org/10.1038/s41598-022-05127-9>

- Sultan, A. R., Tavakol, M., Lemmens-Den Toom, N. A., Croughs, P. D., Verkaik, N. J., Verbon, A., & van Wamel, W. J. B. (2022). Real time monitoring of *Staphylococcus aureus* biofilm sensitivity towards antibiotics with isothermal microcalorimetry. *PLoS ONE*, 17(2 February). <https://doi.org/10.1371/journal.pone.0260272>
- Tan, A. H., Chong, C. W., Lim, S. Y., Yap, I. K. S., Teh, C. S. J., Loke, M. F., Song, S. L., Tan, J. Y., Ang, B. H., Tan, Y. Q., Kho, M. T., Bowman, J., Mahadeva, S., Yong, H. Sen, & Lang, A. E. (2021). Gut Microbial Ecosystem in Parkinson Disease: New Clinicobiological Insights from Multi-Omics. *Annals of Neurology*, 89(3), 546–559. <https://doi.org/10.1002/ana.25982>
- Thiele, I., & Palsson, B. (2010). A protocol for generating a high-quality genome-scale metabolic reconstruction. *Nature Protocols*, 5(1), 93–121. <https://doi.org/10.1038/nprot.2009.203>
- Tkacz, A., Hortala, M., & Poole, P. S. (2018). Absolute quantitation of microbiota abundance in environmental samples. *Microbiome*, 6(1). <https://doi.org/10.1186/s40168-018-0491-7>
- Tripathi, A., Debelius, J., Brenner, D. A., Karin, M., Lomaba, R., Schnabl, B., & Knight, R. (2018). The gut-liver axis and the intersection with the microbiome. In *Nature Reviews Gastroenterology and Hepatology* (Vol. 15, Issue 7, pp. 397–411). Nature Publishing Group. <https://doi.org/10.1038/s41575-018-0011-z>
- Truchado, P., Gil, M. I., Larrosa, M., & Allende, A. (2020). Detection and Quantification Methods for Viable but Non-culturable (VBNC) Cells in Process Wash Water of Fresh-Cut Produce: Industrial Validation. *Frontiers in Microbiology*, 11. <https://doi.org/10.3389/fmicb.2020.00673>
- Vandeputte, D., Kathagen, G., D’Hoe, K., Vieira-Silva, S., Valles-Colomer, M., Sabino, J., Wang, J., Tito, R. Y., De Commer, L., Darzi, Y., Vermeire, S., Falony, G., & Raes, J. (2017). Quantitative microbiome profiling links gut community variation to microbial load. *Nature*, 551(7681), 507–511. <https://doi.org/10.1038/nature24460>
- Wang, E. X., Ding, M. Z., Ma, Q., Dong, X. T., & Yuan, Y. J. (2016). Reorganization of a synthetic microbial consortium for one-step vitamin C fermentation. *Microbial Cell Factories*, 15(1). <https://doi.org/10.1186/s12934-016-0418-6>
- Weghoff, M. C., Bertsch, J., & Müller, V. (2015). A novel mode of lactate metabolism in strictly anaerobic bacteria. *Environmental Microbiology*, 17(3), 670–677. <https://doi.org/10.1111/1462-2920.12493>
- Weiss, J. E., & Rettger, L. F. (1937). The Gram-negative *Bacteroides* of the intestine. *Journal of Bacteriology*, 3, 423–434.
- Whipps J, Lewis K, & Cooke R. (1988). Mycoparasitism and plant disease control. In M. Burge (Ed.), *Fungi in Biological Control Systems* (pp. 161–187). Manchester University Press.
- Widder, S., Allen, R. J., Pfeiffer, T., Curtis, T. P., Wiuf, C., Sloan, W. T., Cordero, O. X., Brown, S. P., Momeni, B., Shou, W., Kettle, H., Flint, H. J., Haas, A. F., Laroche, B., Kreft, J. U., Rainey, P. B., Freilich, S., Schuster, S., Milferstedt, K., ... Wilmes, P. (2016). Challenges in microbial ecology: Building predictive understanding of community function and dynamics. In *ISME Journal* (Vol. 10, Issue 11, pp. 2557–2568). Springer Nature. <https://doi.org/10.1038/ismej.2016.45>
- Xu, Y., Zhong, F., Zheng, X., Lai, H. Y., Wu, C., & Huang, C. (2022). Disparity of Gut Microbiota Composition Among Elite Athletes and Young Adults With Different Physical Activity Independent of Dietary Status: A Matching Study. *Frontiers in Nutrition*, 9(March). <https://doi.org/10.3389/fnut.2022.843076>

- Zanaroli, G., Toro, S. Di, Todaro, D., Varese, G. C., Bertolotto, A., & Fava, F. (2010). *Characterization of two diesel fuel degrading microbial consortia enriched from a non acclimated, complex source of microorganisms*. <http://www.microbialcellfactories.com/content/9/1/10>
- Zemb, O., Achard, C. S., Hamelin, J., De Almeida, M. L., Gabinaud, B., Cauquil, L., Verschuren, L. M. G., & Godon, J. J. (2020). Absolute quantitation of microbes using 16S rRNA gene metabarcoding: A rapid normalization of relative abundances by quantitative PCR targeting a 16S rRNA gene spike-in standard. *MicrobiologyOpen*, 9(3). <https://doi.org/10.1002/mbo3.977>
- Zhang, F., Cui, B., He, X., Nie, Y., Wu, K., Fan, D., Feng, B., Chen, D., Ren, J., Deng, M., Li, N., Zheng, P., Cao, Q., Yang, S., Liu, Y., Zhou, Y., Nie, Y., Ji, G., & Li, P. (2018). Microbiota transplantation: concept, methodology and strategy for its modernization. In *Protein and Cell* (Vol. 9, Issue 5, pp. 462–473). Higher Education Press. <https://doi.org/10.1007/s13238-018-0541-8>
- Ziesack, M., Gibson, T., Oliver, J. K. W., Shumaker, A. M., Hsu, B. B., Riglar, D. T., Giessen, T. W., Dibenedetto, N. V., Bry, L., Way, J. C., Silver, P. A., & Gerber, G. K. (2019). *Engineered Interspecies Amino Acid Cross-Feeding Increases Population Evenness in a Synthetic Bacterial Consortium*. <https://journals.asm.org/journal/msystems>

Acknowledgements

Financial support was provided by the European Regional Development Fund through the project “High throughput platform for growth improvement of microorganisms” (NSP137, 2014–2020.4.02.17-0104), funded by SA Archimedes. This work was also partially supported by the “TUT Institutional Development Program for 2016–2022” Graduate School in Biomedicine and Biotechnology, receiving funding from the European Regional Development Fund under the ASTRA program (2014–2020.4.01.16-0032) in Estonia.

This work was conducted at AS TFTAK, an innovative research centre where I had the opportunity to grow both professionally and personally. This research would not have been possible without the visionary leadership of Raivo Vilu. Over the course of my work there, I gained valuable experience in scientific research, bioprocess development, and collaborative problem-solving. I am grateful to my supervisor, Ranno Nahku, for his guidance and support. I enjoyed the scientific journey we shared and the many projects we worked on together. Kudos to Jekaterina Kazantseva for the guidance in the thesis writing process.

My sincere thanks go to entire Bioprocess group at TFTAK for being awesome colleagues. Special thanks to Isma Belouah and Mariann Vendelin for the insightful discussions and tea breaks that helped me get through even the toughest days. I am also thankful to my colleagues at TalTech Kuressaare College for their support during the thesis writing process.

Lastly, I extend my deepest gratitude to my partner Siim, mother Pille, sister Leena, and brother Aleksander. Thank you for your long-lasting support and motivational talks throughout my studies. To my late father, thank you for everything. I hope this makes you proud.

Abstract

Metabolic characterization and composition control of next generation probiotic consortia

The human gut microbiome plays an important role in host health, contributing to digestion, immune function, and pathogen resistance. While traditional probiotics have long been used to support gut health, their effectiveness is often limited to specific strains and conditions. This has led to growing interest in next-generation probiotics, which include strictly anaerobic commensals with demonstrated health benefits but also complex cultivation requirements. One promising strategy to overcome these limitations is the use of defined microbial consortia, where multiple strains are co-cultivated under controlled conditions to improve stability, and reduce production complexity. However, challenges remain in achieving reproducible growth, maintaining and controlling species ratio, and assessing cell viability in these systems. This thesis addresses these challenges by developing and testing workflows for cultivating and controlling NGP-based consortia with the goal of achieving stability and compositional control.

The main aim of this thesis was to develop and validate workflows for the cultivation, characterization, and compositional control of synthetic consortia composed of next-generation probiotics candidate strains. This work combines experimental and computational methodologies, including isothermal microcalorimetry (IMC), genome-scale metabolic modelling (GEM), flux balance analysis (FBA), microscopy-based image analysis, and quantitative viability assays using PMAxx-qPCR as well as next-generation sequencing (NGS) combined with both PMAxx treatment and spike-in controls. Together, these methods were used to explore the stability, resilience, and cross-feeding among microbial consortia under batch cultivation conditions.

Results were obtained through three publications and an additional set of unpublished data. First, a simplified three-species model consortium (*Akkermansia muciniphila*, *Bacteroides thetaiotaomicron*, and *Faecalibacterium prausnitzii*) was used to explore consortium stability and resilience over serial batch passages using IMC. The consortium exhibited stable heat flow profiles and consistent species ratios. The consortium was also resilient to initial compositional disturbances, returning to its original state within two to four passages.

To extend these findings, a more complex 25-species model consortium was cultivated under anaerobic conditions in serial batch format. Despite achieving high diversity after third passage (Shannon index = 2.26), precise compositional control remained a challenge. To address this, unique substrate approach was proposed and tested, wherein each species was provided a unique carbon source. This trait-based design reduced competition and enabled control of species abundance. Stable two-species co-cultures including *Anaerostipes caccae* with either *Bacteroides thetaiotaomicron* or *Bacteroides vulgatus* were validated using IMC, microscopy, and metabolite analysis. Cross-feeding interactions enhanced butyrate and propionate production. Furthermore, defined media allowed a more accurate application of FBA. While modelling in complex media (Publication I) remained limited due to insufficient data, the combined use of GEMs and empirical validation in Publication II helped to identify key cross-feeding mechanisms, especially involving short-chain fatty acids such as acetate and butyrate.

In Publication III, we evaluated the viability of 20 individual strains and their combined consortia using both PMAxx-qPCR and flow cytometry. PMAxx-qPCR, which selectively

quantifies cells with intact membranes, proved to be a rapid and effective alternative to traditional methods. It provided reliable viability assessments for both individual strains and a 20-strain mixture. However, when the composition of a consortium is unknown, qPCR is not feasible. To address this, we used NGS in combination with PMAxx treatment and spike-in controls, making possible both viability determination and absolute enumeration. Together, these approaches offer alternatives for monitoring cell viability and abundance during cultivation and long-term storage of defined microbial consortia. Moreover, they are adaptable to various types of consortia, including those with unknown composition or greater complexity.

The methodologies developed in this thesis offer a framework for building scalable microbial consortia for industrial use. Nevertheless, limitations remain in extending these workflows to more diverse consortia. Future work should focus on improving compositional control in larger consortia and optimizing media for broader strain coverage. In summary, this thesis demonstrates that co-cultivation using a unique substrate approach can be a scalable method to produce defined consortium. The combination of experimental and modelling approaches provides new insights into microbial interactions and supports the rational design of stable and resilient microbial consortia.

Lühikokkuvõte

Uue põlvkonna probiootiliste koosluste koostise kontroll ja metaboolne iseloomustus

Inimese soolestiku mikrobioomil on oluline roll, aidates kaasa seedimisele, immuunfunktsioonile ja patogeene resistentsusele. Kuigi traditsioonilisi probiootikume on soolestiku tervise toetamiseks juba pikka aega kasutatud, piirdub nende efektiivsus sageli teatud tüvede ja haigusseisunditega. See on toonud kaasa kasvava huvi järgmise põlvkonna probiootikumide vastu, mis hõlmavad rangelt anaeroobseid baktereid. Neil on tõestatud tervisele kasulik mõju, kuid nende kultiveerimine on keeruline. Üks potentsiaalne strateegia on nende kasvatamine kooslusena, et parandada stabiilsust ja imiteerida nende kasvukeskkonda. Siiski on endiselt probleeme reprodutseeritava kasvu saavutamise, liikide suhte säilitamise ja kontrollimisega ning rakkude elujõulisuse hindamisega. See doktoritöö käsitleb neid probleeme, arendades ja testides töövooge koosluste kultiveerimiseks ja kontrollimiseks eesmärgiga saavutada stabiilsus ja koostise kontroll. Selleks kasutati mitmeid eksperimentaalseid ja arvutuslike meetodeid, sealhulgas isotermaalset kalorimeetriat (IMC), genoomi skaalal ainevahetuse modelleerimist (GEM), voobalansi analüüsi (FBA), mikroskoopiat ning PMAx-qPCR meetodit koos *spike-in* kontrolliga, et hinnata rakkude elumust ja hulka.

Doktoritöö raames näidati, et kolmeliikmeline mudelkooslus (*Akkermansia muciniphila*, *Bacteroides thetaiotaomicron*, *Faecalibacterium prausnitzii*) säilitab stabiilse koostise järjestikustes annuskultiveerimistes ning rakkude suhe on võimeline taastuma, kui inokulumis on rakkude suhet muudetud. Nende tulemuste põhjal kultiveeriti 25-liikmelist kooslust järjestikustes annuskultuurides isotermaalses mikrokalorimeetris. Kolmanda annuskultuuri lõpus oli koosluse mitmekesisus kõrge (Shannoni indeks 2.26), kuid liikmete suhtelise arvukuse muutmine oli piiratud. Sellest tulenevalt töötati välja unikaalsete substraatide lähenemine, kus igale liigile oli keskkonnas ainult nende poolt tarbitav peamine süsinikuallikas. Selline lähenemine vähendas konkurentsi ning võimaldas reguleerida liikide suhteid substraadikontsentratsioonide abil. Metaboliitide kvantitatiivne analüüs kinnitas, et testitud kooslused olid stabiilsed ning tõenäoliselt toimub liikide vahel rist-toitumine. Kuna kasutati defineeritud söödet, siis oli lisaks võimalik viia läbi FBA, mis omakorda kinnitas rist-toitumise.

Kolmandas publikatsioonis hinnati PMAx-qPCR meetodi sobivust rakkude elumuse hindamiseks. Analüüsiti 20 erinevat tüve ning nendest koosnevat kooslust ja saadud tulemusi võrreldi voolutsütomeetriaga saadud andmetega. PMAx reagent seondub kovalentselt rakkudega, mille membraan on kompromiteeritud, inhibeerides seeläbi PCR reaktsiooni. Nii voolutsütomeetria kui ka PMAx-qPCR andsid võrreldavaid tulemusi, mis kinnitab viimase sobivust elumuse hindamiseks nii monokultuurides kui ka kooslustes. Siiski, juhtudel kui koosluse täpne koostis pole teada, pole qPCR rakendatav. Selliste proovide jaoks on sobiv kasutada järgmise põlvkonna sekveneerimist, mida kombineeriti käesolevas töös PMAx ja *spike-in* kontrolliga, et hinnata nii rakkude elumust kui ka koguarvu. Tulemused korreleerusid hästi voolutsütomeetria andmetega. Väljatöötatud meetodeid on võimalik rakendada nii koosluste bioprotsesside arendamisel ja säilivuskatsetet biotehnoloogias kui ka muudes valdkondades nagu toit või põllumajandus.

Appendix 1

Supplemental materials

Supplementary Tables
Supplementary tables to Publication I

Table S1. Consortium resilience evaluation by modifying the initial concentration of one species at a time in the inoculum. At the end of each passage (1-5), the relative abundances of *A. muciniphila* (AM), *B. thetaiotaomicron* (BT), and *F. prausnitzii* (FP) was determined. Relative abundances were quantified using 16S rRNA sequencing (n=3). The consortium conditions rAM+BT+FP, AM+rBT+FP, and AM+BT+rFP indicate that the initial concentration of *A. muciniphila*, *B. thetaiotaomicron*, and *F. prausnitzii*, respectively, were reduced (r) at the start of the experiment. Adapted from: Kattel et al., (2024), *MicrobiologyOpen*, Wiley. Licensed under CC BY 4.0.

Condition I		rAM+BT+FP			
Passage	1	2	3	4	5
AM	8.88 ± 1.38	15.09 ± 2.73	25.37 ± 10.11	36.03 ± 1.25	31.02 ± 1.9
BT	85.95 ± 1.54	63.81 ± 0.5	55.44 ± 9.74	44.74 ± 0.57	55.98 ± 2.1
FP	5.17 ± 0.27	21.1 ± 2.26	19.19 ± 1.02	19.23 ± 0.69	13 ± 0.32
Condition II		AM+rBT+FP			
Passage	1	2	3	4	5
AM	38.21 ± 2.04	19.64 ± 2.84	33.74 ± 2.64	35.78 ± 2.53	32.56 ± 4.84
BT	53.18 ± 1.91	56.47 ± 1.41	46.81 ± 2.56	44.64 ± 1.9	54.6 ± 5.32
FP	8.61 ± 0.52	23.88 ± 1.64	19.45 ± 0.08	19.59 ± 0.66	12.84 ± 0.53
Condition III		AM+BT+rFP			
Passage	1	2	3	4	5
AM	40.02 ± 1.16	21.97 ± 2.21	30.33 ± 9.25	36.26 ± 3.67	33.9 ± 0.94
BT	57.51 ± 1.05	56.96 ± 2.54	50.24 ± 7.52	47.46 ± 3.88	53.98 ± 1.15
FP	2.48 ± 0.12	21.07 ± 0.33	19.43 ± 1.74	16.29 ± 0.21	12.12 ± 0.21

Supplementary tables to Publication II

Table S2. Predicted metabolic capabilities with percentage indicating the completeness level of each specific pathway. Adapted from: Kattel et al., (2023), *Anaerobe*, Elsevier. Used under author rights.

Metabolite	Direction	KEGG/ PubChem code	<i>B. adolescentis</i>	<i>B. longum</i>	<i>B. thetaiotaomicron</i>	<i>B. caccae</i>	<i>B. ovatus</i>	<i>B. uniformis</i>	<i>B. vulgatus</i>	<i>A. caccae</i>
			DSM 20087	DSM 20088	DSM 2079	DSM 19024	DSM 1896	DSM 6597	DSM 3289	DSM 14662
Glycogen	deg	C00182	100%	100%	100%	100%	100%	100%	100%	100%
Amylose	deg	C00718	100%	100%	100%	100%	100%	100%	100%	0%
Amylopectin	deg	C00317	100%	0%	100%	100%	100%	100%	100%	0%
Maltodextrin	deg	C01935	100%	100%	100%	100%	100%	100%	100%	0%
Pullulan	deg	C00480	100%	0%	100%	100%	100%	100%	100%	0%
Dextrin	deg	C00721	100%	0%	100%	100%	100%	100%	100%	0%
Pectin	deg	C00714	0%	38%	91%	82%	91%	82%	91%	50%
Rhamnogalacturonan	deg	C131801240	10%	20%	90%	80%	90%	50%	70%	20%
Xylan	deg	C00707	75%	50%	100%	100%	100%	100%	100%	50%
Glucuronoarabinoxylan	deg	C405238131	67%	50%	100%	83%	100%	83%	100%	33%
Sucrose	deg	C00089	100%	100%	100%	50%	50%	100%	50%	100%
Lactose	deg	C00243	86%	100%	86%	86%	86%	86%	71%	100%
Maltose	deg	C00208	100%	100%	100%	100%	100%	100%	67%	100%
Raffinose	deg	C00492	100%	100%	100%	67%	67%	100%	67%	100%
Melibiose	deg	C05402	100%	100%	100%	100%	100%	100%	50%	100%
Trehalose	deg	C01083	50%	50%	50%	50%	50%	100%	50%	50%

Turanose	deg	C19636	100%	100%	100%	100%	100%	100%	67%	67%
Cellobiose	deg	C00185	0%	0%	0%	0%	0%	0%	0%	100%
Melezitose	deg	C08243	0%	0%	0%	0%	0%	0%	0%	0%
D-Glucose	deg	C00031	100%	100%	100%	100%	100%	100%	100%	100%
L-Glucose	deg	C10954115	0%	0%	0%	0%	0%	17%	17%	0%
D-Mannose	deg	C00159	0%	0%	100%	100%	100%	100%	100%	100%
D-Galactose	deg	C00124	80%	100%	80%	80%	80%	80%	80%	100%
D-Allose	deg	C01487	33%	33%	33%	33%	33%	33%	33%	33%
D-Fructose	deg	C00095	0%	0%	100%	100%	100%	100%	100%	100%
D-Tagatose	deg	C00795	0%	0%	0%	0%	0%	0%	0%	0%
D-Allulose	deg	C06468	50%	50%	50%	50%	50%	50%	50%	50%
L-Sorbose	deg	C00247	0%	0%	0%	0%	0%	0%	0%	100%
D-Glucuronate	deg	C00191	0%	60%	100%	100%	100%	100%	80%	80%
D-Mannuronate	deg	C02024	0%	0%	0%	0%	0%	0%	0%	0%
D-Galacturonate	deg	C00333	0%	20%	100%	100%	100%	100%	100%	60%
D-Fructuronate	deg	C00905	0%	50%	100%	100%	100%	100%	75%	75%
D-Methylgalacturonate	deg	Cp7195798	0%	17%	83%	83%	83%	83%	83%	50%
D-Gluconate	deg	C00257	100%	50%	100%	100%	100%	100%	100%	67%
L-Gluconate	deg	C38988608	0%	0%	0%	0%	0%	20%	20%	0%
D-Mannonate	deg	C00514	0%	33%	100%	100%	100%	100%	100%	67%
D-Galactonate	deg	C00880	0%	0%	0%	0%	0%	0%	0%	0%
L-Galactonate	deg	C15930	0%	0%	80%	80%	80%	80%	80%	40%
D-Altronate	deg	C00817	0%	0%	100%	100%	100%	100%	100%	67%

D-Idonate	deg	C44457530	0%	0%	0%	0%	0%	33%	33%	0%
L-Idonate	deg	C00770	33%	0%	33%	33%	33%	33%	33%	67%
L-Gulonate	deg	C00800	0%	40%	80%	80%	80%	80%	60%	60%
D-Glucarate	deg	C00818	0%	0%	0%	0%	0%	0%	0%	25%
Galactarate	deg	C00879	0%	0%	33%	33%	33%	33%	33%	25%
D-Glucosamine	deg	C00329	0%	100%	100%	100%	100%	100%	100%	100%
NAC-D-Glucosamine	deg	C00140	0%	100%	100%	100%	100%	50%	100%	100%
D-Galactosamine	deg	C02262	0%	0%	33%	33%	33%	33%	33%	67%
NAC-D-Galactosamine	deg	C01132	43%	71%	71%	71%	71%	57%	71%	57%
NAC-Neuraminate	deg	C00270	0%	80%	60%	80%	80%	60%	80%	60%
L-Rhamnose	deg	C00507	20%	20%	100%	80%	100%	80%	100%	20%
D-Fucose	deg	C01018	0%	0%	0%	0%	0%	0%	0%	0%
L-Fucose	deg	C01019	20%	40%	100%	100%	100%	40%	67%	20%
D-Sorbitol	deg	C00794	100%	50%	100%	50%	100%	50%	100%	100%
D-Mannitol	deg	C00392	0%	0%	0%	0%	0%	0%	0%	100%
Galactitol	deg	C01697	0%	0%	0%	0%	0%	0%	0%	100%
D-Altritol	deg	C21524	0%	0%	0%	0%	0%	0%	0%	0%
D-myo-Inositol	deg	C00137	0%	22%	56%	56%	56%	56%	33%	86%
D-Ribose	deg	C00121	100%	100%	100%	100%	100%	100%	100%	100%
D-Arabinose	deg	C00216	50%	50%	100%	100%	100%	100%	100%	63%
L-Arabinose	deg	C00259	100%	0%	100%	100%	100%	100%	100%	33%
D-Xylose	deg	C00181	100%	50%	100%	100%	100%	100%	100%	100%
L-Xylose	deg	C01510	0%	0%	0%	0%	0%	0%	0%	0%

D-Lyxose	deg	C00476	50%	50%	50%	100%	50%	50%	50%	50%
L-Lyxose	deg	C01508	25%	0%	25%	25%	25%	25%	25%	25%
D-Ribulose	deg	C00309	100%	57%	100%	100%	100%	100%	100%	71%
L-Ribulose	deg	C00508	100%	0%	100%	100%	100%	100%	100%	50%
D-Xylulose	deg	C00310	100%	50%	100%	50%	100%	50%	100%	100%
L-Xylulose	deg	C00312	67%	33%	67%	33%	67%	33%	67%	67%
D-Ribonate	deg	C01685	50%	50%	50%	50%	50%	50%	50%	50%
D-Arabinonate	deg	C00878	0%	0%	0%	0%	0%	0%	0%	0%
L-Arabinonate	deg	C00545	0%	0%	0%	0%	0%	0%	0%	0%
D-Xylonate	deg	C00502	0%	0%	0%	0%	0%	0%	0%	0%
L-Lyxonate	deg	C05412	0%	0%	0%	0%	0%	0%	0%	0%
Ribitol	deg	C00474	0%	0%	0%	0%	0%	0%	0%	0%
Xylitol	deg	C00379	50%	50%	50%	50%	50%	50%	50%	50%
D-Arabitol	deg	C01904	50%	50%	50%	50%	50%	50%	50%	50%
L-Arabitol	deg	C00532	0%	0%	0%	0%	0%	0%	0%	0%
L-Alanine	syn	C00041	100%	100%	100%	100%	100%	100%	100%	0%
L-Alanine	deg	C00041	100%	100%	100%	100%	100%	100%	100%	100%
L-Arginine	syn	C00062	100%	100%	56%	56%	56%	56%	56%	100%
L-Arginine	deg	C00062	40%	40%	100%	100%	100%	100%	100%	60%
L-Asparagine	syn	C00152	100%	100%	100%	100%	100%	100%	100%	100%
L-Asparagine	deg	C00152	100%	0%	100%	100%	100%	100%	100%	0%
L-Aspartate	syn	C00049	100%	100%	100%	100%	100%	100%	100%	100%
L-Aspartate	deg	C00049	100%	100%	100%	100%	100%	100%	100%	100%

L-Cysteine	syn	C00097	100%	100%	100%	100%	100%	100%	100%	100%
L-Cysteine	deg	C00097	100%	100%	100%	100%	100%	100%	100%	50%
L-Glutamine	syn	C00064	100%	100%	100%	100%	100%	100%	100%	100%
L-Glutamine	deg	C00064	100%	100%	100%	100%	100%	100%	100%	100%
L-Glutamate	syn	C00025	100%	100%	100%	100%	100%	100%	100%	100%
L-Glutamate	deg	C00025	100%	100%	100%	100%	100%	100%	100%	100%
Glycine	syn	C00037	100%	100%	100%	100%	100%	100%	100%	100%
Glycine	deg	C00037	50%	50%	100%	100%	100%	100%	100%	50%
L-Histidine	syn	C00135	89%	89%	100%	100%	100%	100%	100%	100%
L-Histidine	deg	C00135	0%	20%	100%	0%	100%	100%	100%	0%
L-Isoleucine	syn	C00407	100%	100%	100%	100%	100%	100%	100%	100%
L-Isoleucine	deg	C00407	38%	38%	100%	100%	100%	100%	100%	63%
L-Leucine	syn	C00123	100%	100%	100%	100%	100%	100%	100%	100%
L-Leucine	deg	C00123	14%	14%	100%	100%	100%	100%	100%	14%
L-Lysine	syn	C00047	100%	100%	100%	100%	100%	100%	100%	100%
L-Lysine	deg	C00047	0%	0%	100%	100%	100%	100%	100%	33%
L-Methionine	syn	C00073	100%	100%	100%	100%	100%	100%	100%	100%
L-Methionine	deg	C00073	100%	100%	80%	80%	80%	80%	80%	67%
L-Phenylalanine	syn	C00079	100%	100%	100%	100%	100%	100%	100%	100%
L-Phenylalanine	deg	C00079	14%	14%	25%	25%	25%	25%	25%	25%
L-Proline	syn	C00148	100%	100%	100%	100%	100%	100%	100%	100%
L-Proline	deg	C00148	0%	0%	100%	100%	0%	0%	100%	0%
L-Serine	syn	C00065	100%	100%	100%	100%	100%	100%	100%	67%

L-Serine	deg	C00065	100%	100%	100%	100%	100%	100%	100%	100%
L-Threonine	syn	C00188	100%	100%	100%	100%	100%	100%	100%	100%
L-Threonine	deg	C00188	100%	100%	100%	100%	100%	100%	100%	100%
L-Tryptophan	syn	C00078	100%	100%	100%	100%	100%	100%	100%	100%
L-Tryptophan	deg	C00078	13%	13%	100%	0%	100%	100%	13%	10%
L-Tyrosine	syn	C00082	100%	100%	100%	100%	100%	100%	100%	100%
L-Tyrosine	deg	C00082	20%	20%	40%	40%	40%	40%	40%	20%
L-Valine	syn	C00183	100%	100%	100%	100%	100%	100%	100%	100%
L-Valine	deg	C00183	33%	33%	100%	100%	100%	100%	100%	44%
D-Alanine	syn	C00133	100%	100%	100%	100%	100%	100%	100%	100%
D-Alanine	deg	C00133	100%	100%	100%	100%	100%	100%	100%	100%
D-Arginine	syn	C00792	0%	0%	0%	0%	0%	0%	0%	0%
D-Arginine	deg	C00792	0%	0%	0%	0%	0%	0%	0%	0%
D-Aspartate	syn	C00402	100%	0%	0%	0%	0%	0%	0%	0%
D-Aspartate	deg	C00402	100%	0%	0%	0%	0%	0%	0%	0%
D-Cysteine	syn	C00793	0%	0%	0%	0%	0%	0%	0%	0%
D-Cysteine	deg	C00793	0%	0%	0%	0%	0%	0%	0%	0%
D-Glutamine	syn	C00819	0%	0%	0%	0%	0%	0%	0%	0%
D-Glutamine	deg	C00819	100%	100%	100%	100%	100%	100%	100%	100%
D-Glutamate	syn	C00217	100%	100%	100%	100%	100%	100%	100%	100%
D-Glutamate	deg	C00217	100%	100%	100%	100%	100%	100%	100%	100%
D-Lysine	syn	C00739	0%	0%	0%	0%	0%	0%	0%	0%
D-Lysine	deg	C00739	0%	0%	0%	0%	0%	0%	0%	0%

D-Ornithine	syn	C00515	0%	0%	0%	0%	0%	0%	0%	0%
D-Ornithine	deg	C00515	0%	0%	0%	0%	0%	0%	0%	0%
D-Proline	syn	C00763	0%	0%	0%	0%	0%	0%	0%	0%
D-Proline	deg	C00763	0%	0%	0%	0%	0%	0%	0%	0%
D-Serine	syn	C00740	0%	0%	0%	0%	0%	0%	0%	0%
D-Serine	deg	C00740	0%	0%	0%	0%	0%	0%	0%	0%
Beta-alanine	syn	C00099	50%	50%	100%	100%	100%	100%	100%	100%
Beta-alanine	deg	C00099	0%	0%	0%	0%	0%	0%	0%	0%

Table S3. Consumption and production of metabolites by *A. caccae*. The data represent the average consumption/production (mM) \pm standard error (n = 3). Adapted from: Kattel et al., (2023), *Anaerobe*, Elsevier. Used under author rights.

Amount of acetate in the medium	Sorbitol	Acetate	Butyrate	Ethanol	Formate	Lactate	Malate	Propionate	Succinate
0 mM	-5.87 \pm 0.00	ND	1.46 \pm 0.01	0.66 \pm 0.21	0.03 \pm 0.01	5.24 \pm 0.04	ND	ND	ND
2 mM	-5.34 \pm 0.00	-2.15 \pm 0.00	3.85 \pm 0.02	0.63 \pm 0.04	0.17 \pm 0.01	2.78 \pm 0.01	ND	ND	ND
4 mM	-5.30 \pm 0.00	-4.26 \pm 0.03	6.06 \pm 0.01	0.51 \pm 0.16	0.47 \pm 0.01	0.45 \pm 0.01	ND	ND	ND
6 mM	-5.51 \pm 0.00	-4.20 \pm 0.01	6.85 \pm 0.01	0.74 \pm 0.04	0.74 \pm 0.02	0.08 \pm 0.01	ND	ND	ND
8 mM	-5.61 \pm 0.00	-3.83 \pm 0.03	6.59 \pm 0.03	0.58 \pm 0.02	0.80 \pm 0.01	0.12 \pm 0.03	ND	ND	ND
10 mM	-5.40 \pm 0.00	-4.39 \pm 0.03	6.88 \pm 0.05	0.94 \pm 0.05	0.97 \pm 0.01	0.08 \pm 0.00	ND	ND	ND
20 mM	-5.36 \pm 0.00	-4.44 \pm 0.05	6.56 \pm 0.03	0.73 \pm 0.14	1.04 \pm 0.01	0.14 \pm 0.00	ND	ND	ND

Table S4. Consumption and production of metabolites by *B. thetaiotaomicron*. The data represent the average consumption/production (mM) \pm standard error (n = 3). * - Formate concentration could not be determined due to signal interference from the lactate peak. NA – not available, ND – not detected. Adapted from: Kattel et al., (2023), *Anaerobe*, Elsevier. Used under author rights.

Amount of lactate in the medium	Xylose	Acetate	Butyrate	Ethanol	Formate	Lactate	Malate	Propionate	Succinate
0 mM	-4.98 \pm 0.00	2.72 \pm 0.01	ND	-0.13 \pm 0.14	0.08 \pm 0.02	ND	ND	0.62 \pm 0.01	1.18 \pm 0.01
2 mM	-4.45 \pm 0.00	3.46 \pm 0.02	ND	-0.05 \pm 0.02	0.25 \pm 0.01	-1.77 \pm 0.00	ND	1.24 \pm 0.02	1.73 \pm 0.01
4 mM	-4.41 \pm 0.00	4.16 \pm 0.04	ND	-0.28 \pm 0.24	0.28 \pm 0.01	-3.01 \pm 0.04	ND	1.52 \pm 0.02	1.79 \pm 0.01
6 mM	-4.88 \pm 0.00	3.97 \pm 0.01	ND	-0.31 \pm 0.07	0.46 \pm 0.00	-2.16 \pm 0.01	ND	1.38 \pm 0.00	1.88 \pm 0.00
8 mM	-4.57 \pm 0.00	4.15 \pm 0.03	ND	-0.20 \pm 0.03	0.39 \pm 0.01	-2.84 \pm 0.03	ND	1.47 \pm 0.01	1.91 \pm 0.02
10 mM	-4.84 \pm 0.00	4.17 \pm 0.00	ND	-0.15 \pm 0.03	0.67 \pm 0.02	-2.62 \pm 0.04	ND	1.48 \pm 0.01	1.91 \pm 0.01
20 mM	-4.76 \pm 0.00	4.49 \pm 0.00	ND	0.05 \pm 0.08	NA*	-3.21 \pm 0.03	ND	1.56 \pm 0.01	2.19 \pm 0.00

Table S5. Expected gDNA ratios based on optical density measurements and experimentally determined values from qPCR. The data represent the average gDNA ratio \pm standard error ($n = 3$). Adapted from: Kattel et al., (2023), Anaerobe, Elsevier. Used under author rights.

Sample	gDNA ratio, %		
	<i>A. caccae</i>	<i>B. thetaiotaomicron</i>	<i>B. vulgatus</i>
theoretical ratio	33%	33%	33%
1st mixture	12% \pm 1%	47% \pm 2%	41% \pm 1%
theoretical ratio	80%	10%	10%
2nd mixture	52% \pm 2%	27% \pm 1%	21% \pm 1%
theoretical ratio	10%	80%	10%
3rd mixture	4% \pm 0%	87% \pm 1%	10% \pm 0%
theoretical ratio	10%	10%	80%
4th mixture	4% \pm 0%	15% \pm 1%	81% \pm 1%

Table S6. gDNA ratios were measured at the end of each batch using qPCR. Values represent the average gDNA ratio \pm standard error ($n = 3$). Adapted from: Kattel et al., (2023), Anaerobe, Elsevier. Used under author rights.

Sample	gDNA ratio, %		
	<i>A. caccae</i>	<i>B. thetaiotaomicron</i>	<i>B. vulgatus</i>
Day 1 <i>A. caccae</i> + <i>B. thetaiotaomicron</i>	5% \pm 1%	95% \pm 1%	
Day 2 <i>A. caccae</i> + <i>B. thetaiotaomicron</i>	5% \pm 0%	95% \pm 0%	
Day 3 <i>A. caccae</i> + <i>B. thetaiotaomicron</i>	4% \pm 1%	96% \pm 1%	
Day 1 <i>A. caccae</i> + <i>B. vulgatus</i>	6% \pm 1%		94% \pm 1%
Day 2 <i>A. caccae</i> + <i>B. vulgatus</i>	10% \pm 1%		90% \pm 1%
Day 3 <i>A. caccae</i> + <i>B. vulgatus</i>	8% \pm 1%		92% \pm 1%

Supplementary figures to Publication I

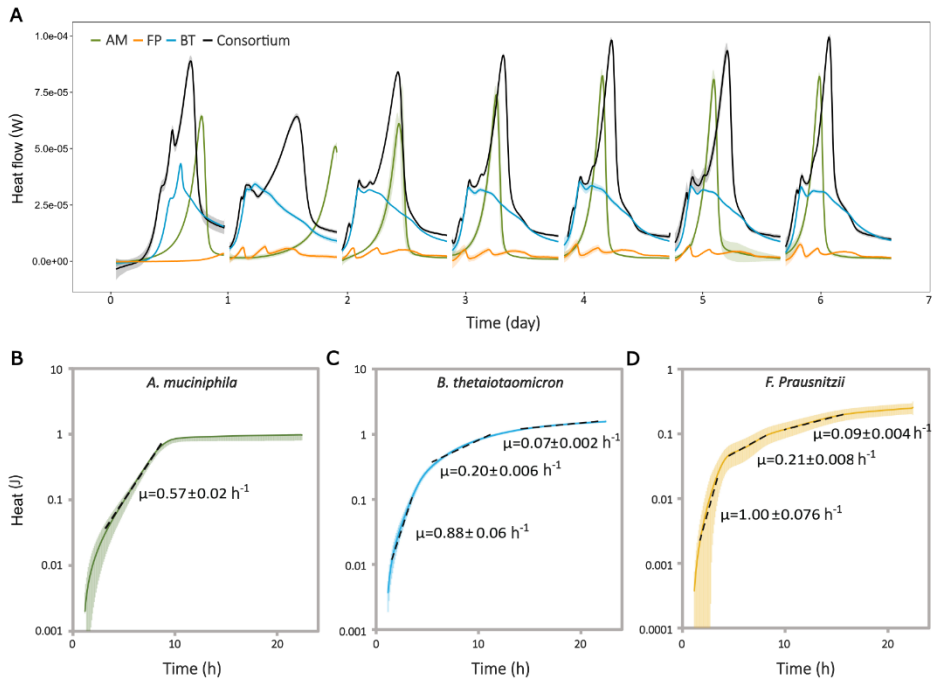


Figure S1. Growth kinetics of the monoculture and the consortium in the YCFAM medium. (A) Heat flow (W) released by monocultures and consortium. Growth was monitored over seven serial passages using the IMC. Full line and ribbon represent the average and standard deviation of the heat flow, respectively ($n=3$), for each passage. *A. muciniphila*, *B. thetaiotaomicron*, *F. prausnitzii*, and the consortium are represented by the green, blue, yellow, and black lines, respectively. (B-D) The specific growth rate(s) for each strain were calculated based on heat (J) data collected from the fifth, sixth, and seventh batch cultivations. The full line and ribbon represent the average and standard deviation, respectively, ($n = 3$). Reproduced from: Kattel et al., (2024), *MicrobiologyOpen*, Wiley. Licensed under CC BY 4.0.

Appendix 2

Publication I

Kattel, A., Aro, V., Lahtvee, P. J., Kazantseva, J., Jöers, A., Nahku, R., & Belouah, I. (2024). Exploring the resilience and stability of a defined human gut microbiota consortium: An isothermal microcalorimetric study. *MicrobiologyOpen*, 13(4).
<https://doi.org/10.1002/mbo3.1430>

Appendix 3

Publication II

Kattel, A., Morell, I., Aro, V., Lahtvee, P. J., Vilu, R., Jöers, A., & Nahku, R. (2023). Detailed analysis of metabolism reveals growth-rate-promoting interactions between *Anaerostipes caccae* and *Bacteroides* spp. *Anaerobe*, 79.

<https://doi.org/10.1016/j.anaerobe.2022.102680>

Appendix 4

Publication III

Kallastu, A., Malv, E., Aro, V., Meikas, A., Vendelin, M., Kattel, A., Nahku, R., & Kazantseva, J. (2023). Absolute quantification of viable bacteria abundances in food by next-generation sequencing: Quantitative NGS of viable microbes. *Current Research in Food Science*, 6(December 2022), 100443. <https://doi.org/10.1016/j.crf.2023.100443>

Curriculum vitae

Personal data

Name: Anna Kattel
Date of birth: 19.11.1995
Place of birth: Põlva, Estonia
Citizenship: Estonian
ORCID: 0000-0002-8105-278X

Contact data

E-mail: anna.kattel11@gmail.com

Education

2019–2025 Tallinn University of Technology, Applied Chemistry and Biotechnology, PhD
2017–2019 Tallinn University of Technology, Applied Chemistry and Biotechnology, MSc
2014–2017 Tallinn University of Technology, Applied Chemistry and Biotechnology, BSc
2011–2014 Tartu Tamme Gümnaasium, High school

Language competence

Estonian Native
English Fluent

Professional employment

2024– ... Tallinn University of Technology, Specialist in valorisation of natural raw materials
2024 AS TFTAK, Senior research specialist
2022–2024 AS TFTAK, Project manager
2019–2022 AS TFTAK, Researcher

Supervised theses

2023 Liselle Kaldaru “Developing production of next-generation probiotic co-cultures using a unique substrate”

Publications

Kattel, A., Aro, V., Lahtvee, P. J., Kazantseva, J., Jöers, A., Nahku, R., & Belouah, I. (2024). Exploring the resilience and stability of a defined human gut microbiota consortium: An isothermal microcalorimetric study. *MicrobiologyOpen*, 13(4). <https://doi.org/10.1002/mbo3.1430>

Pismennõi, D., **Kattel, A.**, Belouah, I., Nahku, R., Vilu, R., & Kobrin, E. G. (2023). The Quantitative Measurement of Peptidoglycan Components Obtained from Acidic Hydrolysis in Gram-Positive and Gram-Negative Bacteria via Hydrophilic Interaction Liquid Chromatography Coupled with Mass Spectrometry. *Microorganisms*, 11(9). <https://doi.org/10.3390/microorganisms11092134>

Kattel, A., Morell, I., Aro, V., Lahtvee, P. J., Vilu, R., Jöers, A., & Nahku, R. (2023). Detailed analysis of metabolism reveals growth-rate-promoting interactions between *Anaerostipes caccae* and *Bacteroides* spp. *Anaerobe*, 79. <https://doi.org/10.1016/j.anaerobe.2022.102680>

Kallastu, A., Malv, E., Aro, V., Meikas, A., Vendelin, M., **Kattel, A.**, Nahku, R., & Kazantseva, J. (2023). Absolute quantification of viable bacteria abundances in food by next-generation sequencing: Quantitative NGS of viable microbes. *Current Research in Food Science*, 6(December 2022), 100443. <https://doi.org/10.1016/j.crfs.2023.100443>

Conferences

September 2023 Life Sciences Baltics; Vilnius, Lithuania

July 2022 Microbiome Connect: Europe; Amsterdam, Netherlands. Oral presentation

September 2019 Intensive course “Pro-, pre-, syn- and postbiotics: the effect on our microbiota and health”; Tartu, Estonia

Elulookirjeldus

Isikuandmed

Nimi: Anna Kattel
Sünniaeg: 19.11.1995
Sünnikoht: Põlva, Eesti
Kodakondsus: Eesti
ORCID: 0000-0002-8105-278X

Kontaktandmed

E-post: anna.kattel11@gmail.com

Hariduskäik

2019–2025 Tallinna Tehnikaülikool, Keemia ja biotehnoloogia PhD
2017–2019 Tallinna Tehnikaülikool, Rakenduskeemia ja biotehnoloogia, MSc
2014–2017 Tallinna Tehnikaülikool, Rakenduskeemia ja biotehnoloogia, BSc
2011–2014 Tartu Tamme Gümnaasium

Keelteoskus

Eesti keel Emakeel
Inglise keel Kõrgtase

Teenistuskäik

2024–... Tallinna Tehnikaülikool, biotoorme väärindamise ekspert
2024 AS TFTAK, vanemarendusspetsialist
2022–2024 AS TFTAK, projektijuht
2019–2022 AS TFTAK, nooremteadur

Juhendatud lõputööd

2023 Liselle Kaldaru “Uue põlvkonna probiootikumide koosluste tootmise arendamine kasutades unikaalsete substraatide lähenemist”

Publikatsioonid

Kattel, A., Aro, V., Lahtvee, P. J., Kazantseva, J., Jöers, A., Nahku, R., & Belouah, I. (2024). Exploring the resilience and stability of a defined human gut microbiota consortium: An isothermal microcalorimetric study. *MicrobiologyOpen*, 13(4). <https://doi.org/10.1002/mbo3.1430>

Pismennõi, D., **Kattel, A.**, Belouah, I., Nahku, R., Vilu, R., & Kobrin, E. G. (2023). The Quantitative Measurement of Peptidoglycan Components Obtained from Acidic Hydrolysis in Gram-Positive and Gram-Negative Bacteria via Hydrophilic Interaction Liquid Chromatography Coupled with Mass Spectrometry. *Microorganisms*, 11(9). <https://doi.org/10.3390/microorganisms11092134>

Kattel, A., Morell, I., Aro, V., Lahtvee, P. J., Vilu, R., Jöers, A., & Nahku, R. (2023). Detailed analysis of metabolism reveals growth-rate-promoting interactions between *Anaerostipes caccae* and *Bacteroides* spp. *Anaerobe*, 79. <https://doi.org/10.1016/j.anaerobe.2022.102680>

Kallastu, A., Malv, E., Aro, V., Meikas, A., Vendelin, M., **Kattel, A.**, Nahku, R., & Kazantseva, J. (2023). Absolute quantification of viable bacteria abundances in food by next-generation sequencing: Quantitative NGS of viable microbes. *Current Research in Food Science*, 6(December 2022), 100443. <https://doi.org/10.1016/j.crfs.2023.100443>

Konverentsid

September 2023 Life Sciences Baltics; Vilnius, Lithuania

Juuli 2022 Microbiome Connect: Europe; Amsterdam, Holland. Suuline ettekanne

September 2019 Intensiivkursus “Pro-, pre-, syn- ja postbiootikumid: mõju meie mikrobiootale ja tervisele”; Tartu, Eesti